NIT

AUG 1971
RECEIVED
NASA STI FACILITY
INPUT BRANCH

R-8756

CR-119928

ADVANCED IGNITION SYSTEMS
FINAL REPORT

SEP 1971
RECEIVED
NASA STI FACILITY
INPUT BRANCH

Rocketdyne
North American Rockwell

6633 Canoga Avenue
Canoga Park, California 91304

FACILITY FORM 602

N71-35152
(ACCESSION NUMBER)

134
(PAGES)

CR-119928
(NASA CR OR TMX OR AD NUMBER)

(THRU)

G 3
(CODE)

33
(CATEGORY)

Rocketdyne
North American Rockwell

6633 Canoga Avenue
Canoga Park, California 91304

R-8756 CR-119328

ADVANCED IGNITION SYSTEMS
FINAL REPORT

Contract NAS8-25126

PREPARED BY

Rocketdyne Engineering
Canoga Park, California

APPROVED BY

P. N. Fuller
J-2 Program Manager

NO OF PAGES 128 & x

REVISIONS

DATE 30 July 1971

DATE	REV BY	PAGES AFFECTED	REMARKS

FORM R18-G REV. 5-69

FOREWORD

This report was prepared by Rocketdyne, a division of North American Rockwell Corporation, under Contract NAS8-25126 and Rocketdyne G.O. 09288.

ABSTRACT

Two ignition system concepts were experimentally evaluated during laboratory testing for application in hydrogen/oxygen engine system incorporating a multiple-combustor thrust chamber. Both concepts, designated the Resonant Flow Igniter and the Combustion Wave Igniter, proved operationally feasible for the specific engine system application. The ignition concepts are unique and can be used to ignite any hydrogen/oxygen combustion device. The ignition system design requirements are discussed, ignition system configurations for a specific application are described, and the results of feasibility testing with prototype igniter hardware are detailed.

CONTENTS

Foreword iii
Abstract iii
Introduction and Summary 1
Ignition Systems 3
  Engine System Requirements 3
  Resonant Flow Ignition Device 3
  Resonant Flow System 8
  Combustion Wave Ignition Device 8
  Combustion Wave System 12
Resonant Ignition Devices 17
  Resonance Heating Phenomenon 17
  Ignition and Combustion 22
  Test Program Objectives 23
  Resonance Igniter Testing 23
  Resonant Flow Experiments 54
  Conclusions 65
Combustion Wave Ignition Device 69
  Combustion Wave Phenomenon 69
  Test Program Objectives 79
  Combustion Wave Igniter Testing 79
  Optimum Combustion Wave Ignition System 100
  Conclusions 104
References 105
Appendix A
Advanced Igniter Energy Requirements A-1
Appendix B
Related Experience in Resonance Ignition B-1
Appendix C
Igniter Test Facility C-1

ILLUSTRATIONS

1. No. 2 Test Bed Assembly 4
2. No. 2 Test Bed Start Sequence 5
3. No. 2 Test Bed Igniter Port 6
4. Resonant Flow Igniter 7
5. Resonant Flow Ignition System 9
6. No. 2 Test Bed Start Sequence (Resonant Igniter) 10
7. Combustion Wave Igniter Element 11
8. Combustion Wave Ignition System 13
9. Combustion Wave Ignition System 14
10. No. 2 Test Bed Start Sequence (Combustion Wave Igniter) 15
11. H_2/O_2 Autoignition 18
12. Resonance Heating Phenomenon 20
13. Resonance Igniter Nomenclature 25
14. Resonance Igniter Assembly (Used During Geometry Optimization and Combustion Characteristics Tests) 27
15. Resonance Igniter Assembly (With Uncooled Throat) 28
16. Oxidizer Augmentation Assembly 29
17. Resonance Temperature vs G/d 33
18. Resonance Temperature vs Pressure Ratio 35
19. Resonance Temperature vs Time 36
20. Resonance Temperature vs Total Pressure 37
21. Ignition Trace 39
22. c* Efficiency vs Mixture Ratio (at H_2 Total Pressure ~165 psia) . . 46
23. c* Efficiency vs Mixture Ratio (at H_2 Total Pressure ~210 psia) . . 47
24. c* Efficiency vs Mixture Ratio (at H_2 Total Pressure ~265 psia) . . 48
25. Primary Mixture Ratio vs Overall Mixture Ratio 53
26. Oxidizer Augmentation Ignition Limits 55
27. Resonant Flow Igniter Design 56
28. Resonant Flow Test Hardware 58
29. Resonance Tube Configurations 59
30. Removed Gas Temperature vs G/d 61
31. Pressure Ratio vs G/d 62

32. Removed Gas Percent vs G/d 63
33. Removed Gas Temperature vs Percent 64
34. Chapman-Jouguet Ratios vs Energy Release 73
35. Energy Release vs Mixture Ratio 74
36. Influence of Initial Conditions on Chapman-Jouguet Temperature Ratio 76
37. Influence of Initial Conditions on Chapman-Jouguet Pressure Ratio 77
38. Induction Length vs Mixture Ratio 78
39. Combustion Wave Element Design 80
40. Combustion Wave Igniter Element 82
41. Combustion Wave Igniter Premixer 83
42. Precombustor 84
43. Test Setup 85
44. Combustion Wave Map 94
45. Ignition Temperature vs Time 95
46. Pilot Ignition Map (Precombustor/Pilot Element) 97
47. Pilot Ignition Map (Precombustor/Precombustor) 98
48. Dual-Element Test Results 99
49. Optimized Combustion Wave Ignition System 101
50. Optimized Combustion Wave Igniter Element 102
51. Optimized Combustion Wave Igniter Engine Start Sequence 103

TABLES

1. Resonance Igniter Test Program 32
2. Combustion Characteristics, Nonoptimized Resonance Igniter 40
3. Combustion Characteristics, Optimized Resonance Igniter 45
4. Oxidizer Augmentation Results 51
5. Effect of Initial Conditions on Chapman-Jouguet Conditions 75
6. Combustion Wave Ignition Test Program 87
7. Combustion Wave Igniter Test Results 88

INTRODUCTION AND SUMMARY

As a result of tradeoff studies completed during the last quarter of CY 1970, two igniter concepts were selected for further detailed study with the objective of selecting an advanced ignition system for the No. 2 test bed, a multicombustor aerospike engine system. Both the Resonant Flow and the Combustion Wave Igniter concepts proved sufficiently sound analytically to warrant experimental testing on the prototype component level. Tests conducted at No. 2 test bed ignition-stage operating conditions proved that both concepts are operationally feasible for the No. 2 test bed, and that either concept has the development potential to be a simple, reliable, lightweight, low-cost ignition system for multicombustor thrust chambers.

The Resonant Flow igniter concept has been selected as the primary ignition system for the No. 2 test bed. Although both concepts offer simplicity and operational reliability, the Resonant Flow concept is favored because no external energy source is required for ignition and the technology advancement potential is higher. The fundamental operation of this device is based on a gas-dynamic resonance phenomenon that is generated using pressurized ambient-temperature hydrogen and results in the production of a small quantity of high-temperature hydrogen for autoignition with ambient-temperature oxygen. Three configurations of resonant igniters were experimentally evaluated in a total of 193 laboratory tests to determine optimized geometry, to evaluate oxidizer augmentation, and to verify the feasibility of hot gas extraction from a resonance tube. Based on these test results, the Resonant Flow concept was judged feasible for the No. 2 test bed ignition system.

The Combustion Wave igniter is the backup ignition device for the No. 2 test bed. This concept operates by propagating a combustion wave through unburned, premixed, hydrogen/oxygen gas to ignite a coaxial pilot element at the injector face. The combustion wave is initiated by sparking a premix chamber and manifold filled with the unburned propellant gases. The combustion wave igniter was laboratory tested to determine the feasibility of propagating the combustion wave through representative lengths of standard tubing with right-angle bends, to verify the ignition of multiple pilot elements with a single, manifolded combustion wave, and

to evaluate the ignition limits of the pilot elements. The 106 tests performed during this evaluation proved the concept feasible.

A detailed description of the system configurations, analytical considerations, test hardware, and test results for the Resonant Flow and Combustion Wave igniters is presented in the following sections.

IGNITION SYSTEMS

ENGINE SYSTEM REQUIREMENTS

The candidate ignition systems selected for the No. 2 test bed (Fig. 1) must be capable of providing a sufficient ignition source for 10 segmented combustors. Although the No. 2 test bed is to be ignited at test site ambient conditions, the ignition system must also be capable of reliable vacuum ignitions. No moving parts are permitted in the ignition device because of the adverse effect on reliability. The ignition system must be operationally independent of the engine start sequence in that an ignition source must be established prior to opening the engine system main oxidizer valve and prior to turbopump spinup. The No. 2 test bed start sequence is presented in Fig. 2. The ignition devices must sustain combustion in engine mainstage to maintain injector performance at a high level.

Igniter flowrates and energy output during the ignition stage must be comparable to or exceed the values determined for main propellant ignition during J-2S engine system testing at AEDC (Appendix A). The ignition system must establish an ignition source sufficient for main propellant ignition in the 1.0-second interval between Engine Start signal and Mainstage Start signal. The ignition device must be capable of being installed in a common igniter port that is cast into the oxidizer dome of the No. 2 test bed combustors (Fig. 3).

RESONANT FLOW IGNITION DEVICE

The Resonant Flow ignition device (Fig. 4) is activated by admitting pressurized gaseous hydrogen through a sonic nozzle into a coaxially located resonance tube. The resonance phenomenon produces a small percentage of hot (1800 to 2000 R) hydrogen which flows into a primary combustor through an orifice at the downstream end of the resonance tube. A small quantity of the gaseous oxidizer flow is admitted to the primary combustion region through orifices to cause primary ignition. Secondary ignition of the fuel and oxidizer flow bypassed around the primary combustor occurs in the discharge tube. The hot igniter gases exit through the discharge tube to the injector face of the combustor and ignite the main propellants.

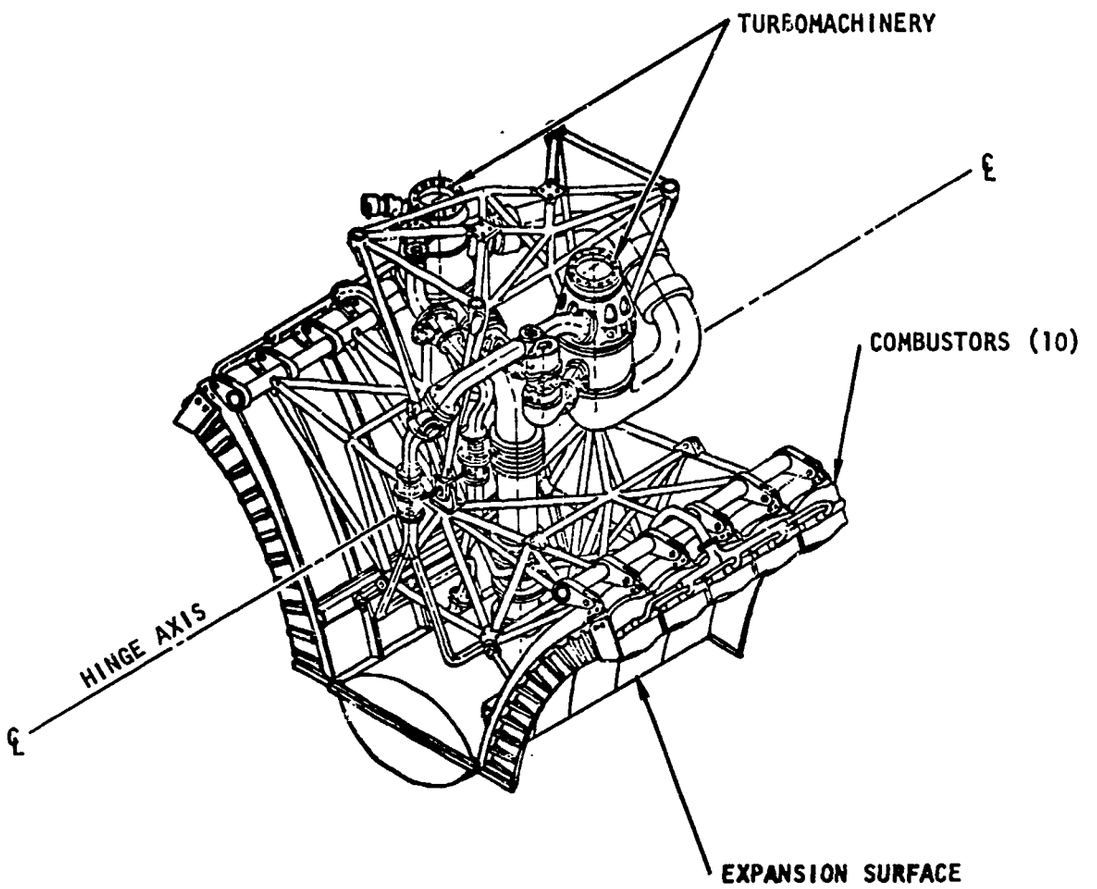

Figure 1. No. 2 Test Bed Assembly

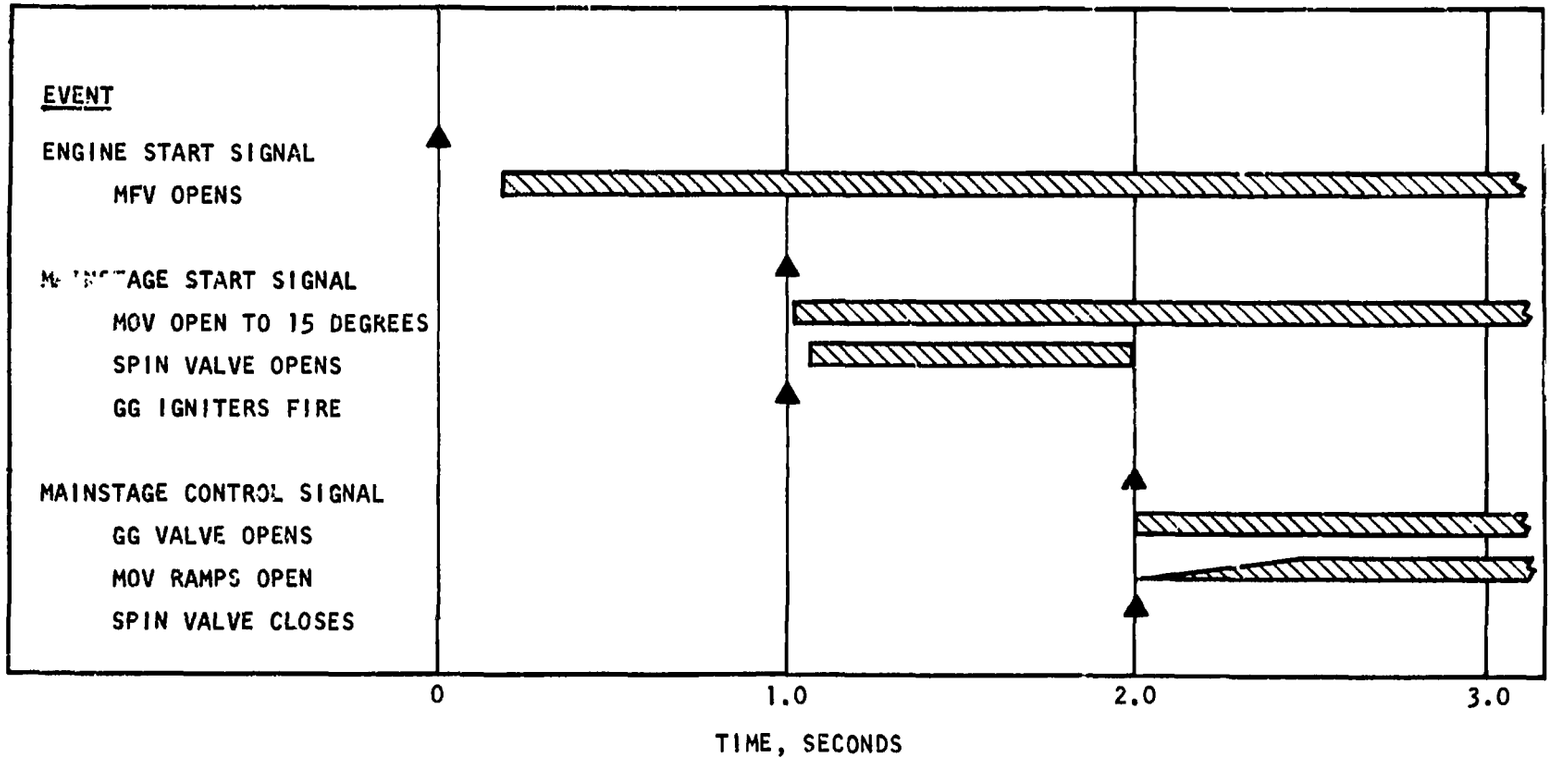

Figure 2. No. 2 Test Bed Start Sequence

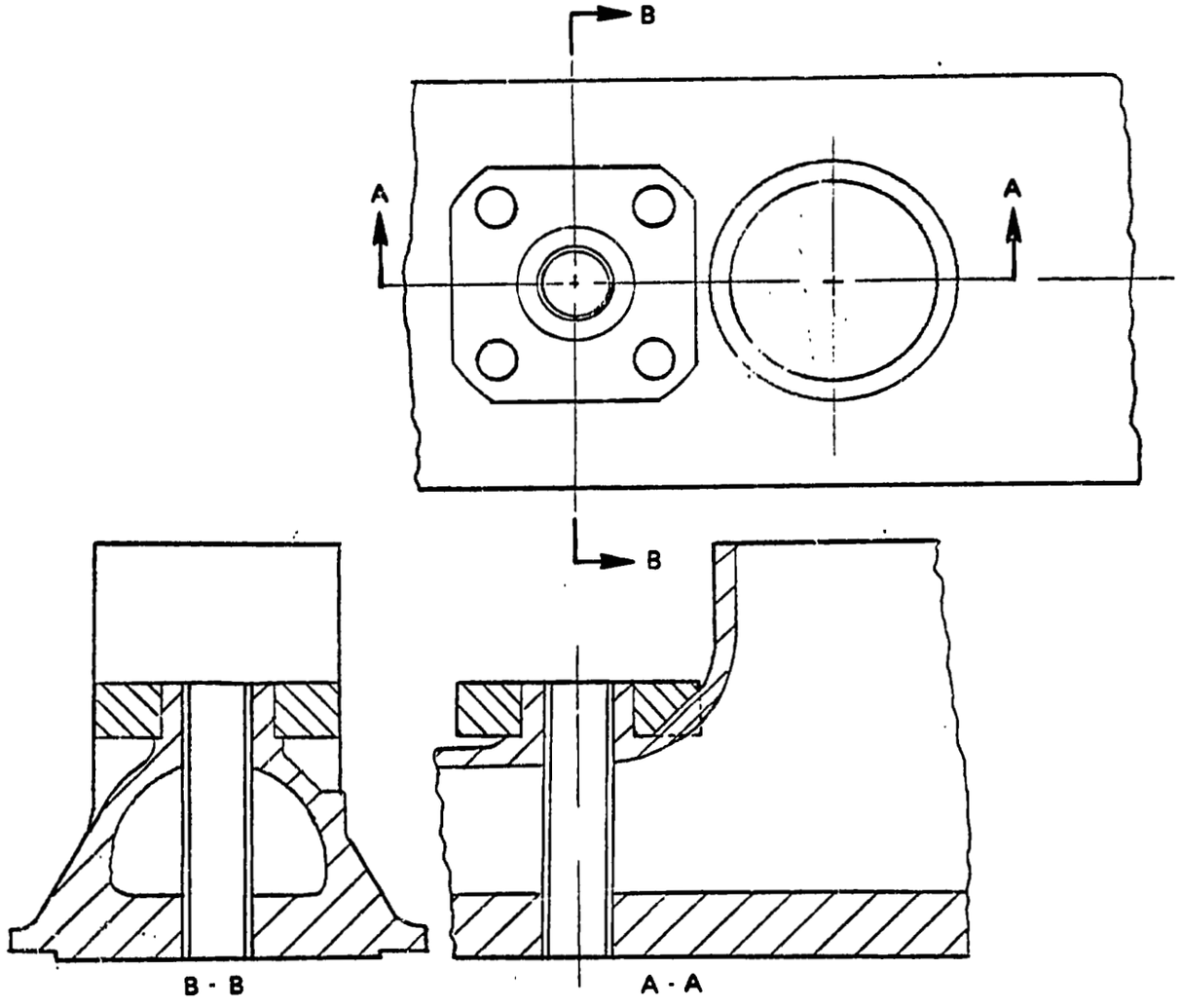

Figure 3. No. 2 Test Bed Igniter Port

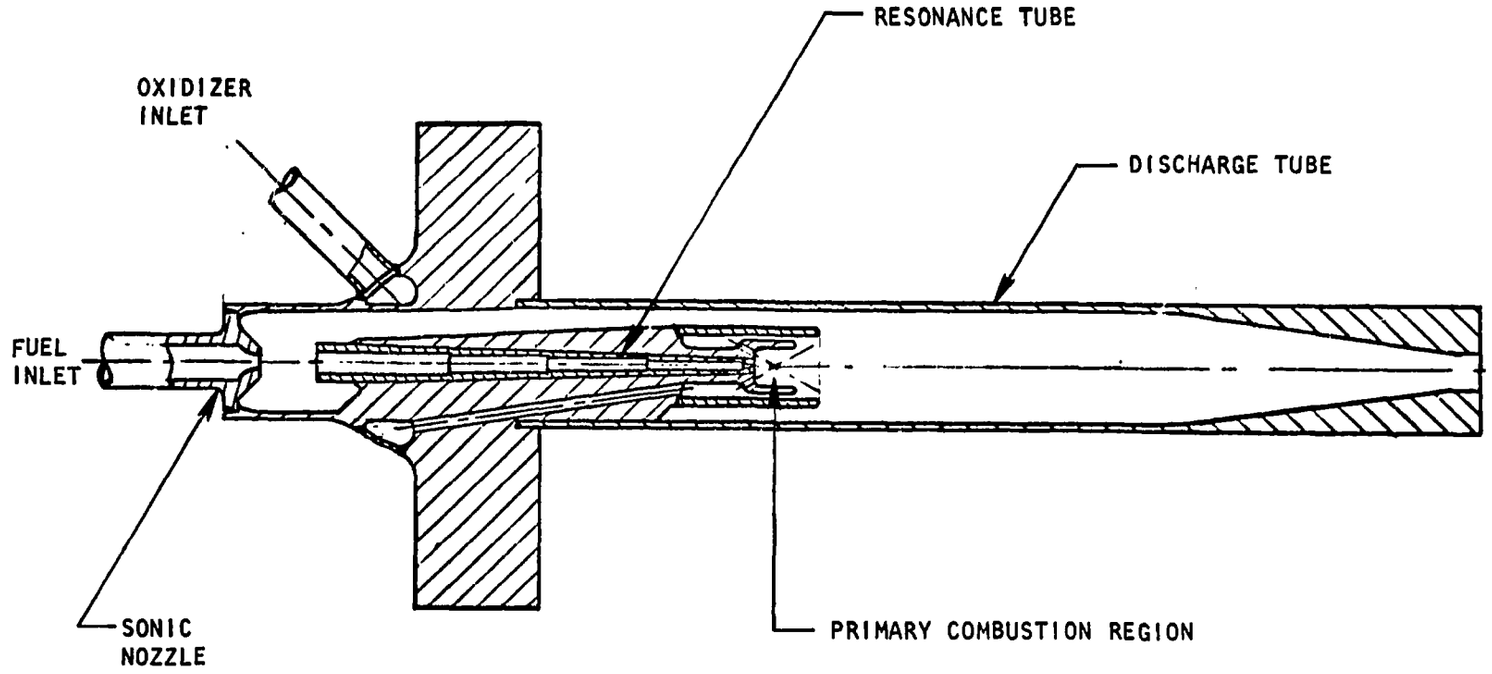

Figure 4. Resonant Flow Igniter

RESONANT FLOW SYSTEM

The Resonant Flow ignition system meeting engine requirements employs 10 ignition devices (as shown in Fig. 4) installed through the common igniter ports supplied on the combustors. A schematic of the ignition system is shown in Fig. 5. The system is comprised of a set of pressurized propellant tanks isolated with igniter propellant valves, a set of igniter bootstrap valves to control propellant flow from upstream of the engine system main valves, 10 resonant flow ignition devices, and a set of propellant supply manifolds. The ignition system will be sequenced in the following manner:

1. At Engine Start signal the main fuel valve and igniter propellant valves will open, admitting pressurized gaseous propellants to the Resonant Flow ignition devices.
2. When ignition has been detected, permission for Mainstage Start signal is received, and the engine main oxidizer valve is opened to 15 degrees.
3. At Mainstage Control signal, 2.0 seconds after engine start, the igniter bootstrap valves are opened, and the igniter propellant valves are closed.

The detailed start sequence for the No. 2 test bed with the Resonant Flow igniter is shown in Fig. 6.

COMBUSTION WAVE IGNITION DEVICE

The Combustion Wave ignition element (shown in Fig. 7) is a set of triaxial tubes that are flush mounted in the combustor injector face. The core of the triaxial element is the combustion wave tube, and the annuli form the pilot element that is ignited by the passage of the combustion wave. The combustion wave for any number of these elements is supplied from a premix chamber equipped with an integrated spark plug and exciter unit, which is being developed by Rocketdyne under contract NAS3-14351.

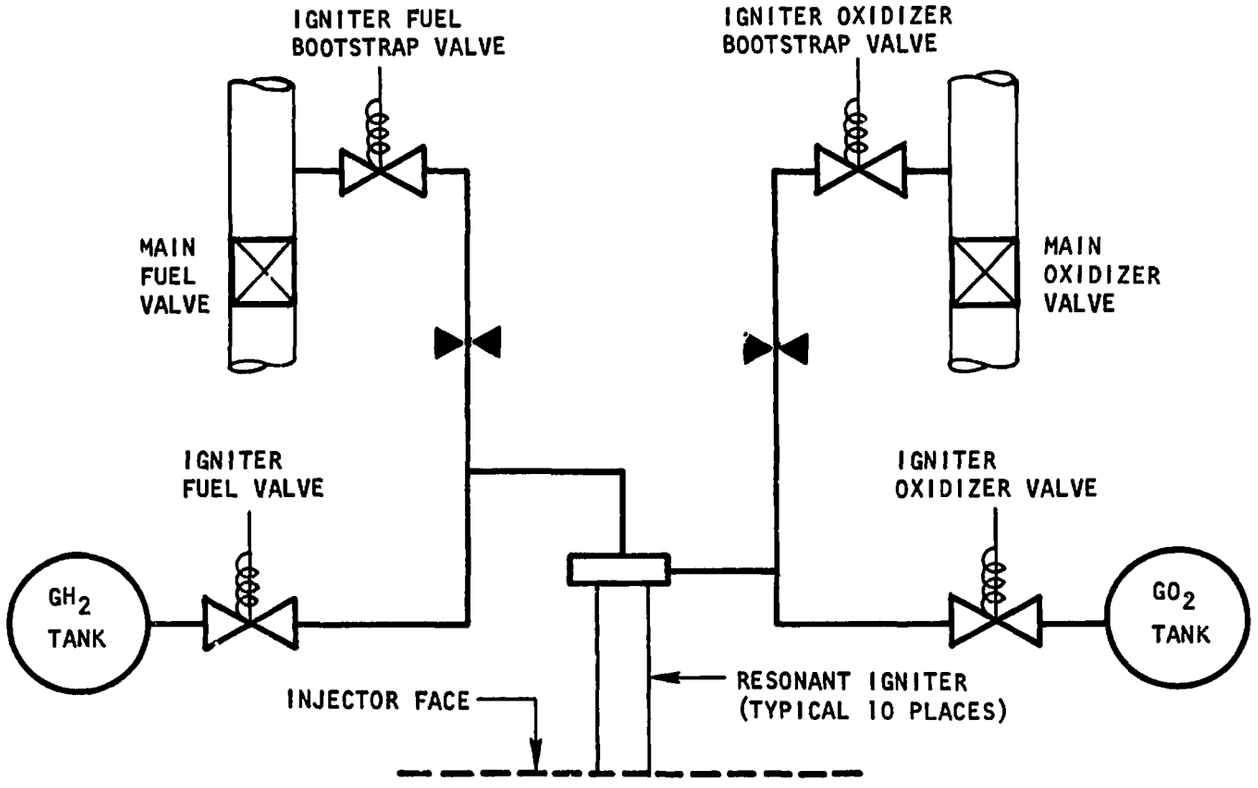

Figure 5. Resonant Flow Ignition System

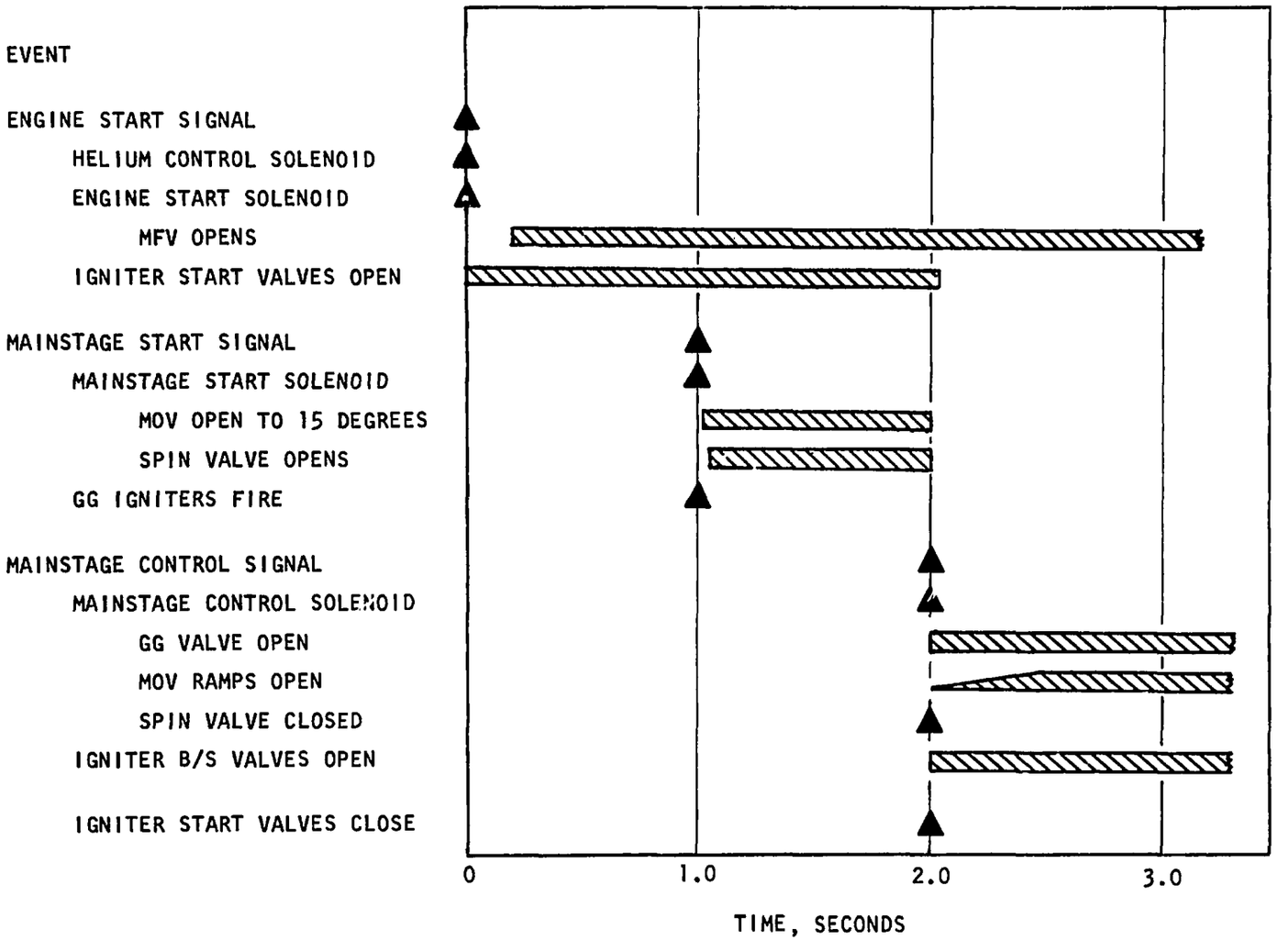

Figure 6. No. 2 Test Bed Start Sequence (Resonant Igniter)

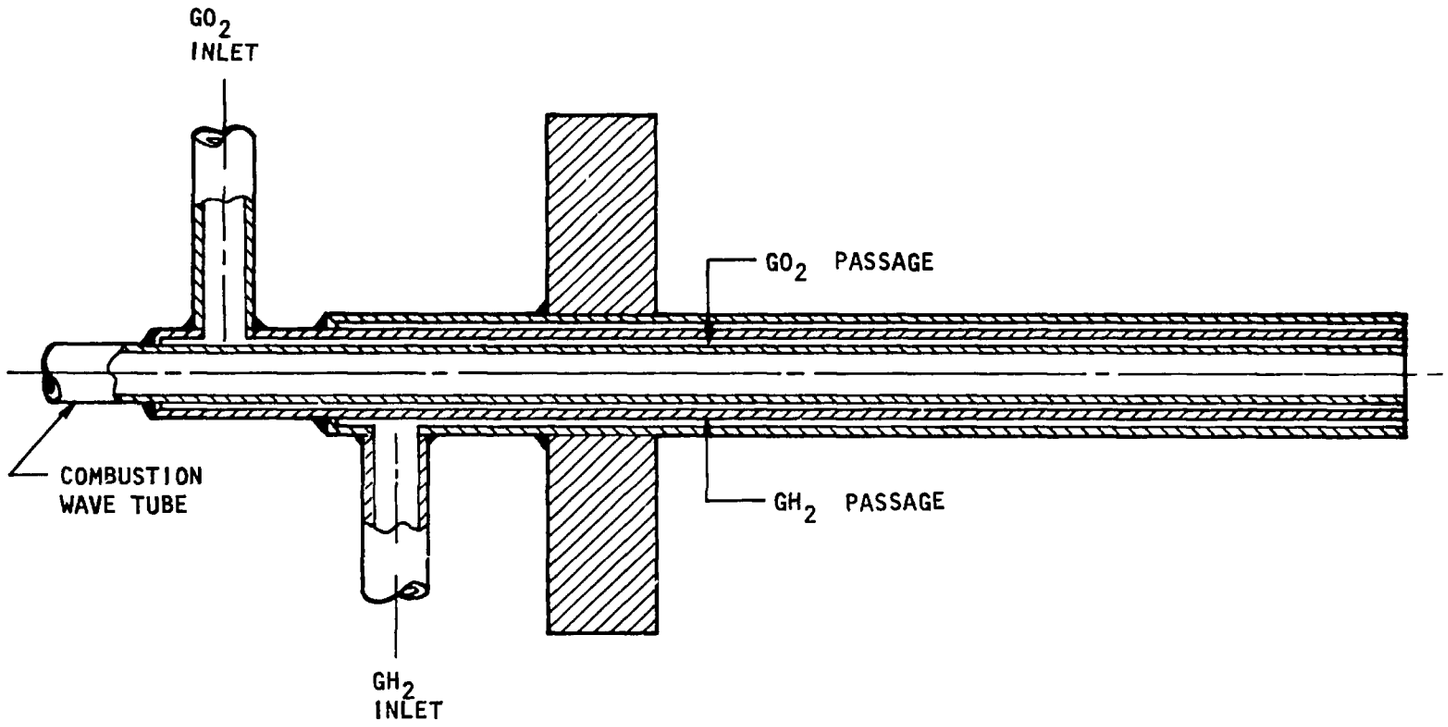

Figure 7. Combustion Wave Igniter Element

COMBUSTION WAVE SYSTEM

In the Combustion Wave system (Fig. 8) ignition energy is supplied from a centrally located premix chamber incorporating a single, integrated spark plug and exciter unit. A combustion wave manifold, constructed of standard 1/4-inch tubing, is attached to the premix chamber and terminates in 10 combustion wave/pilot elements mounted in the common igniter ports on the thrust chamber combustors. A typical installation on a multisegment unit is shown in Fig. 9. Fuel is supplied to the premix chamber and pilot fuel manifold under engine tank head pressure from the fuel turbopump discharge ducting and is controlled by a single igniter fuel valve. Check valves are provided in the premix chamber fuel and oxidizer lines to prevent backflow to the pump discharge lines when the combustion wave is generated in the premix chamber. Oxidizer is supplied, under engine tank head pressure, from the oxidizer pump discharge duct to the premix chamber and the oxidizer pilot manifold. An oxidizer pilot valve is provided in the pilot supply line and an igniter valve is installed in the premix chamber oxidizer line. The ignition system is sequenced as follows:

1. At Engine Start signal, the main fuel valve, igniter fuel valve, igniter oxidizer valve, and oxidizer pilot valve are opened and the combustion wave and pilot manifolds are primed with gaseous propellants.
2. Upon expiration of an ignition delay timer, the spark plug is fired, the igniter oxidizer valve is closed, the combustion wave is generated, and the pilot elements are ignited.
3. The combustion wave manifold continues to be supplied with fuel at pump discharge conditions throughout the start transient and in mainstage. The pilot propellant manifolds are supplied with both oxidizer and fuel during start and mainstage.

The engine start sequence for the No. 2 test bed with the Combustion Wave ignition system is shown in Fig. 10.

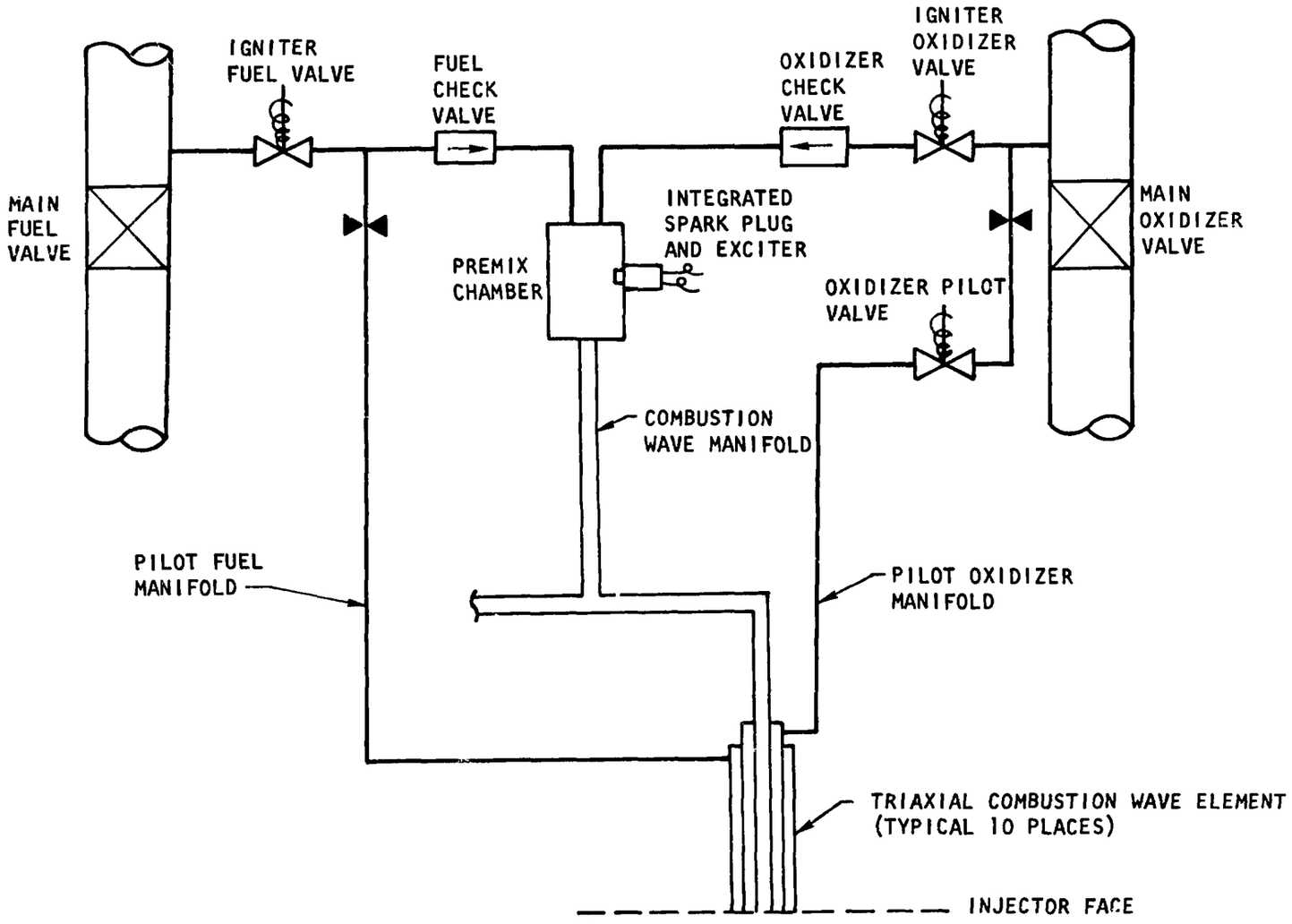

Figure 8. Combustion Wave Ignition System

FOLDOUT FRAME 1

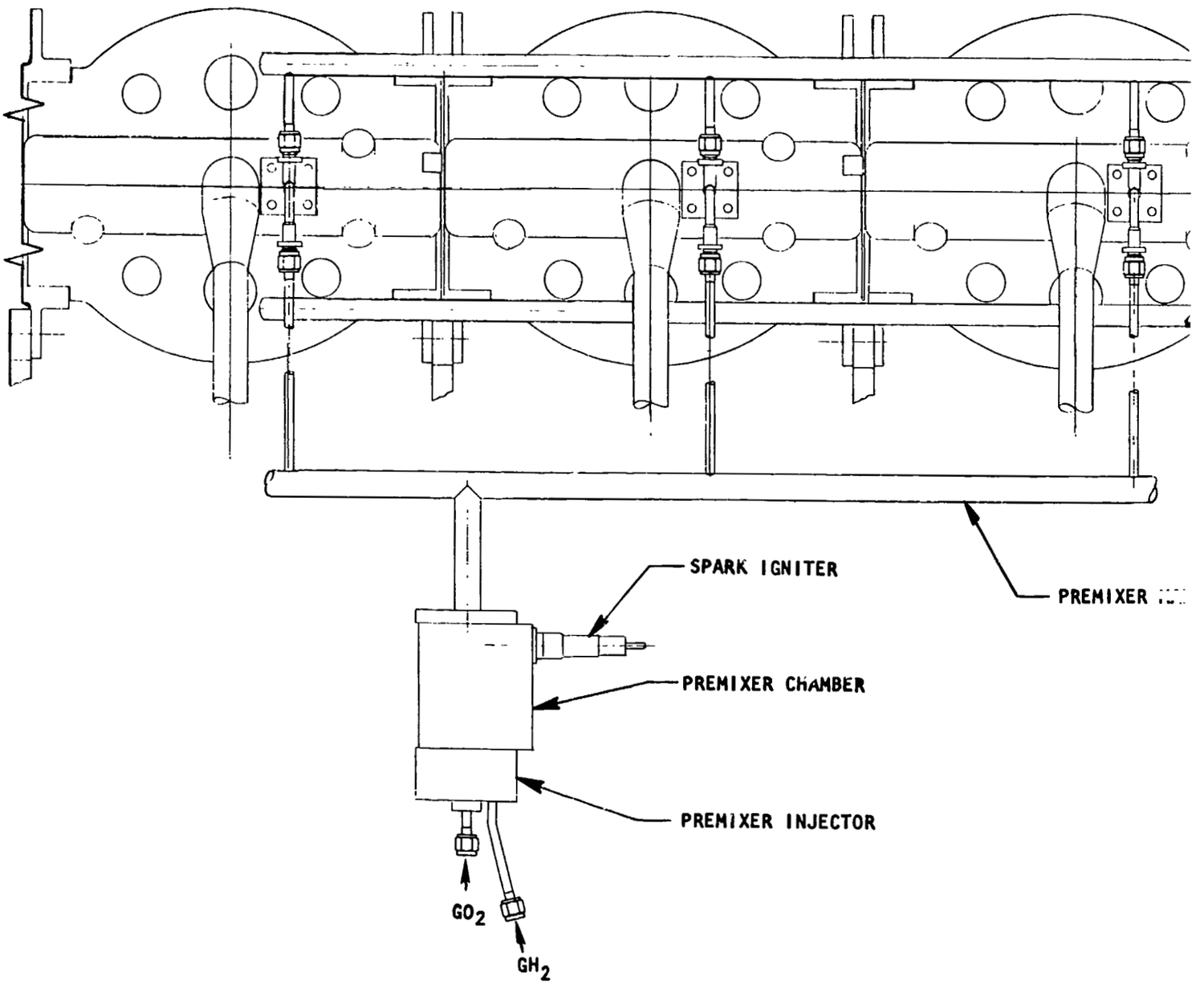

FOLDOUT FRAME 2

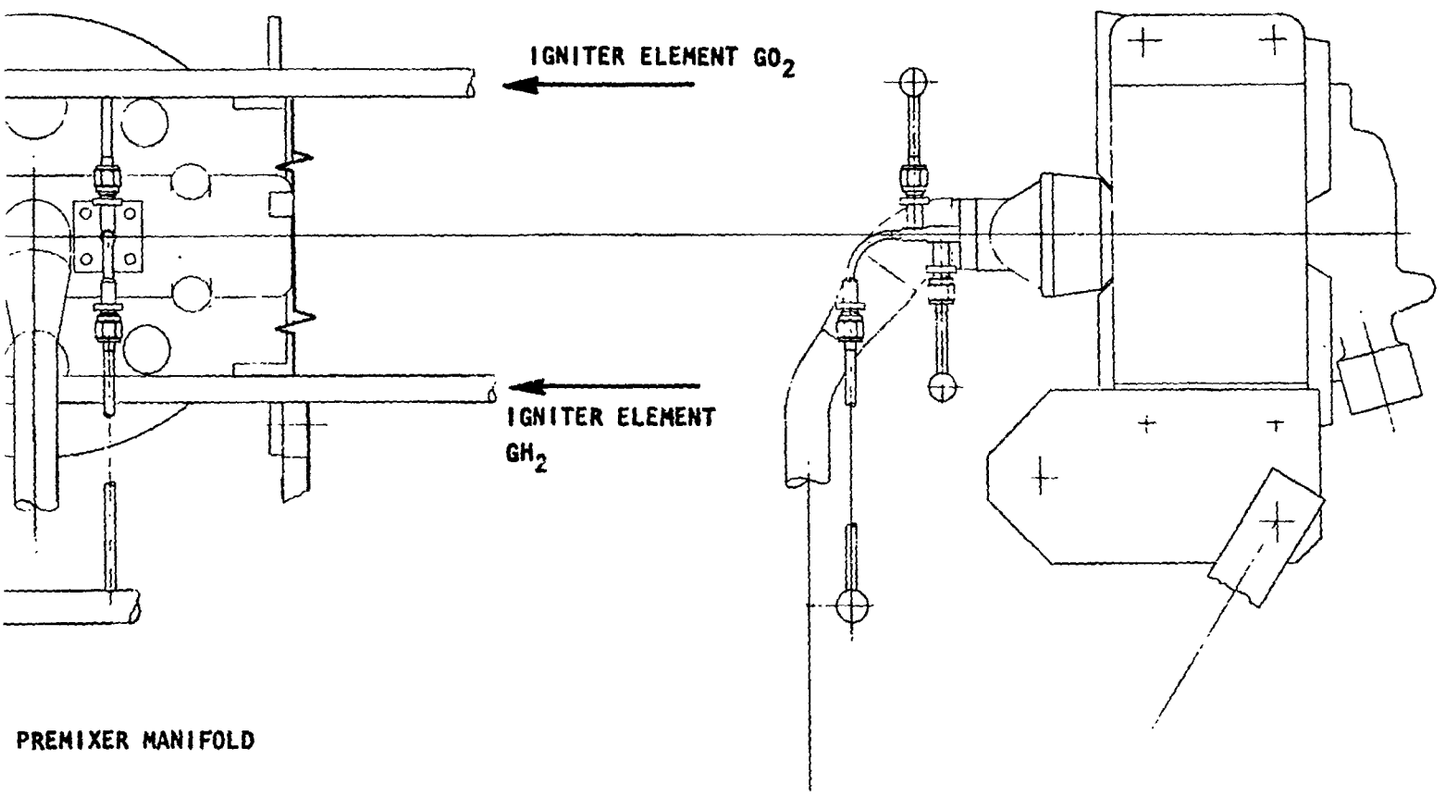

Figure 9. Combustion Wave Ignition System

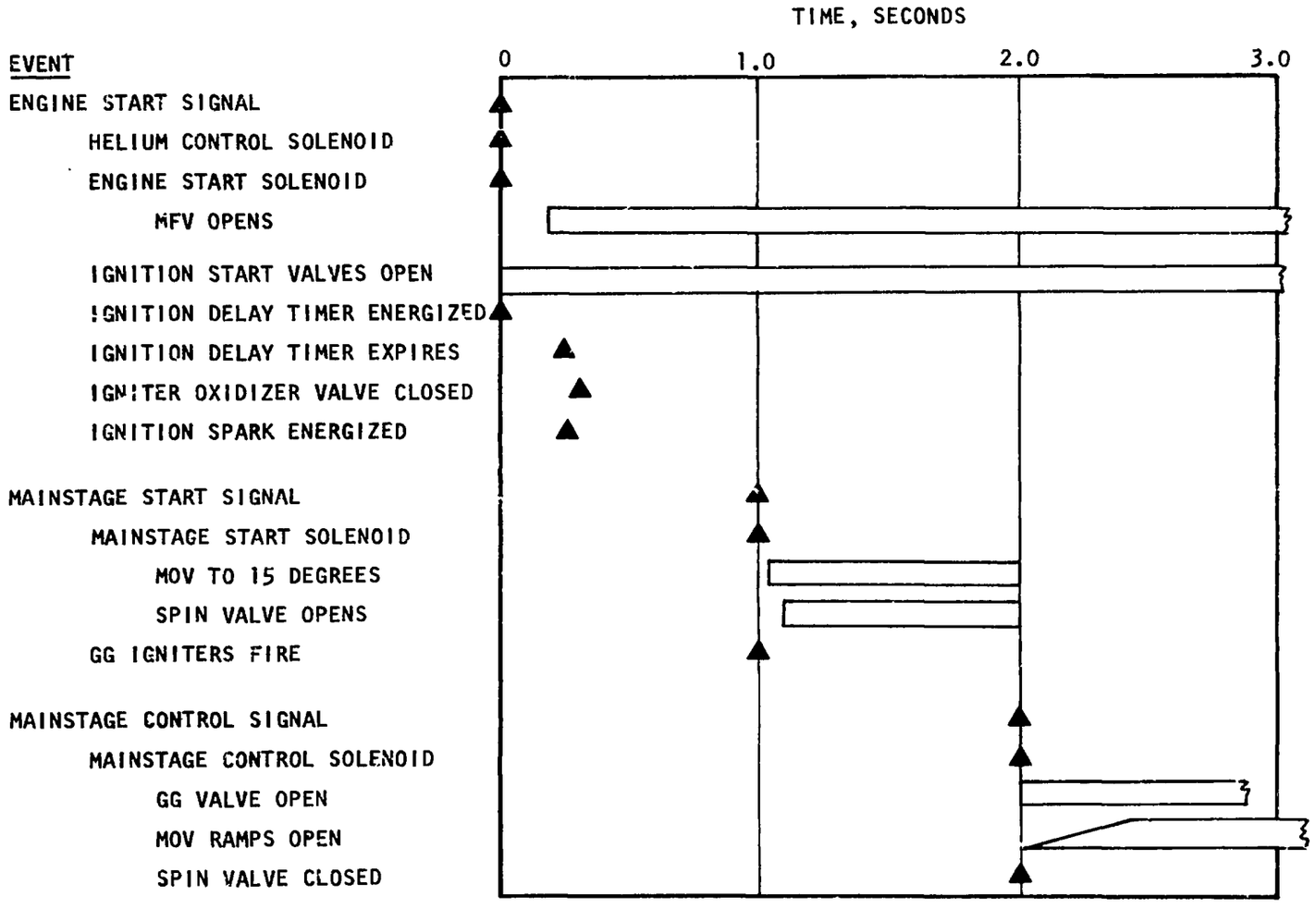

Figure 10. No. 2 Test Bed Start Sequence (Combustion Wave Igniter)

RESONANT IGNITION DEVICES

RESONANCE HEATING PHENOMENON

The operation of the igniter to be discussed is based upon a gas-dynamic resonance phenomenon. This igniter, to be referred to as the Resonance igniter, requires no external energy inputs or catalytic surface reactions, and makes hydrogen and oxygen propellants appear virtually hypergolic from a system point of view. In the case of segmented thrust chambers, where each segment must be ignited individually and simultaneously, the resonance igniter offers advantages over other ignition systems in terms of integration, simplicity, ease of operation, and lightweight packaging.

The igniter consists of two opposed tubes that serve as oxidizer and fuel inlets (Fig. 11). One of the propellants (in the gaseous state) is introduced through one of the tubes and is allowed to resonate in the opposed tube which is initially close-ended. The resonance phenomena cause heating of the gas, and after a finite period of time, the other propellant is introduced, forcing the heated gas out of the tube while ignition occurs at the interface of the two propellants. When steady-state flow is established, both oxidizer and fuel feed into a larger diameter tube where combustion is sustained. While either propellant can be used as the lead gas, experimental efforts conducted under Rocketdyne IR&D in early 1970 indicated the most rapid heating and the highest temperatures could be obtained with low molecular weight gases. The hydrogen propellant was, therefore, selected as the lead gas.

To reiterate the operational procedure, the hydrogen is introduced slightly before the oxygen (by 0.005 to 0.010 second). The hydrogen resonates in the oxygen tube and a portion of the hydrogen gas becomes heated (Mode I, Fig. 11). The oxygen is then injected into this hot hydrogen and ignites (Mode II, Fig. 11). Combustion is sustained in the larger diameter tube, thus providing a hot gas torch for main propellant ignition.

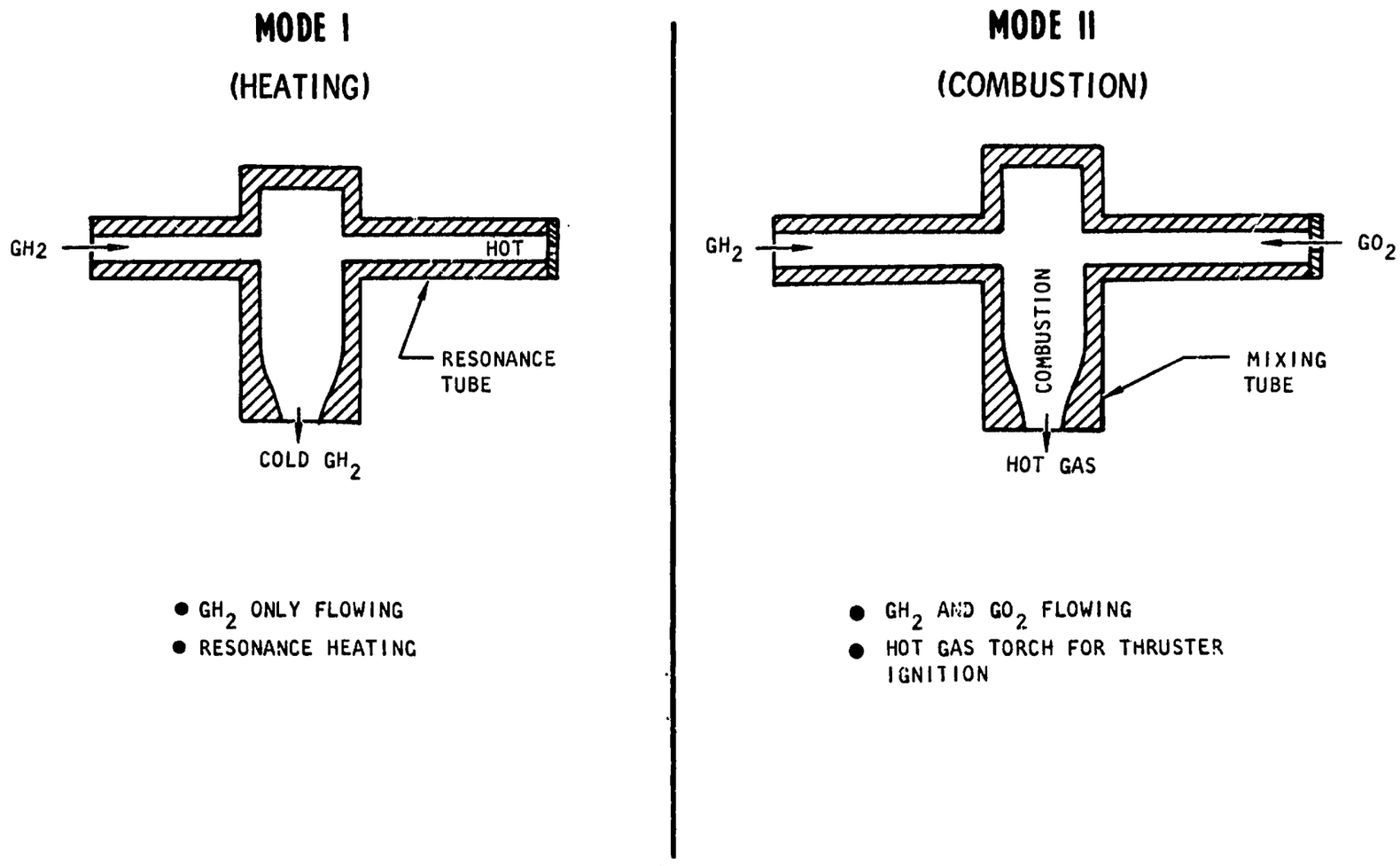

Figure 11. H_2/O_2 Autoignition

Many attempts have been made to understand and theorize the phenomena of resonance and the attending temperature rise that occurs when a gas jet impinges on a cavity. At the present time, there is a good qualitative understanding of resonant heating and the conditions under which it occurs.

Perhaps the best explanation of the flow structure during resonance can be deduced from the experimental observations presented in Ref. 1. Based on these observations, the following is a brief summary of the event sequence that occurs during one cycle of resonance tube operation:

1. The jet that issues from the flow tube is underexpanded and thus freely expands into the mixing chamber as shown in Fig. 12. The normal shock (shock disk) stands at the inlet of the tube and, for a fraction of the cycle period, a steady in-flow is established during which time most of the flow passes into the tube. A series of shocks travels down the tube, irreversibly compressing a fraction of the gas volume.
2. For a very short fraction of the cycle period, a transition occurs between in-flow and out-flow due to reflections of compressions waves. A strong shock leaves the tube and advances into the jet (Fig. 12b).
3. A steady out-flow is temporarily established during which the two jets impinge on each other with most of the mass flow existing through the region formed by the two shock disks (Fig. 12c).
4. Because the closed-end tube contains only a fixed gas mass, the above out-flow phase is accompanied with a decrease in pressure (and mass flow-rate) in the closed-end tube, allowing the jet to move back to its original position (Fig. 12d).

It should be noted that the shock movements in the tube as depicted in Fig. 12 are repsentative for the fundamental resonance mode. Higher modes are known to exist. These modes create more complex shock interactions as they move along the tube.

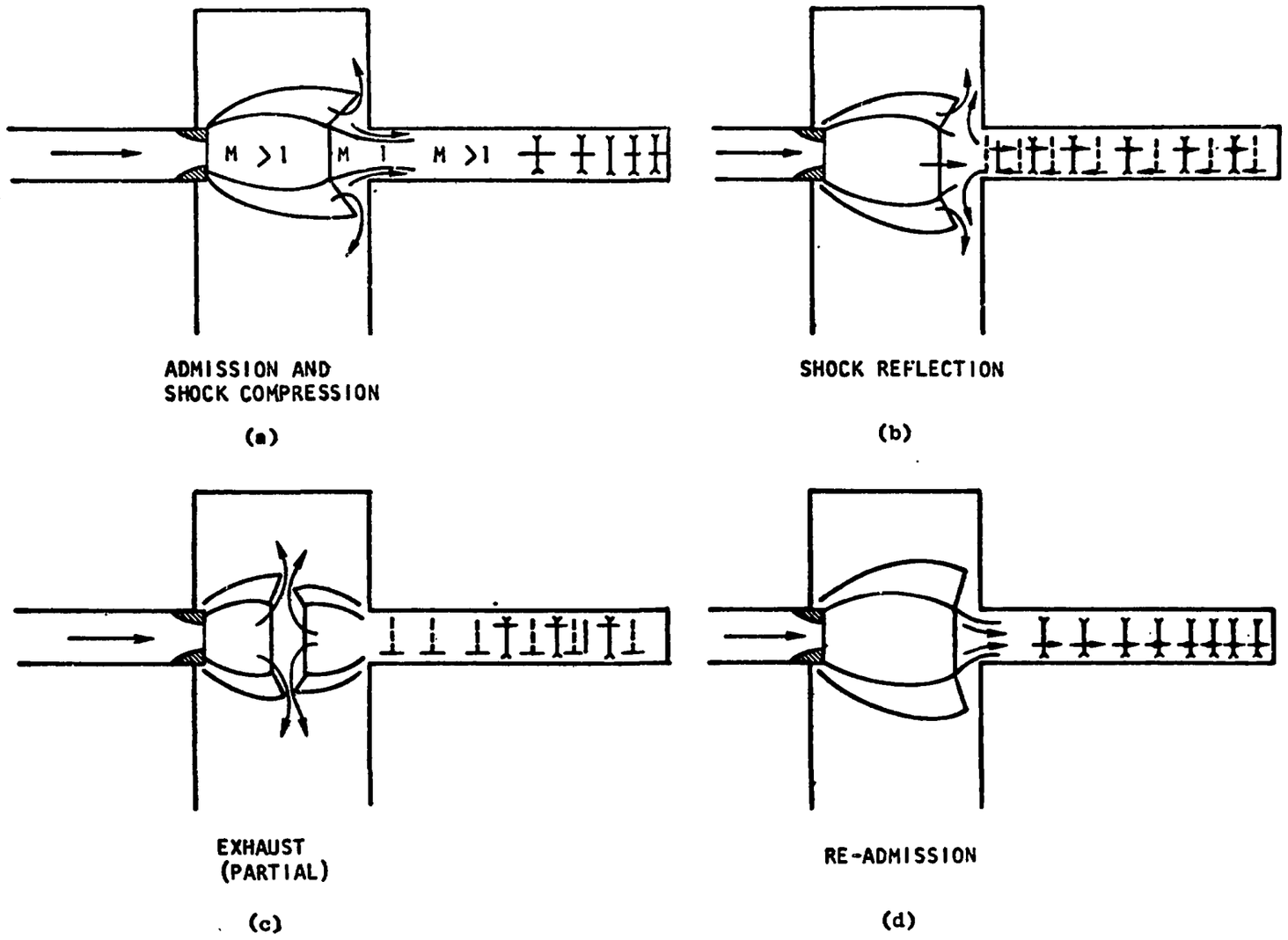

Figure 12. Resonance Heating Phenomenon

Using a number of simplifying assumptions, an equation was derived in Ref. 2 for calculating the upper limit of temperature rise in a resonant tube. The equation has the following form:

$$\Delta T = 2\ (\gamma + 1)\ \overline{T}$$

where

ΔT = the temperature rise above jet stagnation temperature
γ = ratio of specific heats
$\overline{T}$ = average gas temperature in tube after resonance has been established

The above equation indicates that for diatomic gases ($\gamma = 1.4$) the temperature rise from open to closed end of the tube can be as high as 4.8 times the mean tube temperature. Temperatures measured experimentally have achieved approximately half of this temperature rise. Whereas average temperatures can be measured with reasonable accuracy, the local gas (along tube centerline) temperature rise and fluctuations are extremely difficult to determine experimentally. Even with a high-response thermocouple the measurement of gas temperature rise times is influenced by both the presence of thermocouple as a flow obstruction, and the heat transfer between the gas and the surrounding heat sink.

Schlieren observations (and theoretical estimates) indicate that local maximum temperatures are achieved within milliseconds (Ref. 3). However, the literature, as well as the experiments performed at Rocketdyne, indicate that it takes several seconds to achieve steady-state maximum temperature readings. Since heat transfer influences temperature measurements as well as maximum achievable temperature rise, tests have to be conducted with thermally insulated tubes. Thermal insulation substantially reduces heat transfer losses and increases the measurable rate of temperature rise.

Several other methods are also available for increasing the temperature rise. One is to taper the resonant tube to take advantage of shock strengthening caused by

convergence (Ref. 4). Another way of increasing the temperature rise is to use either a monatomic gas or one of low molecular weight (i.e., hydrogen) as the driving gas.

IGNITION AND COMBUSTION

The chemical and gas dynamic processes involved in achieving ignition and sustaining combustion of low-temperature H_2/O_2 gas by means of resonance ignition are complex. However, based on past experimental observations, a number of conclusions relating to ignition and combustion can be drawn:

1. A minimum temperature must be established by resonance before ignition occurs. This resonance ignition temperature does not necessarily correspond to accepted minimum ignition temperatures as obtained from conventional static (bomb) experiment. According to Ref. 5 it appears that under flow conditions the ignition temperature of H_2/O_2 mixture lies below 980 F over a wide range of pressures, mixture ratios, and flow velocities. The reduced minimum ignition temperature may be attributed (according to Ref. 6) to the observation of high-temperature regions in the resonance tube.
2. The method of introducing oxygen and the rate at which it is introduced appears to be directly related to obtaining the proper mixing and mixture ratio for ignition.
3. Following ignition, the combustion process begins in the resonance tube and ignition is completed in the mixing chamber. If the mixing chamber is too short, completion of combustion will be inhibited by the drop in temperature resulting from the sudden expansion of the gases as they leave the mixing chamber, resulting in quenching.

Related experience at Rocketdyne in the area of resonant ignition is presented in Appendix B.

TEST PROGRAM OBJECTIVES

The purpose of this effort was to study the application of the resonance igniter to the No. 2 test bed. Although the feasibility and operational reliability of the resonance igniter was demonstrated in previous investigations (see Appendix B), the present effort was directed toward a particular application, namely the ignition of segmented thrust chambers which requires low igniter flowrates per individual igniter and simple mechanical features.

The program consisted of two major aspects both primarily experimental in nature: (1) operation of a resonance igniter scaled to meet the flowrate requirements of the No. 2 test bed, and (2) a feasibility study of a modified version of the resonance igniter (to be referred to as the Resonant Flow igniter) that would ultimately lead to system simplifications.

The test program was divided into four phases:

1. Geometry optimization
2. Combustion characteristics
3. Oxidizer augmentation
4. Valveless heating

Details pertaining to each of the above phases will be given in the Test Results section of this report.

RESONANCE IGNITER TESTING

A resonance igniter meeting the No. 2 test bed operational requirements was designed, fabricated, and tested. All tests were performed at the Thermodynamics Laboratory of the Los Angeles Division.

The following topics pertaining to the resonance igniter will be discussed: (1) criteria used in establishing the required flowrates, (2) methods used in determining the igniter hardware geometry, (3) the test hardware design features, and (4) test results.

With respect to the Resonant Flow igniter the following subjects will be discussed: (1) description and basis for the concept, (2) hardware design, and (3) test results.

The test facility used was common to both igniter configurations, and a description of this facility is given in Appendix C.

Flowrate Determination

In recent H_2/O_2 thrust chamber investigations (Ref. 7), it was determined that igniter flowrate necessary to light off a thrust chamber was approximately 30 percent of the ignition-stage flowrate of the injector elements immediately adjacent to the igniter gas stream. The above igniter was running at mixture ratios ranging between 0.8 and 1.0. Since the nominal ignition-stage flowrate per segment of the No. 2 test bed is 0.25 lb/sec, and 6 out of the 68 elements in each segment surround the igniter gas port, the total flow per igniter was calculated to be 0.0070 lb/sec. These criteria were verified for the ignition requirements of large rocket engines by a study conducted on J-2S altitude ignition (Appendix A).

Assuming that the resonance igniter will be running at a mixture ratio of 1.0, the hydrogen flowrate (which determines the igniter geometry) was nominally set at 0.0035 lb/sec. Based on system evaluations it was also determined that both the hydrogen and oxygen propellants will be at ambient temperature (530 R) and that a total pressure of 165 psia will be available at the igniter inlets.

Geometrical Scaling Procedure

Operation of the resonance igniter is predicated upon the proper relationship between a number of critical dimensions. These relationships, given in terms of dimensionless ratios, were established in a previous program (Ref. 8) for a resonance igniter having a nominal total flowrate of 0.040 lb/sec. During this program, the following ratios were found for the optimized igniter configuration (see Fig. 13 for nomenclature).

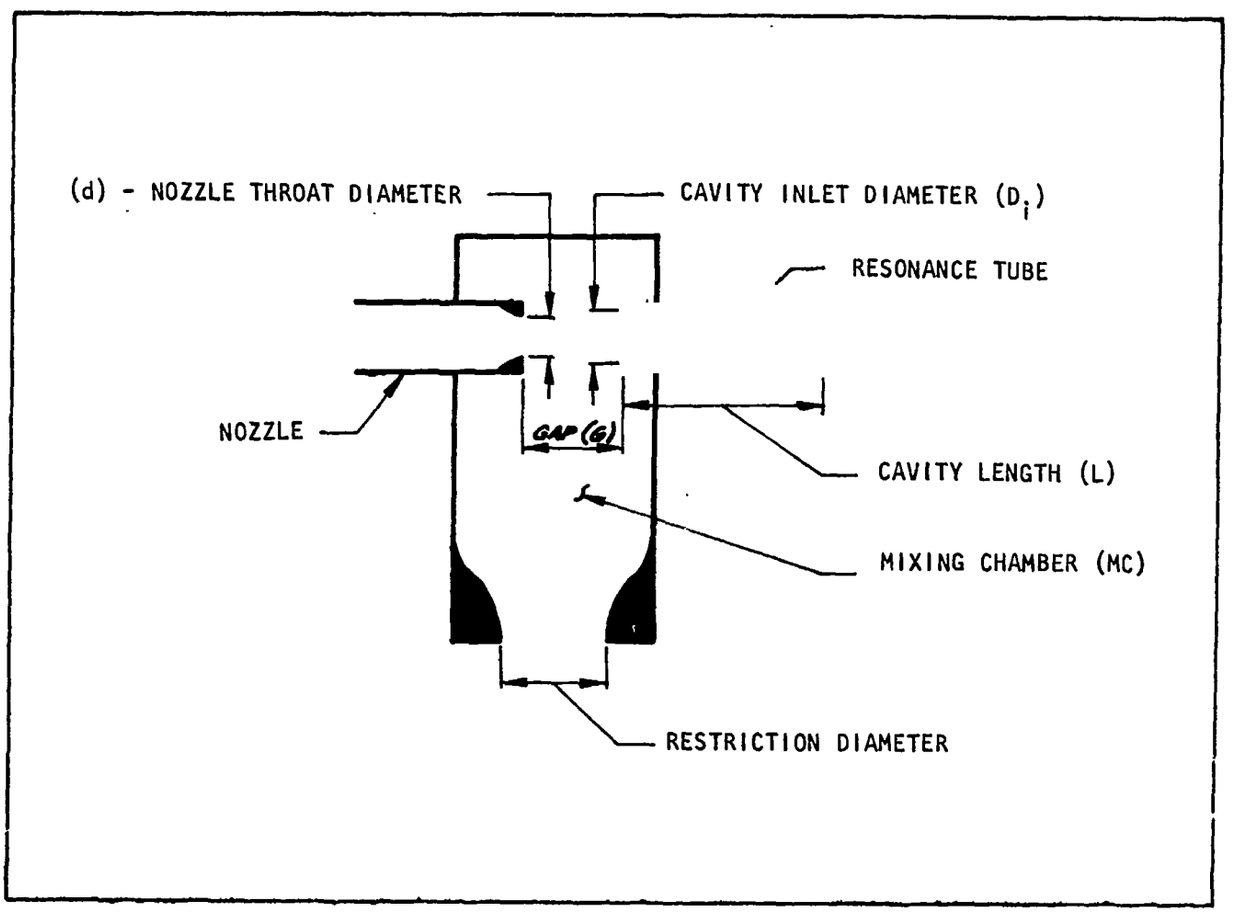

Figure 13. Resonance Igniter Nomenclature

1. Gap to nozzle throat diameter: $G/d = 3.426$

2. Hydrogen inlet total pressure to mixing chamber pressure $P_T/P_{MC} = 5.2$. Note that since sonic flow conditions exist at both the nozzle and at the restriction located at the end of the mixing chamber, the above ratio also determines the area ratio of these two orifices.

3. Resonance tube length to cavity inlet diamter: $L/D_i = 9.6$

4. Cavity inlet diamter to nozzle throat diameter: $D_i/d = 1.3$

All of the above ratios can be dimensionalized by knowing the nozzle throat diameter. For a nominal hydrogen flowrate of 0.0035 lb/sec (total temperature of 530 R and inlet total pressure of 165 psia), the nozzle throat diameter was calculated to be 0.071 inch.

Design Description

The resonance igniter assembly consists of four main components: igniter body, hydrogen inlet nozzle, oxygen inlet resonance cavity, and the throat tube that contains the restriction and allows access to the thrust chamber injector face. The basic hardware shown in Fig. 14 (photograph shown in Fig. 15) was used during the geometry optimization and combustion characteristics test phases. The hardware shown in Fig. 16 was used during the oxidizer augmentation test phase.

Figure 14 shows the assembly of the resonance igniter designed and fabricated specifically for this experimental task. The hardware will handle a nominal total flowrate of 0.0070 lb/sec of hydrogen and oxygen, running at a mixture ratio of 1.0, with the propellants at ambient temperature and total inlet pressure of 165 psia. A detailed description of the design is given in the following paragraphs.

The hydrogen nozzle has a rounded entrance that ends sharply at the sonic throat. A portion of the outer surface of the nozzle end is exposed to combustion gases; however, it is made of Nickel 200 and cooled by the hydrogen flowing through it. The nozzle assembly incorporates spacers for precise setting of the expansion gap,

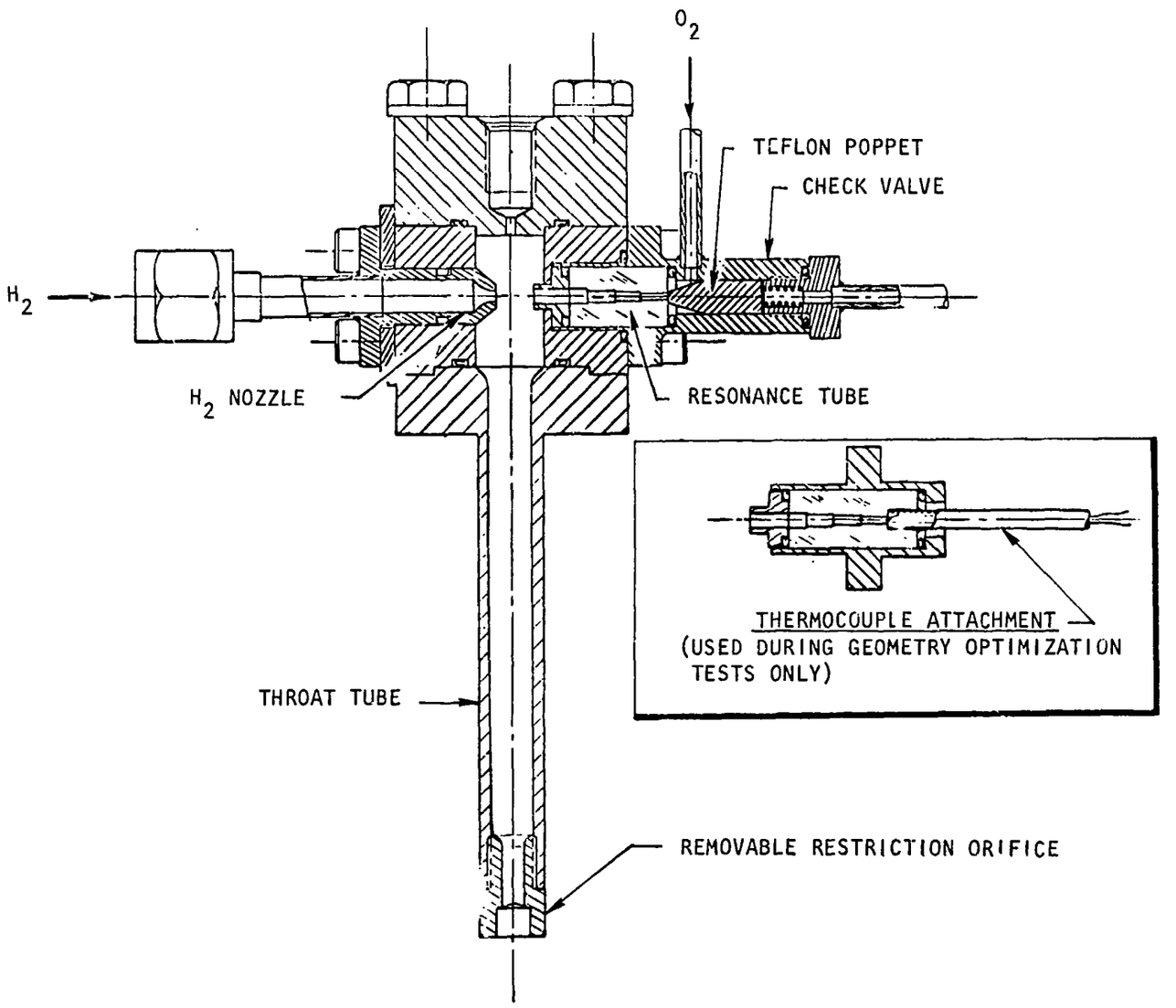

Figure 14. Resonance Igniter Assembly (Used During Geometry Optimization and Combustion Characteristics Tests)

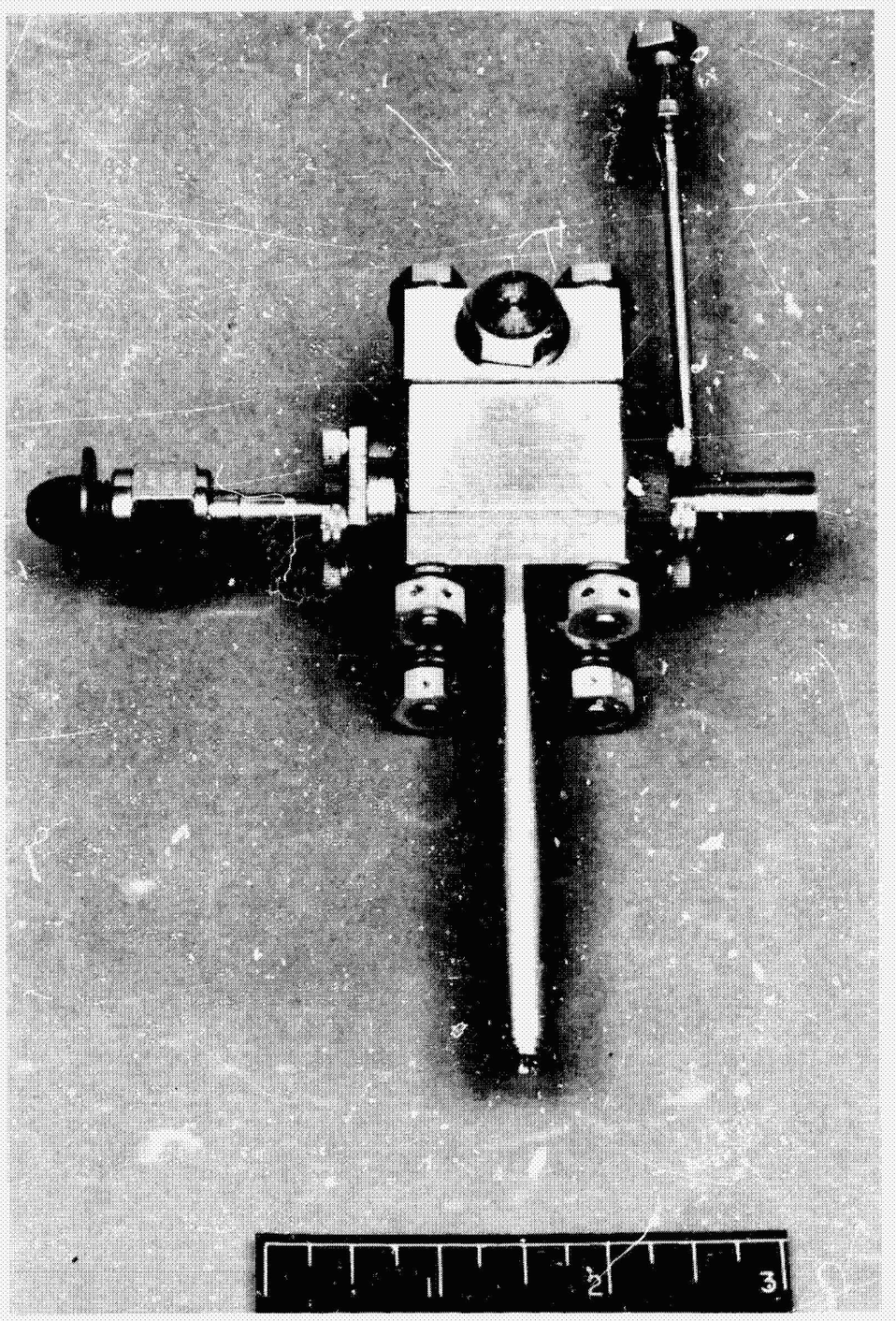

1CT62-3/11/71-C1H

Figure 15. Resonance Igniter Assembly (With Uncooled Throat)

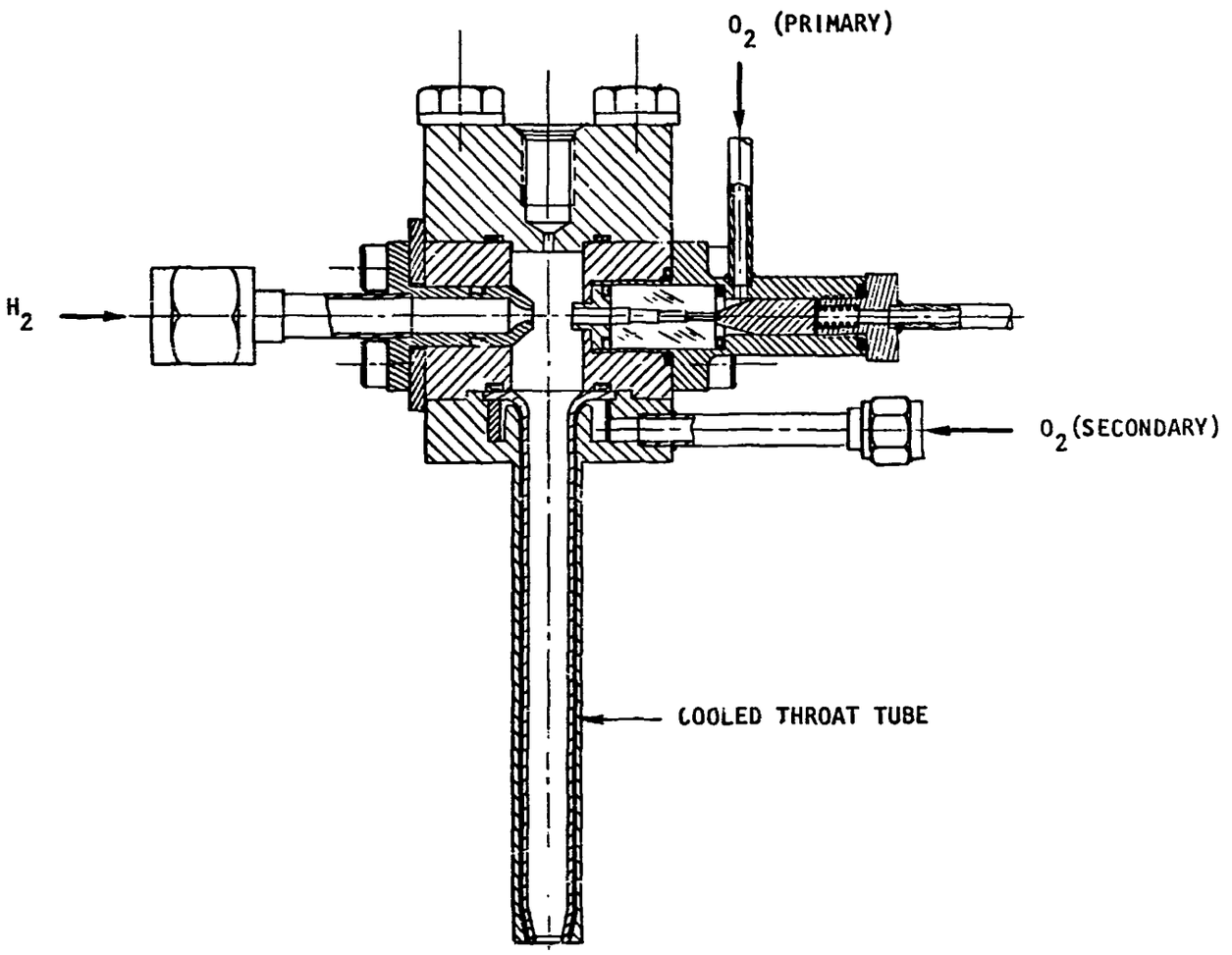

Figure 16. Oxidizer Augmentation Assembly

which permits proper tuning of the resonance phenomena. The nozzle is short coupled to reduce fill time and has straight-through flow to produce a fully developed jet.

Constructed of Nickel 200, the mixing chamber provides flow area away from the resonating jet during the start transient and serves as a combustion mixing chamber during steady-state operation. Flow area around the expanding jet is required to remove the reflected gas without distorting the jet and deflecting it away from the resonance cavity entrance. The mixing chamber diameter has been scaled from the previously tested hardware. The igniter body also serves as the fixture which supports and maintains proper orientation of the other components.

The oxygen inlet and cavity consists of the oxygen-pressure-actuated oxygen valve and the resonance cavity, which is designed and scaled based on previous igniter cavitities. The cavity inlet is Nickel 200 to reduce erosion of the inlet tip.

Located at the small end of the resonance cavity, the igniter oxidizer valve (also referred to as the check valve) was designed as a simple oxygen-pressure-actuated poppet valve. This would allow multiple igniters to be connected in parallel with one main oxygen control valve and thus only one solenoid.

The end face of the resonance cavity formed the valve seat to eliminate any volume between the cavity and the poppet. The poppet, which is cylindrical with a truncated conical end, was machined from Teflon for a close fit with the honed stainless-steel body. The compression spring and end cap-spring carrier were also stainless steel. The end of the spring carrier also served as a poppet stop and secondary seal for the poppet in the open position, and the spring cavity was vented to prevent poppet oscillation. Initial spring compression was set to hold the poppet closed against the hydrogen pressure and to open or close at 40-psi oxygen pressure.

The throat tube contains the hot igniter gases as they flow through the main injector. The initial uncooled throat tube shown is made of 321 CRES and has replaceable throat inserts for quick cold-flow tuning adjustment. After the exact

throat diameter was determined it was designed to be machined in a Nickel 200 insert and welded in place for hot-fire testing. The same throat diameter was machined into a convectively cooled (dump cooled) throat tube which provided oxygen augmentation at the main injector face, thus boosting the mixture ratio from approximately 1 to 3.

Test Results

The test matrix shown in Table 1 included geometry optimization, combustion, oxidizer augmentation, and valveless heating investigations. Test results are discussed in the following paragraphs.

Geometry Optimization. A resonance igniter configuration is considered optimum when the combined settings of all critical dimensions result in the maximum attainable gas temperature in a given period of time. Generally, maximum ignition reliability is achieved with an optimum geometrical configuration.

The geometry optimization test phase involved hydrogen only, measuring the gas temperature at the end of the resonance cavity while parametrically varying the gap distance and the restriction diameter. Throughout these tests the resonance cavity geometry was kept constant. The geometry of the resonance cavity (Fig. 14), was a scaled version of one of the cavities tested in Ref. 8. Among these cavities, the geometry chosen for the present investigation resulted in the highest performance.

Throughout this test series, hydrogen inlet total pressure was maintained at approximately 165 psia, and the inlet total temperature was kept at ambient conditions (520 to 530 R). The hydrogen resonance temperature was measured by means of an exposed-tip chromel-alumel thermocouple, with 3-mil-diameter wires to ensure high response rates. The thermocouple tip was sealed with epoxy near the end of the resonance tube and along the cavity centerline. The resonance tube was fabricated from Lava (aluminum silicate), a material chosen for its low thermal conductivity and ease of machinability.

Table 1. Resonance Igniter Test Program

Test	Variables	Results
Geometry Optimization	Gap distance, restriction diameter, thermocouple at end of resonance cavity (H_2 flow only)	Optimization of geometry (maximum temperature in minimum time)
Combustion Characteristics	Valve sequencing, mixture ratios, propellant inlet pressures (H_2 and O_2 flow)	Ignition and combustion characteristics
Oxidizer Augmentation	Igniter mixture ratios, secondary O_2 flowrate	Ignition limits and combustion characteristics
Valveless Heating	Resonance cavity geometry, gap distance, restriction diameter	Removed hydrogen flowrate and temperature

During initial tests, the restriction diameter of 0.161 inch was fixed, and the gap distance was varied in discrete increments by shimming the hydrogen nozzle. Results of these tests are given in Fig. 17, which shows the hydrogen resonance temperature as a function of gap-to-nozzle diameter ratio. It is seen that the maximum temperature for two time slices (temperature reached after 50 and 100 milliseconds of hydrogen valve opening) is reached with a gap ratio of 3.240. This compares to an optimum gap ratio of 3.426 found in Ref. 8. For this gap setting (G/d = 3.240) and the restriction diameter of 0.161 inch, the corresponding ratio of inlet hydrogen total pressure to mixing chamber pressure (P_T/P_{MC}) was 5.58.

The next series of geometry optimization tests consisted of measuring the gas resonance temperature, keeping the gap distance fixed while varying the restriction diameter hence varying the pressure ratio (P_T/P_{MC}). The gap distance chosen was at the (approximate) optimum gap ratio shown in Fig. 17 (G/d = 3.210). The

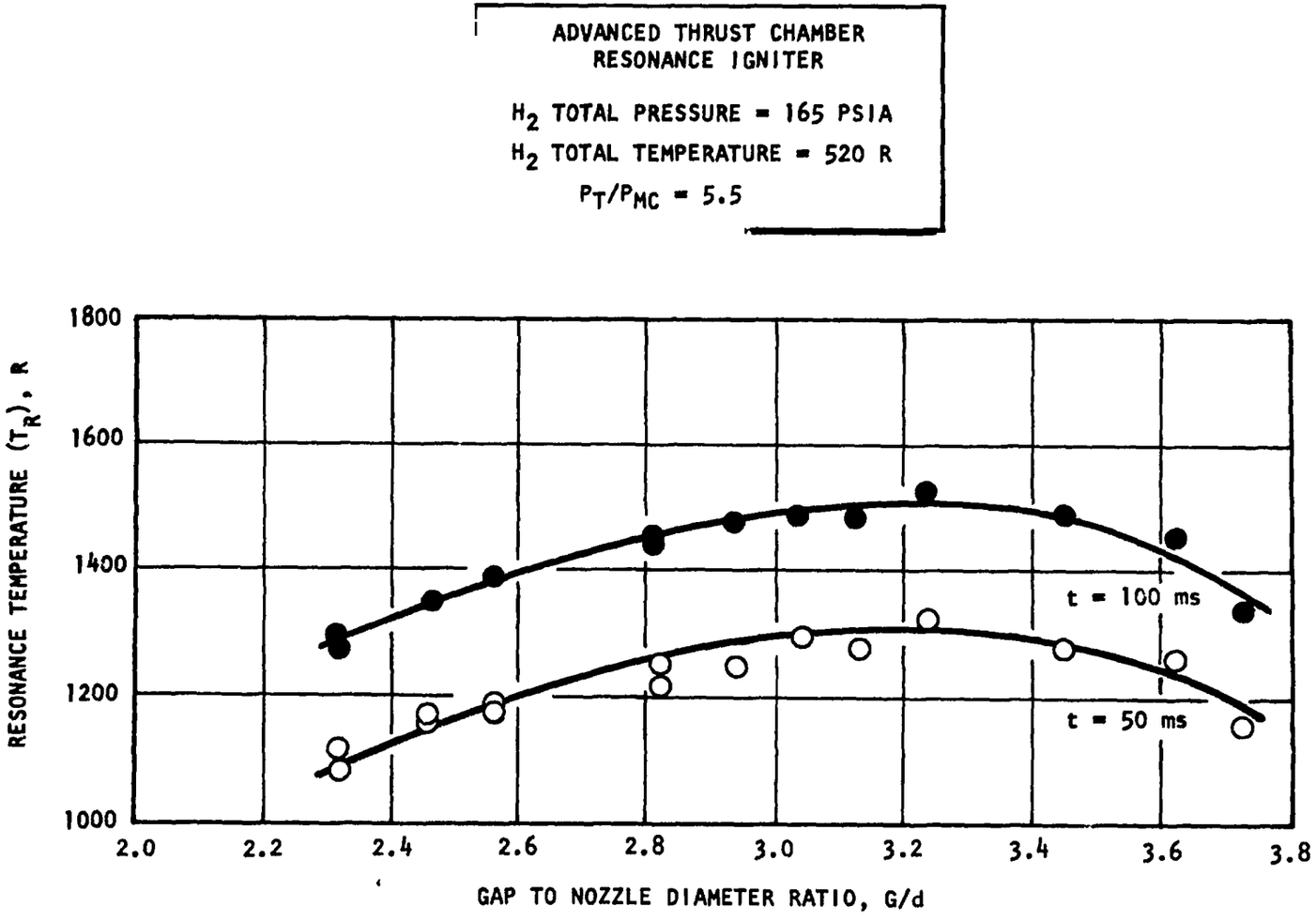

Figure 17. Resonance Temperature vs G/d

results of these tests as shown in Fig. 18 indicate that maximum temperatures were reached when the steady-state pressure ratio (P_T/P_{MC}) was 5.0. This pressure ratio was obtained with a restriction diameter of 0.157 inch.

As a result of the above two test series, the resonance igniter configuration deemed optimum is one which had a gap of 0.228 inch ($G/d = 3.21$) and a restriction diameter of 0.157 ($P_T/P_{MC} = 5.0$). For the above configuration, the time transients for the resonance temperature and mixing chamber pressure are given in Fig. 19. In this figure, time zero is taken as the instant when the inlet hydrogen valve is activated. It should be noted that the temperature-time relation indicated was taken directly from the thermocouple readings and consequently these readings include the lags normally associated in actual transient gas temperature measurements such as bead/wire thermal capacity and heat transfer losses. It is estimated that the actual gas temperatures during the first 20 milliseconds could be twice as high as the measured readings.

It should be reiterated that all of the above tests were conducted with ambient-temperature hydrogen having an inlet total pressure of 165 psia. The last phase of this test series was conducted with the optimum configuration, and the inlet total pressure was varied over a wide range (118 psia$<P_T<$416 psia) and the hydrogen resonance temperature was measured. The results are presented in Fig. 20 for time slices of 50 and 100 milliseconds (time after opening of hydrogen valve). It can be seen that substantial resonance temperature gains can be obtained by running the igniter at the maximum available hydrogen total pressure.

Combustion Characteristics. The main purpose of this test series was to determine the operational characteristics of the resonance igniter when both hydrogen and oxygen are allowed to flow into the device. For all combustion tests the sequence of events was the same: (1) the hydrogen inlet valve (Marotta) was opened, (2) the oxygen valve (Marotta) was opened (forcing the opening of the check valve) 3 to 5 milliseconds after opening of the hydrogen valve, (3) both propellants flowed through the igniter for approximately 200 milliseconds, (4) the oxygen valve was closed, and (5) the hydrogen valve was closed. Occurrences of ignition

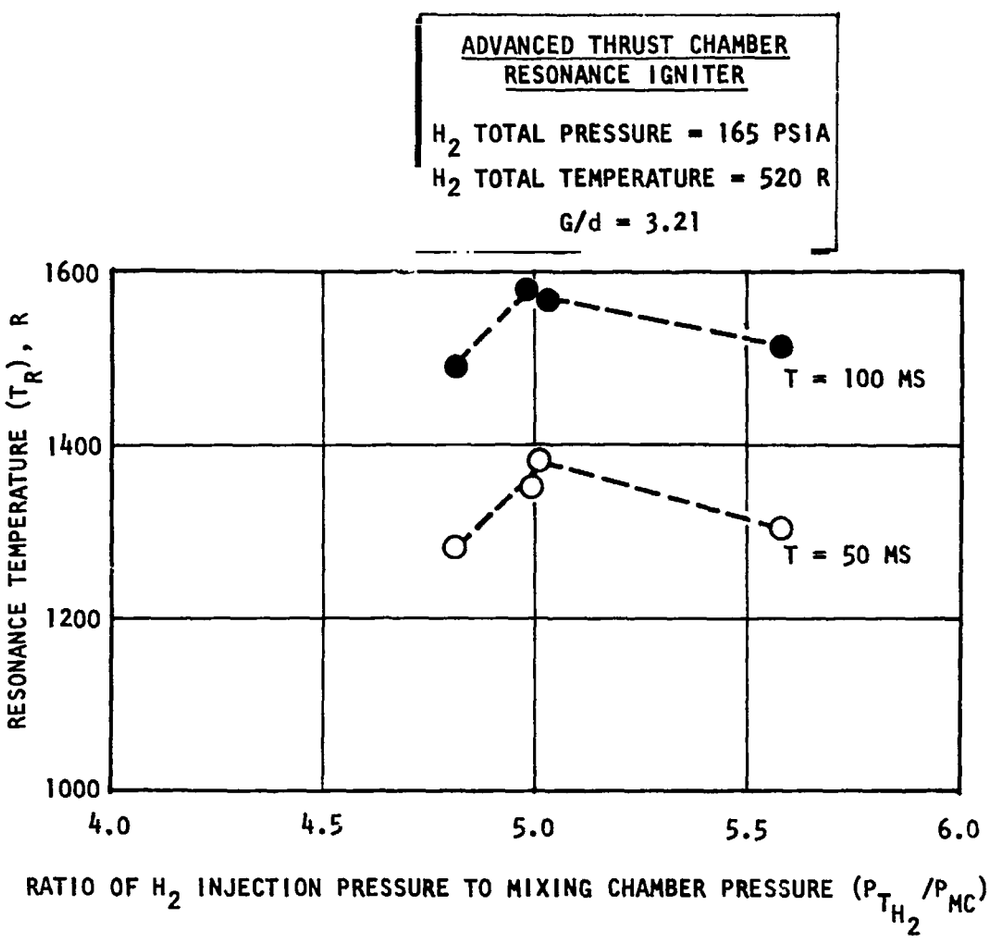

Figure 18. Resonance Temperature vs Pressure Ratio

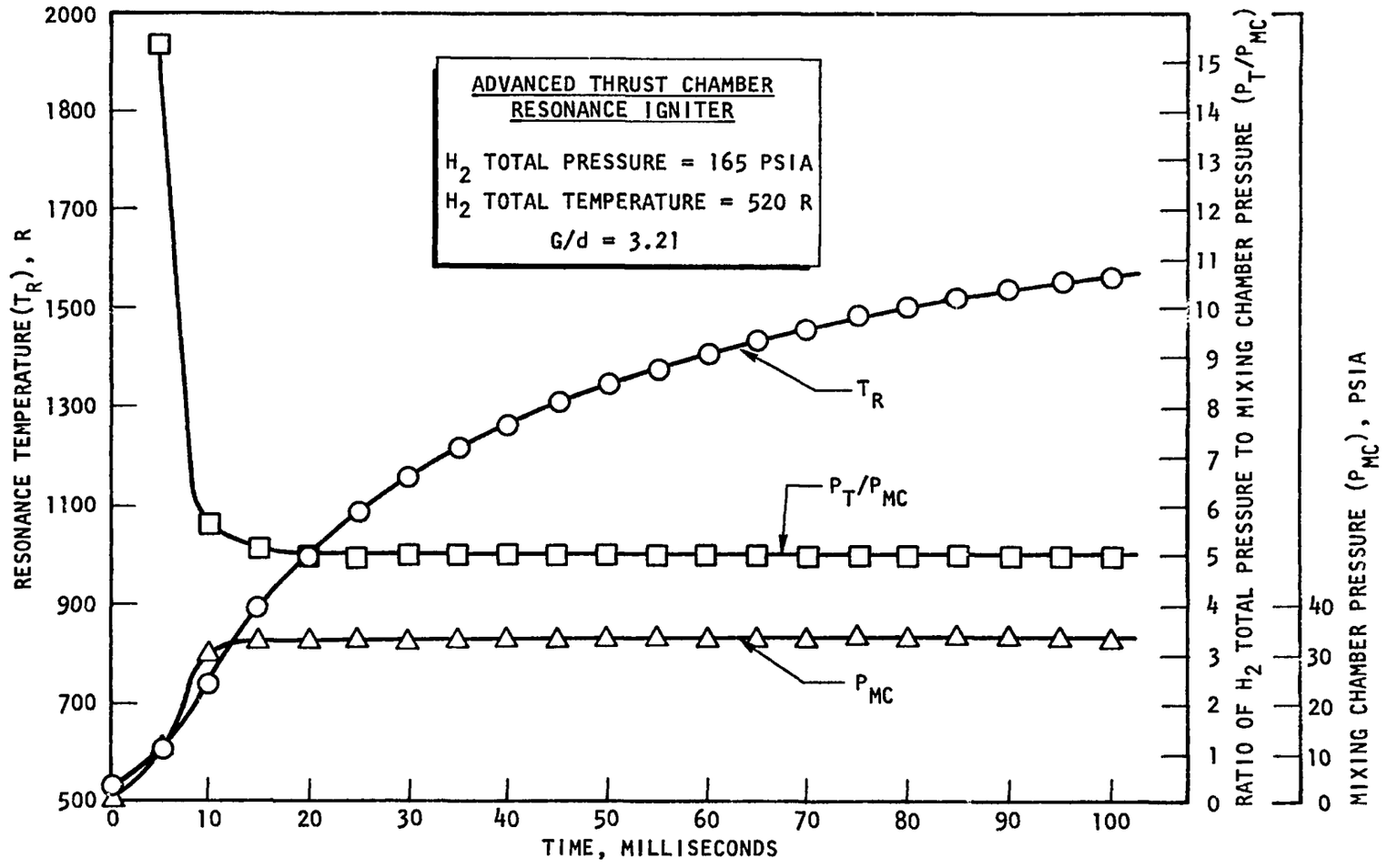

Figure 19. Resonance Temperature vs Time

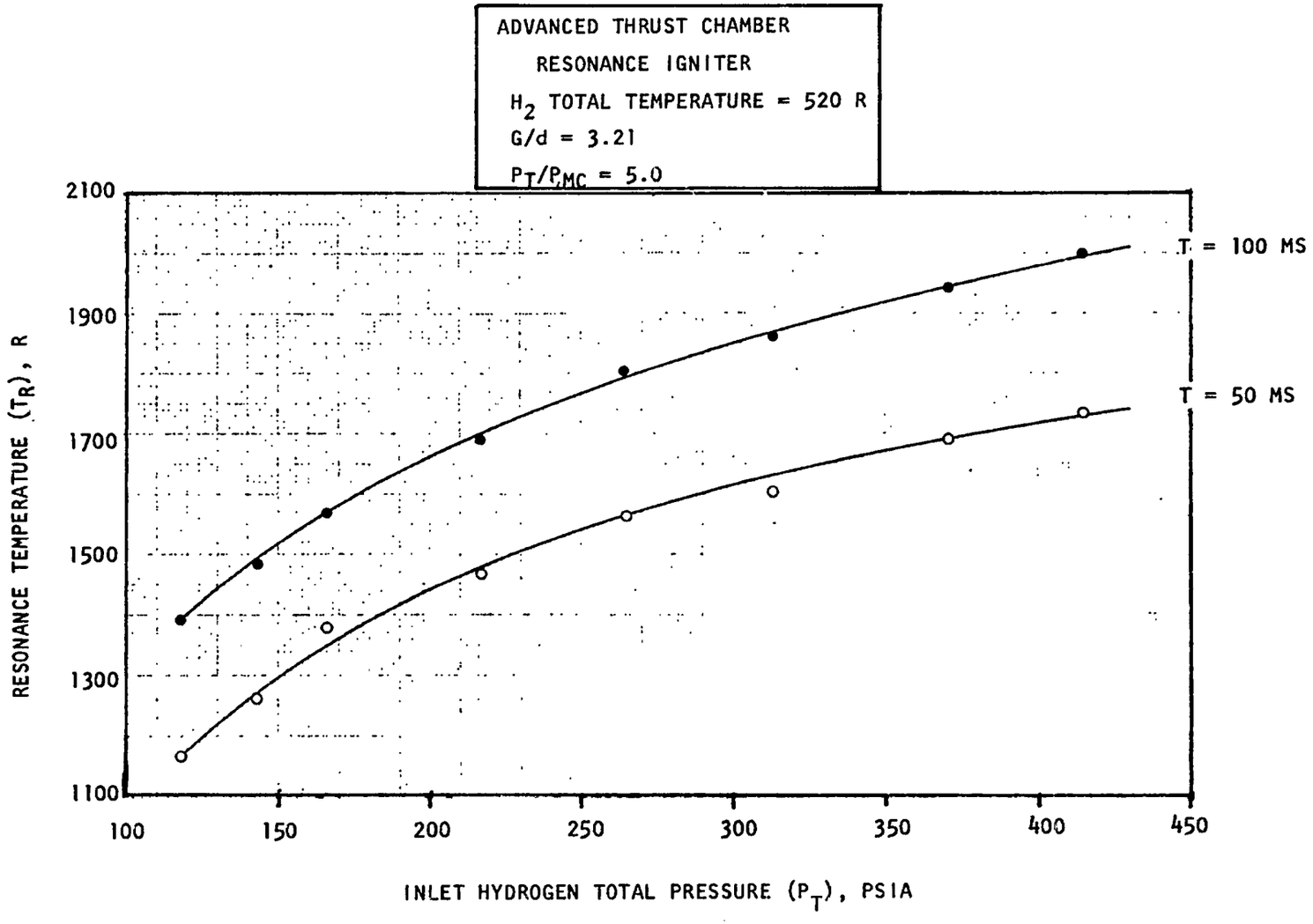

Figure 20. Resonance Temperature vs Total Pressure

and combustion were detected by means of a transducer that measured the mixing chamber pressure. A typical mixing chamber pressure trace showing the sequence of events is shown in Fig. 21.

The initial test series was conducted prior to the geometry optimization tests. Although the test plan reflected the more logical procedure (i.e., geometry optimization followed by combustion characteristics tests), problems of sealing the thermocouples to the resonance cavity forced a delay in the geometry optimization start date. Facility availability and scheduling however did permit testing for combustion characteristics using the igniter configuration with dimensions based on the numbers quoted in the Geometrical Scaling Procedure section of this report (i.e., $G/d = 3.426$, $P_T/P_{MC} = 5.2$).

A total of 87 tests was run with this configuration. The hydrogen inlet total pressure was varied between 145 and 267 psia, and the oxygen inlet total pressure was varied to provide a mixture ratio ($\dot{W}_{O_2}/\dot{W}_{H_2}$) range from 0.48 to 1.20. Table 2 gives a listing of all ignition tests. Figures 22, 23, and 24 show the energy release efficiency (η_{c*}) as a function of mixture ratio for three levels of inlet hydrogen total pressure (165, 210, and 265 psia). Although the data scatter (which may be due in part to check valve leaks) does not permit firm conclusions to be drawn, it appears that the energy release efficiency does increase with increasing propellant feed pressures.

The energy release efficiency is defined as:

$$\eta_{c*} = \frac{c^* \text{ actual}}{c^* \text{ theoretical}}$$

where

$$c^* = \frac{P_c A_t g}{\dot{W}}$$

P_c = mixing chamber stagnation pressure
A_t = restriction geometrical throat area
g = acceleration of gravity
$\dot{W}$ = total flowrate through the igniter

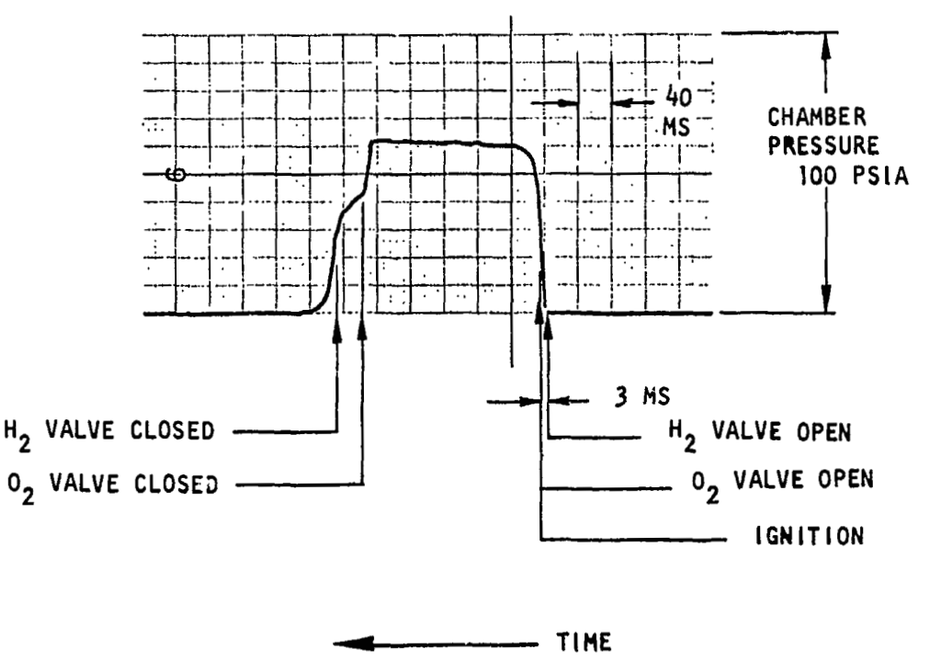

Figure 21. Ignition Trace (Test 2, Table 3)

Table 2. Combustion Characteristics, Nonoptimized Resonance Igniter

Test No.	Total Flowrate, lbm/sec	Mixture Ratio	Ignition Delay* ($\tau_{0.9P_c}$), milliseconds	P_{H_2}, psia	P_{O_2}, psia	Remarks
1	0.0057	0.68	29	154	153	
2	0.0057	0.68	30	152	153	
3	0.0058	0.68	32	157	153	
4	0.0062	0.72	40	158	164	
5	0.0062	0.72	41	157	163	
6	0.0060	0.71	40	156	164	
7	0.0075	1.08	--	156	173	No ignition
8	0.0067	0.81	55	162	174	
9	0.0068	0.94	55	154	174	
10	0.0067	0.86	57	159	174	
11	0.0072	1.00	55	156	181	
12	0.0077	1.20	--	156	179	No ignition
13	0.0071	0.97	49	154	180	
14	0.0071	0.97	60	160	181	
15	0.0074	0.57	44	207	203	
16	0.0074	0.57	50	205	203	
17	0.0073	0.59	48	204	203	
18	0.0082	0.74	51	206	219	
19	0.0082	0.72	43	209	220	
20	0.0081	0.72	35	[illegible]	220	
21	0.0087	0.74	42	217	228	

*Ignition delay includes an 8-millisecond H_2 valve actuation time.

Table 2. (Continued)

Test No.	Total Flowrate, lbm/sec	Mixture Ratio	Ignition Delay* ($\tau_{0.9P_c}$), milliseconds	P_{H_2}, psia	P_{O_2}, psia	Remarks
22	0.0085	0.74	44	215	228	
23	0.0083	0.69	41	215	228	
24	0.0090	0.84	53	215	236	
25	0.0091	0.86	49	215	237	
26	0.0101	1.06	--	216	236	No ignition
27	0.0092	0.88	50	215	237	
28	0.0088	0.49	34	265	251	
29	0.0090	0.53	30	264	251	
30	0.0089	0.51	28	265	252	
31	0.0094	0.59	33	264	266	
32	0.0118	1.00	--	264	265	No ignition
33	0.0094	0.59	33	264	266	
34	0.0118	1.00	--	264	264	No ignition
35	0.0103	0.75	44	264	280	
36	0.0103	0.75	43	264	280	
37	0.0101	0.71	40	266	281	
38	0.0111	0.88	54	264	291	
39	0.0109	0.85	49	266	291	
40	0.0112	0.87	55	265	291	
41	0.0059	0.55	37	168	155	
42	0.0059	0.55	30	168	155	

*Ignition delay includes an 8-millisecond H_2 valve actuation time.

Table 2. (Continued)

Test No.	Total Flowrate, lbm/sec	Mixture Ratio	Ignition Delay* ($\tau_{0.9P_c}$), milliseconds	P_{H_2}, psia	P_{O_2}, psia	Remarks
43	0.0058	0.53	31	167	155	
44	0.0062	0.72	33	160	166	
45	0.0062	0.72	30	158	166	
46	0.0060	0.67	38	161	164	
47	0.0066	0.83	43	161	174	
48	0.0069	0.97	48	155	174	
49	0.0068	1.00	41	152	174	
50	0.0067	0.92	60	154	172	
51	0.0068	1.00	46	152	179	
52	0.0069	0.97	46	157	179	
53	0.0069	0.97	45	156	179	
54	0.0069	1.03	43	153	179	
55	0.0078	0.61	37	210	204	
56	0.0078	0.62	40	210	205	
57	0.0078	0.62	37	210	204	
58	0.0085	0.85	56	198	215	
59	0.0081	0.72	37	205	215	
60	0.0082	0.74	38	205	215	
61	0.0086	0.79	43	211	226	
62	0.0085	0.70	47	217	226	
63	0.0102	1.04	--	217	225	No ignition

*Ignition delay includes an 8-millisecond H_2 valve actuation time.

Table 2. (Continued)

Test No.	Total Flowrate, lbm/sec	Mixture Ratio	Ignition Delay* ($\tau_{0.9P_c}$), milliseconds	P_{H_2}, psia	P_{O_2}, psia	Remarks
64	0.0086	0.72	37	216	226	
65	0.0092	0.88	56	215	236	
66	0.0091	0.82	45	216	236	
67	0.0091	0.86	46	216	236	
68	0.0092	0.82	45	216	236	
69	0.0090	0.50	24	267	253	
70	0.0114	0.87	--	267	251	No ignition
71	0.0091	0.49	27	267	253	
72	0.0096	0.57	30	268	268	
73	0.0096	0.60	34	268	268	
74	0.0095	0.58	34	268	268	
75	0.0101	0.48	38	266	278	
76	0.0101	0.48	38	267	278	
77	0.0101	0.48	34	268	278	
78	0.0111	0.85	50	267	292	
79	0.0111	0.85	49	267	293	
80	0.0112	0.87	50	268	293	
81	0.0059	0.51	31	171	154	
82	0.0060	0.54	33	170	154	
83	0.0060	0.54	33	171	154	
84	0.0060	0.54	32	170	160	

*Ignition delay includes an 8-millisecond H_2 valve actuation time.

Table 2. (Concluded)

Test No.	Total Flowrate, lbm/sec	Mixture Ratio	Ignition Delay* ($\tau_{0.9P_c}$), milliseconds	P_{H_2}, psia	P_{O_2}, psia	Remarks
85	0.0059	0.51	28	170	156	
86	0.0058	0.49	32	170	145	
87	0.0078	1.00	--	169	171	No ignition
88	0.0064	0.64	44	169	172	
89	0.0064	0.64	36	170	172	
90	0.0063	0.62	34	170	172	
91	0.0067	0.72	34	171	180	
92	0.0068	0.74	33	170	180	
93	0.0068	0.74	31	170	181	
94	0.0083	0.66	43	218	226	
95	0.0084	0.68	33	218	227	
96	0.0083	0.66	40	218	227	
97	0.0084	0.68	31	217	227	
98	0.0091	0.54	27	264	254	
99	0.0090	0.50	28	270	255	
100	0.0091	0.49	25	270	255	
101	0.0091	0.49	25	270	255	

*Ignition delay includes an 8-millisecond H_2 valve actuation time.

Table 3. Combustion Characteristics, Optimized Resonance Igniter

Test No.	Total Flowrate, lb_m/sec	Mixture Ratio	Ignition Delay ($\tau_{0.9P_c}$), milliseconds	P_{H_2} psia	P_{O_2}, psia	Remarks
1	0.0057	0.58	54	160	160	
2	0.0060	0.67	43	160	169	
3	0.0065	0.78	60	160	176	
4	0.0069	0.92	47	160	184	
5	0.0057	0.58	50	157	156	
6	0.0061	0.74	44	155	166	
7	0.0067	0.91	47	152	174	
8	0.0069	1.03	43	152	180	
9	0.0065	0.91	39	153	172	
10	0.0064	0.94	40	152	172	
11	0.0064	0.94	36	153	172	
12	0.0063	0.91	28	152	172	
13	0.0064	0.94	30	152	172	
14	0.0063	0.91	27	152	171	
15	0.0067	1.03	26	151	178	
16	0.0064	0.94	28	152	173	
17	0.0064	0.94	26	152	173	
18	0.0056	0.81	23	138	148	
19	0.0055	0.83	37	137	147	
20	0.0055	0.77	33	139	147	
21	0.0062	1.00	35	136	158	
22	0.0060	0.94	36	133	151	
23	0.0063	1.03	28	134	158	
24	0.0062	1.00	29	135	157	
25	0.0106	1.00	28	235	279	

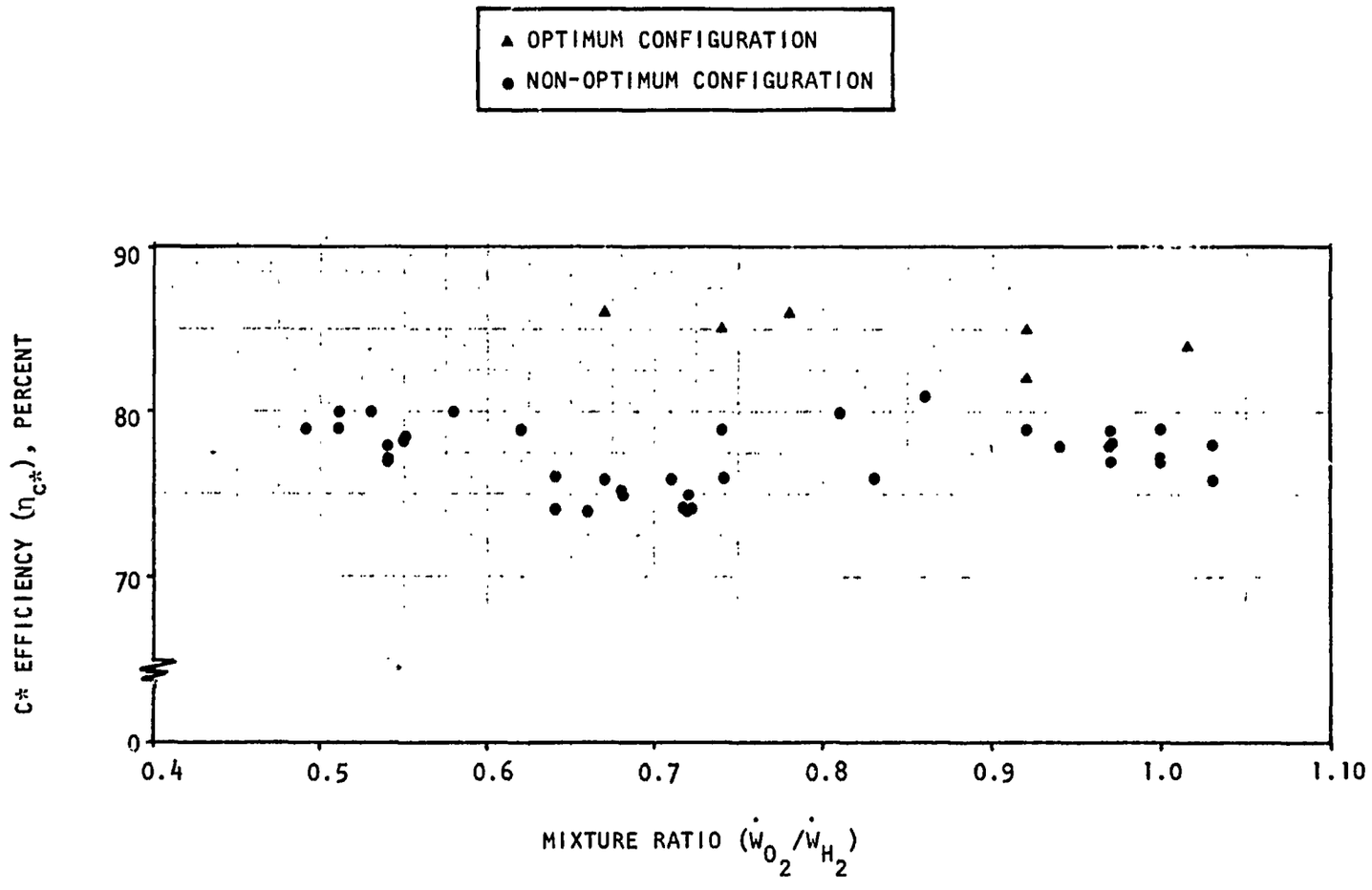

Figure 22. c* Efficiency vs Mixture Ratio (at H_2 Total Pressure ~ 165 psia)

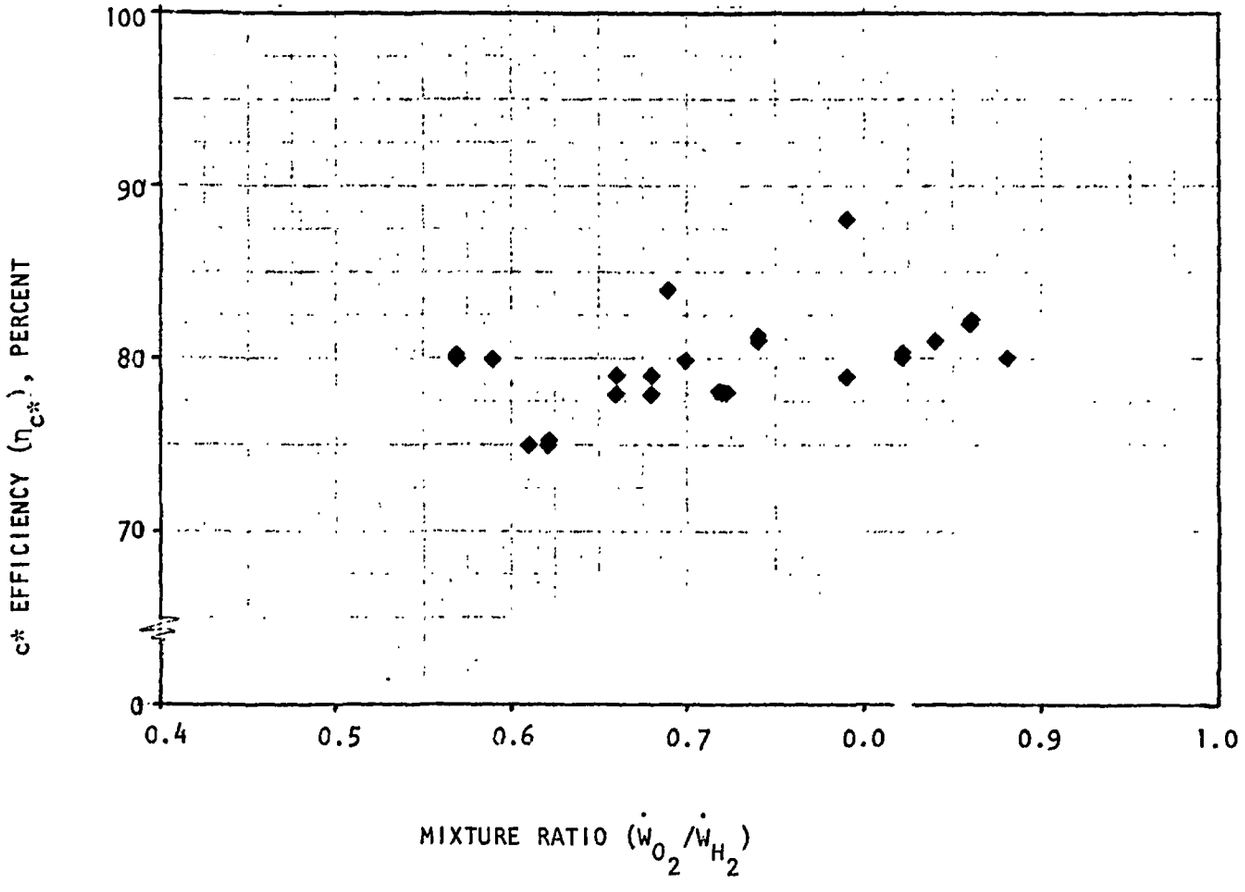

Figure 23. c* Efficiency vs Mixture Ratio (at H_2 Total Pressure ~ 210 psia)

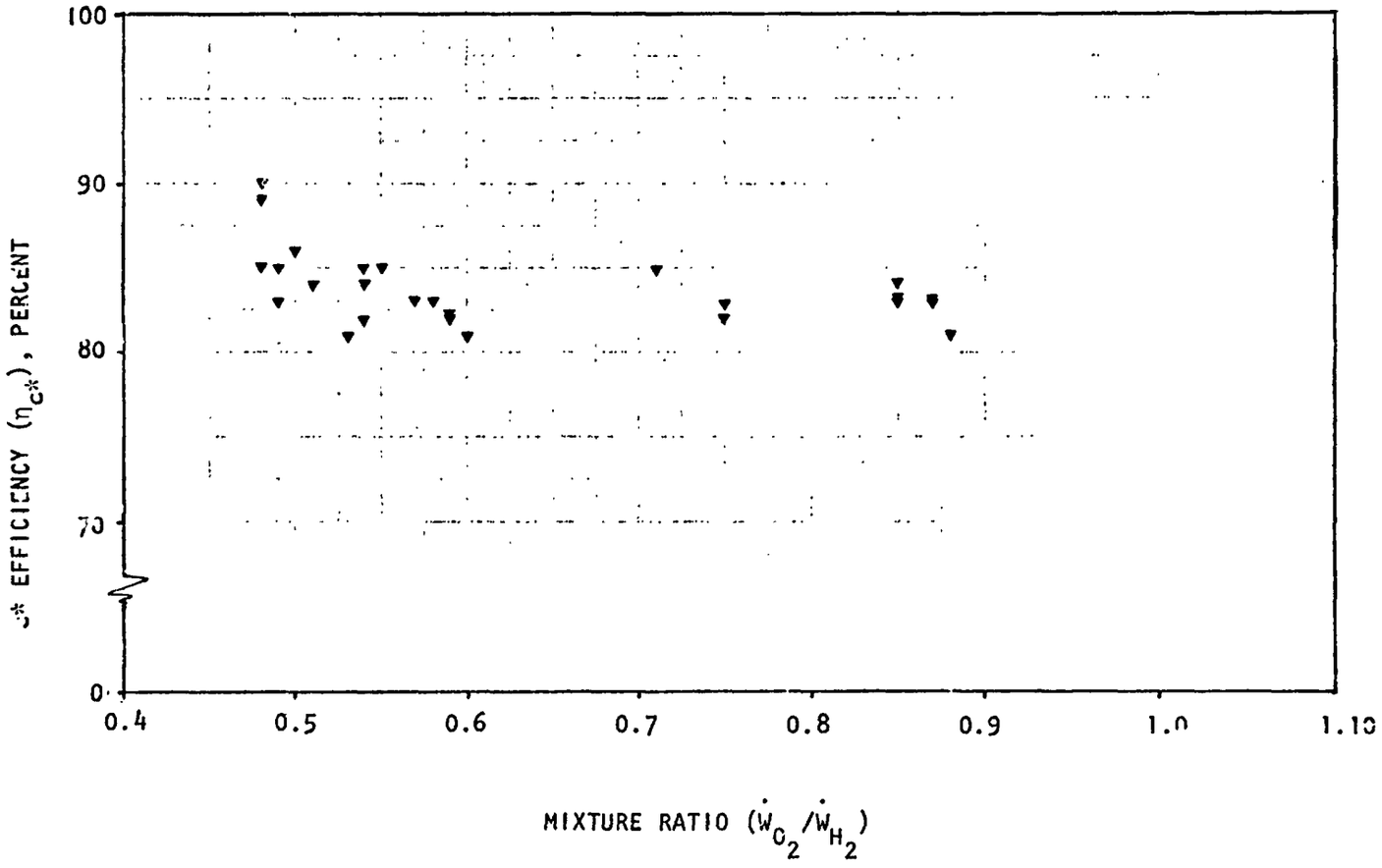

Figure 24. c* Efficiency vs Mixture Ratio (at H_2 Total Pressure ~ 265 psia)

From Table 2 it can be seen that 79 out of the 87 tests resulted in ignition. The reasons for the eight no-ignition cases may be attributed to the following factors: (1) the resonance igniter configuration was not optimized, and (2) during the tests a small flowrate leak was observed at the back-end of the check valve. Taken individually, both factors will cause a decrease in the resonance temperature of hydrogen, although the latter of the two factors mentioned is probably the more serious in that small amounts of gas removed from the end of the resonance cavity will cause a substantial reduction in temperature (see Valveless Heating section of this report).

Upon completion of this test series, the geometry optimization task was undertaken. During this time the check valve was refurbished (scratches on the Teflon pintle had most likely caused the leakage problem). Combustion characteristics testing was resumed with the refurbished check valve and with the igniter having the optimized configuration. All subsequent hydrogen/oxygen tests resulted in ignition and sustained combustion. A listing of test series with the geometrically optimum hardware is given in Table 3. In the first eight tests in this series there was no noticeable propellant leakage and the improved energy release efficiencies are reflected in Fig. 22. The other tests (No. 9 through 25) did have a gradual increase in the leakage rate which again resulted in lowered energy release efficiencies.

The reliability of the check valve proved to be inadequate for a system incorporating 10 parallel ignition devices, and prompted the investigation of the valveless resonant igniter discussed under Resonant Flow Experiments.

In addition to the above tests a series of 21 pulses was made (igniter firings in rapid succession with approximately 500-milliseconds intervals), with all pulses resulting in ignition and sustained combustion. These pulse data were recorded on the Brush traces but not on the Astro Data tape. Both hydrogen and oxygen inlet total pressures were maintained at 115 and 165 psia, respectively.

To summarize, 147 tests were made with both a nonoptimized and an optimized resonance igniter configuration. All except eight of the tests resulted in

ignition and sustained combustion. The major cause for the no-ignition cases could be traced to gas leakage in the oxidizer check valve.

Oxygen Augmentation. Data obtained during thrustor experiments (Ref. 7) with spark and catalytic igniters have indicated that igniter (torch) temperatures greater than 2000 R were desirable for reliable ignition of H_2/O_2 combustors. Also, if the igniter were to be used ultimately without separate valving (i.e., igniter firing duration equal to main chamber firing duration), some form of igniter cooling would be required.

To achieve both objectives, cooling and temperature increase of igniter gases, tests 1 through 32 (listed in Table 4) were run with oxygen and hydrogen through the igniter, and with oxygen passing through the external cooling circuit and dumped out at the exit plane of the throat tube assembly through an annular orifice (see Fig. 16). The dumped oxygen was directed into the ignited low mixture ratio (referred to in Table 4 as primary mixture ratio) gases and resulted in higher overall mixture ratio combustion. To prevent sudden expansion of the gases as they flowed from the igniter into the vacuum chamber, a 9-inch-long, 1/2-inch-diameter pipe was welded onto the plane interfacing the igniter and the vacuum chamber. This open-ended pipe also provided for the support of a thermocouple (10-mil wires, chromel-alumel, shielded tip) located 6 inches from the igniter exit plane. The thermocouple permitted ignition and combustion occurrences to be monitored. Test runs were approximately 200 milliseconds long and only transient temperature readings were obtained.

Propellant flowrates into the igniter were monitored by controlling the inlet pressures. A bypass (which included a flow-metering orifice) in the oxygen feed line provided secondary flow into the cooling circuit. Consequently, both the oxygen flowing into the resonance cavity and into the cooling circuit had equal inlet total pressures. The relationship between the primary and overall mixture ratios is shown in Fig. 25.

Table 4. Oxidizer Augmentation Results

Test No.	Total (Primary) Flowrate, lb_m/sec	Mixture Ratio (Primary)	Mixture Ratio (Overall	Delay ($\tau_{0.9P_c}$), milliseconds	P_{H_2} psia	P_{O_2} psia	Remarks
1	0.0056	1.00	--	34	130	147	No augmentation flow
2	0.0056	0.93	2.76	38	132	147	Ignition of primary flow but no combustion of secondary oxidizer
3	0.0056	0.92	2.76	29	132	147	↓
4	0.0064	1.21	--	32	134	166	No augmentation flow
5	0.0064	1.21	3.28	31	132	166	Ignition of primary flow but no combustion of secondary oxidizer
6	0.0068	1.34	--	36	133	176	No augmentation flow
7	0.0067	1.31	3.55	37	133	176	
8	0.0067	1.31	3.52	33	132	175	
9	0.0067	1.31	--	30	132	175	No augmentation flow
10	0.007	1.29	--	30	137	184	No augmentation flow
11	0.0070	1.33	3.60	30	137	184	
12	0.0070	1.33	3.60	34	137	184	
13	0.0070	1.33	3.60	28	138	184	
14	0.0080	0.90	--	33	192	216	No augmentation flow
15	0.0080	0.90	2.86	29	192	215	Ignition of primary flow but no combustion of secondary oxidizer

Table 4. (Concluded)

Test No.	Total (Primary) Flowrate, lb_m/sec	Mixture Ratio (Primary)	Mixture Ratio (Overall)	Delay ($\tau_{0.9P_c}$), milliseconds	P_{H_2} psia	P_{O_2} psia	Remarks
16	0.0086	1.05	3.14	31	191	229	Ignition of primary flow but no combustion of secondary oxidizer
17	0.0092	1.19	3.43	28	191	240	↓
18	0.0096	1.29	3.62	28	192	252	
19	0.0096	1.29	3.64	31	192	253	
20	0.0096	1.29	3.64	31	192	253	
21	0.0084	0.60	--	28	240	242	No augmentation flow
22	0.0085	0.58	2.34	22	240	241	Ignition of primary flow but no combustion of secondary oxidizer
23	0.0093	0.72	2.59	33	244	260	↓
24	0.0105	0.98	3.04	28	240	268	
25	0.0112	1.11	3.36	26	242	297	
26	0.0118	1.23	3.58	34	242	310	
27	0.0118	1.23	3.58	34	242	310	
28	0.0117	1.21	3.57	31	243	310	
29	0.0069	1.46	3.93	31	130	185	
30	0.0071	154	4.18	37	132	195	
31	0.0073	1.61	4.39	35	130	196	
32	0.0077	1.66	4.48	36	135	215	

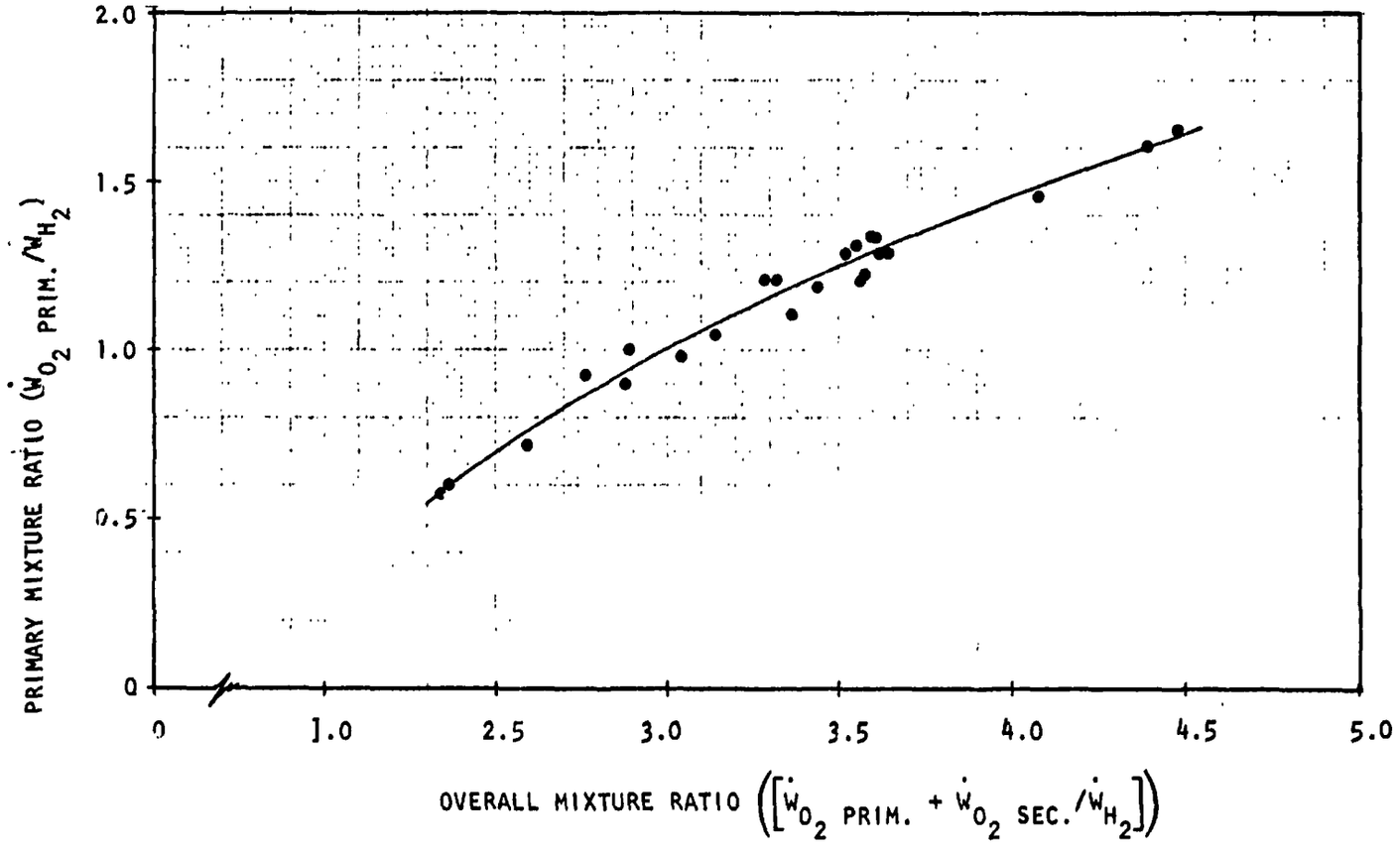

Figure 25. Primary Mixture Ratio vs Overall MIxture Ratio (Oxidizer Augmentation)

All tests run during this phase of the program resulted in ignition of the primary mixtures. During the test series the lower limit of the primary mixture ratios necessary to ignite the secondary oxidizer flow was established. Figure 26 shows all of the oxygen augmentation test points, with the open symbols representing tests in which the overall mixture ignited, and the closed symbol representing test where only the primary mixture ignited (numbers adjacent to the symbols giving the number of tests at each condition). Figure 26 indicates that for three levels of hydrogen inlet total pressures (130, 190, and 240 psia) the ignition limit for the secondary oxygen actually caused a cooling of the primary igniter gases. Hence, to ensure gas temperature augmentation, the igniter primary mixture ratio should be above 1.3. It should be pointed out that this ignition limit could be lowered by modifying the secondary flow injection pattern at the exit plane (i.e., discrete injection ports and steeper injection angle to increase mixing rate).

RESONANT FLOW EXPERIMENTS

Valveless Heating.

In previous sections of the report it was indicated that gas leakage problems arose as a result of the presence of the check valve. In the following paragraphs a method of eliminating the check valve will be discussed. Basically, the concept involves the extraction of high-temperature hydrogen from the end of the resonance cavity. Oxygen is then allowed to impinge on the hydrogen causing ignition of the two streams. Figure 27 shows a design of a valveless resonance igniter where the extracted hydrogen essentially serves as an ignition pilot for all of the propellant gases passing through the igniter hardware. This Resonant Flow igniter has no moving parts, and would lead to simple engine firing operational procedures.

The extraction of hot gases from the resonance cavity was first investigated by Sprenger (Ref. 9) in an attempt to understand the physics of gas temperature separation in the Ranque-Hilsch tube. Reference 9 indicated that starting with air at ambient temperature (530 R) and 70 psia, the air temperature reached 780 R when approximately 3 percent of the total mass flow was removed from a straight tube resonance configuration. The maximum temperature achieved in this configuration was 1260 R as measured at the end of the close-ended cavity (i.e., no gas removed).

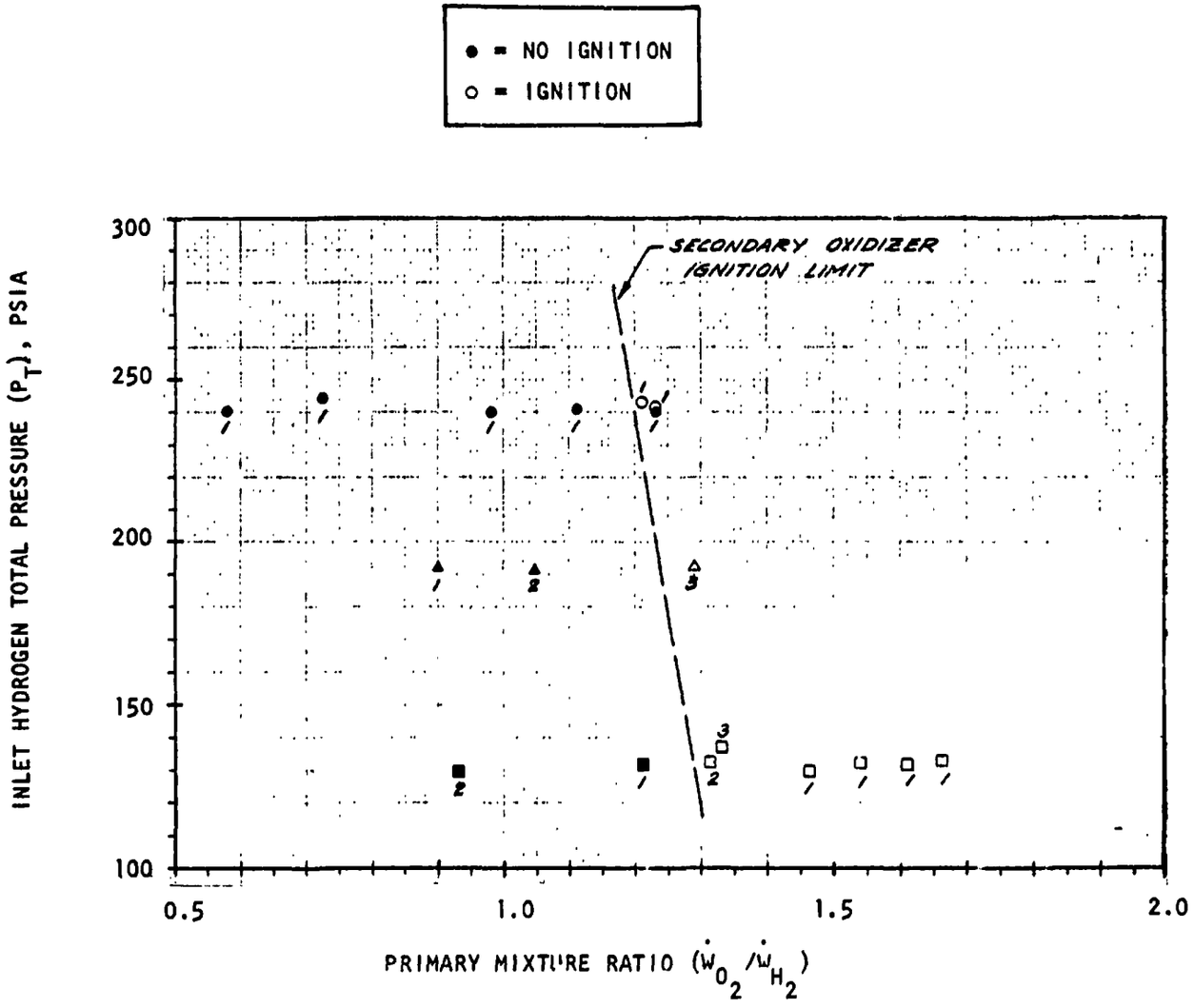

Figure 26. Oxidizer Augmentation Ignition Limits

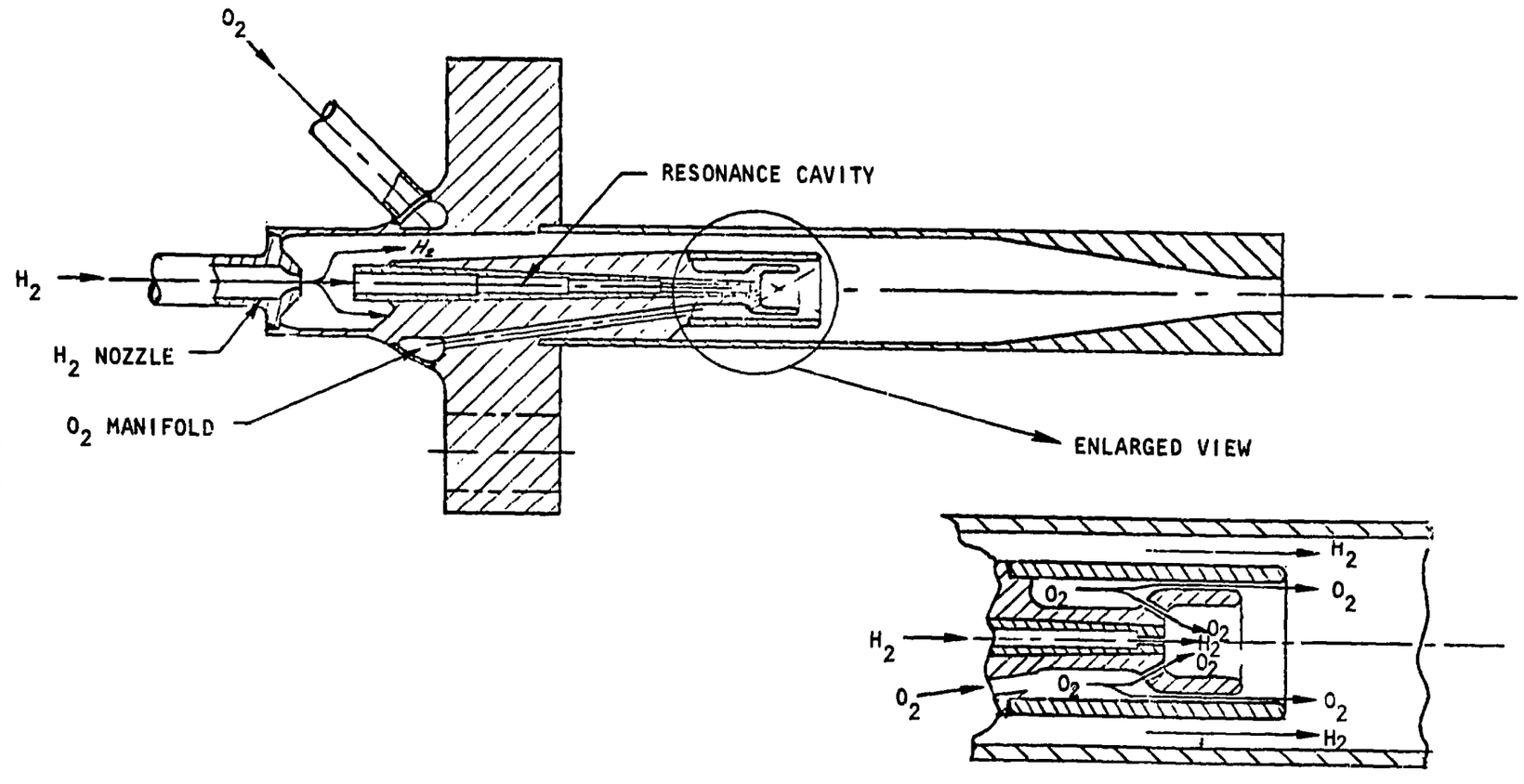

Figure 27. Resonant Flow Igniter Design

Test Hardware Description

During a recently completed experimental program conducted under a NASA-LeRC contract (Ref. 9), a variable-geometry device was developed to study the phenomena and parameters that affect the performance of the resonance igniter. The variable-geometry phenomena hardware, which is equipped with a thermocouple attachment as required during gas heating test, is shown in Fig. 28. The same hardware, with minor modifications, was used during the present program (NASA approval was obtained prior to testing). The modifications were made to permit hot-gas extraction and placement of instrumentation for temperature and pressure measurements. As shown in Fig. 28, the end of the resonance tube was capped with a stainless-steel disk which contained a small-diameter hole to allow hot-gas extraction (a series of these capping disks with varying hole sizes were used to vary the flowrate). A total temperature probe was placed along the resonance tube axis approximately 1/4 inch away from the extraction orifice. The removed gases flowed into a plenum chamber created by a second orifice located downstream of the resonance tube capping disk. By measuring the pressure and temperature in the plenum and knowing the area of the second orifice, the removed gas flowrates were calculated. A series of 5 stepped-tapered resonance cavities of different lengths were tested (Fig. 29). The test entailed variations of extraction flowrates, gap distances, and mixing chamber pressures. For all tests, the inlet hydrogen total pressure was maintained at approximately 200 psia, and the inlet hydrogen total temperature was held at 520 R.

Test Results

For each resonance cavity the same test procedure was followed: (1) the gap was at a known fixed distance, (2) an orificed capping disk was placed at the end of the resonance tube, (3) the hydrogen inlet valve was activated, and (4) the mixing chamber pressure was modulated by remote control of an hydraulically activated valve (Annin). As the hydrogen was flowing, the modulation of the mixing chamber pressure caused temperature variations in the hydrogen flowing through the orificed capping disk. The temperature variation, with the corresponding mixing chamber pressure changes were observed on a Brush recorder. When the removed gas temperature reached a maximum, the pertinent flow parameters were recorded on the digital

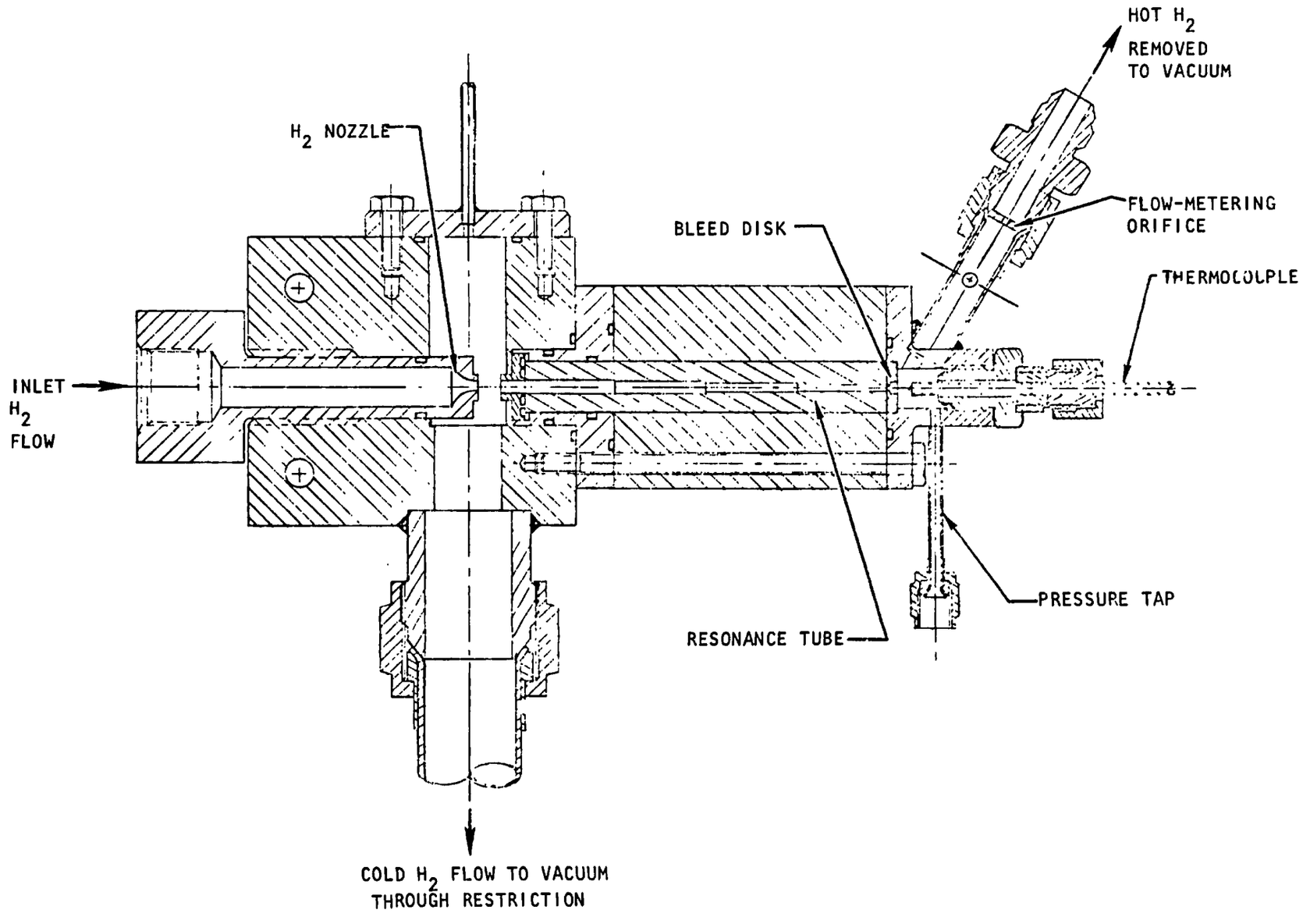

Figure 28. Resonant Flow Test Hardware

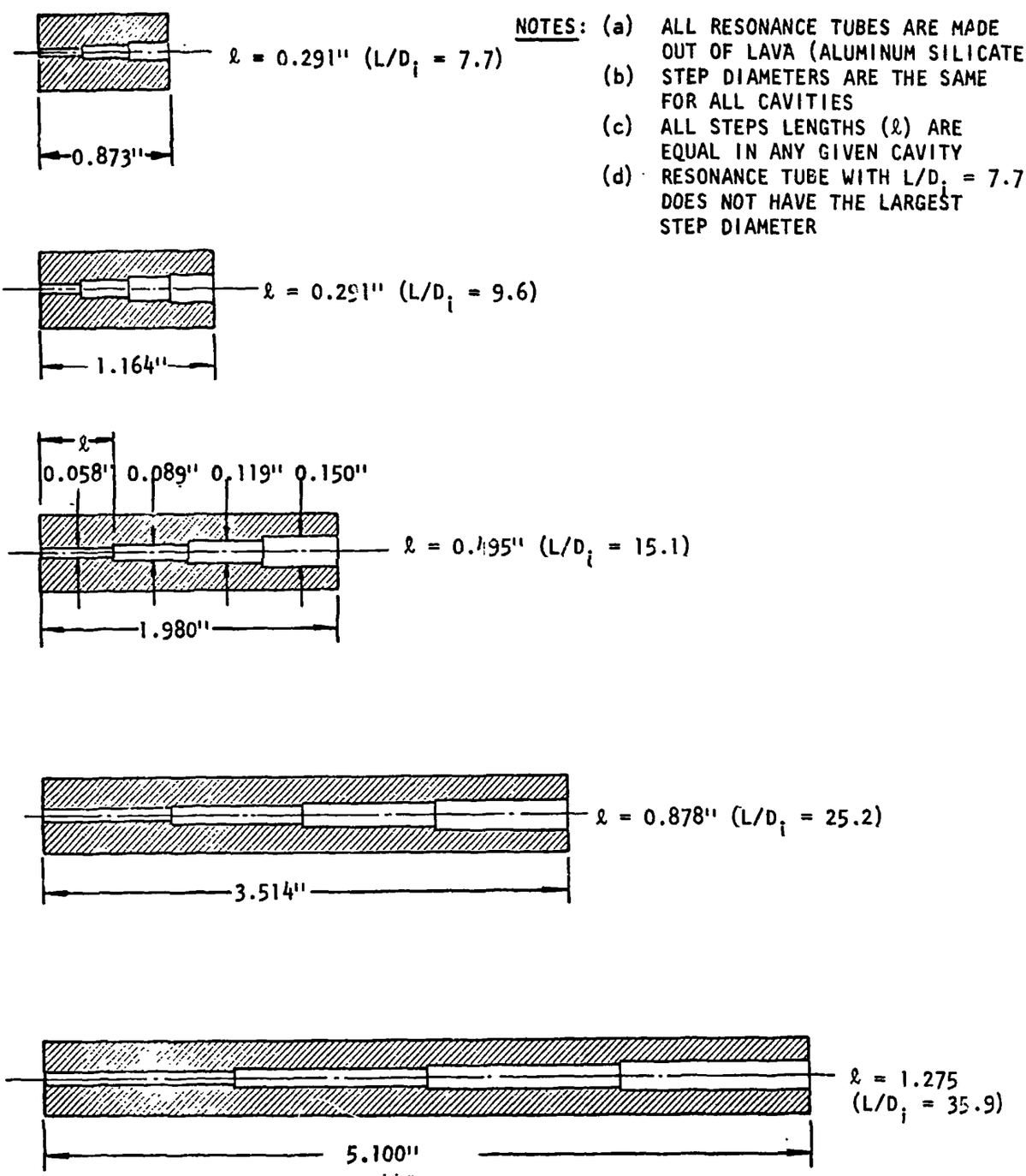

Figure 29. Resonance Tube Configurations

system (Astro Data). The above procedure was repeated for an incremental change in the gap setting. When all the extreme limits of the gap distance were reached, a new test series was initiated with another capping disk having a different orifice diameter

Typical test results are shown in Fig. 30, 31, and 32 for the 3.514-inch-long (L/D = 25.2) resonance tube (see Fig. 29). For three different capping disk orifice diameters, Fig. 30 shows the removed gas temperature as a function of the ratio of gap distance to resonance cavity orifice diameter (G/d). Figure 31 shows the corresponding ratio of hydrogen inlet total pressure to mixing chamber pressure, again as a function of (G/d). Figure 32 shows the calculated removed gas flowrate, given here as a percentage of the total hydrogen flow through the sonic nozzle. The major reason for the decreasing flowrate of the removed gas, as the gap distance is increased, follows an expected trend based on the physics of the resonance phenomenon. As the gap distance increases, the pressure in the mixing chamber (necessary to achieve maximum temperature of the removed gases) decreases (Fig. 31). A constant hydrogen inlet total pressure and a decreasing mixing chamber pressure results in a higher free jet plume expansion, hence a higher Mach number upstream of the normal shock associated with higher Mach number flows results in increasing downstream loss in total pressure. Hence the resonance cavity "sees" a lower hydrogen total pressure with increasing gap distance resulting in decreasing flow through a fixed orifice located at the end of the resonance cavity.

A summary of the test results obtained with all of the resonance cavity configurations is given in Fig. 33. The removed gas temperature is shown as a function of the removed hot hydrogen flowrate (given as a percentage of the total hydrogen flowrate into the variable geometry hardware) for various resonance cavity configurations. Temperatures up to 1780 R were reached with the resonance cavity having an L/D of 25.2. It should be noted that the L/D quoted in Fig. 33 is the ratio of resonance cavity length (including the fixed stainless-steel inlet length) to maximum cavity diameter. Because it is generally recognized that temperatures near 1460 R will lead to ignition of gaseous hydrogen and oxygen propellants, the present investigation indicates the feasibility of the gas removal concept as an igniter which will eliminate the need for the oxidizer valve and thus considerably simplify the resonance igniter hardware.

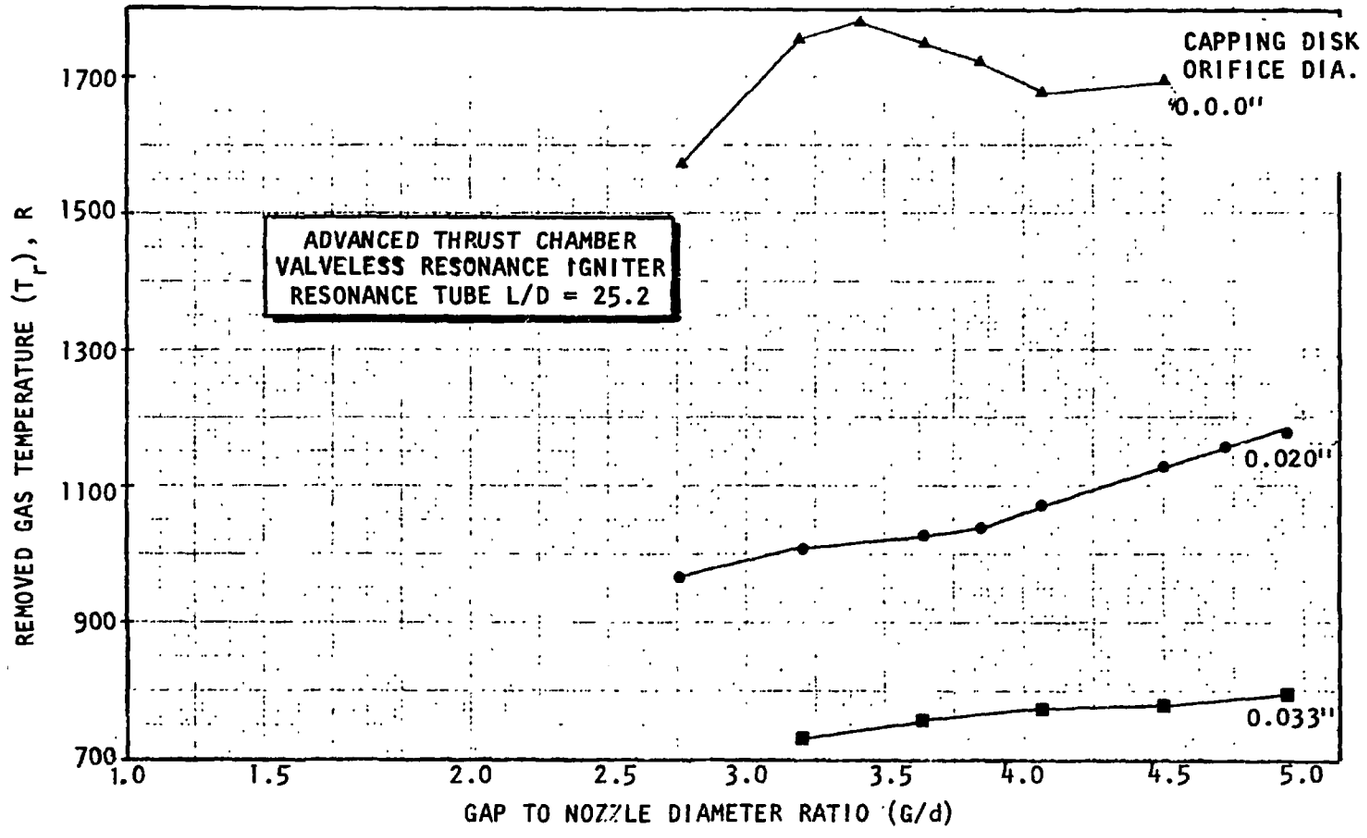

Figure 30. Removed Gas Temperature vs G/d

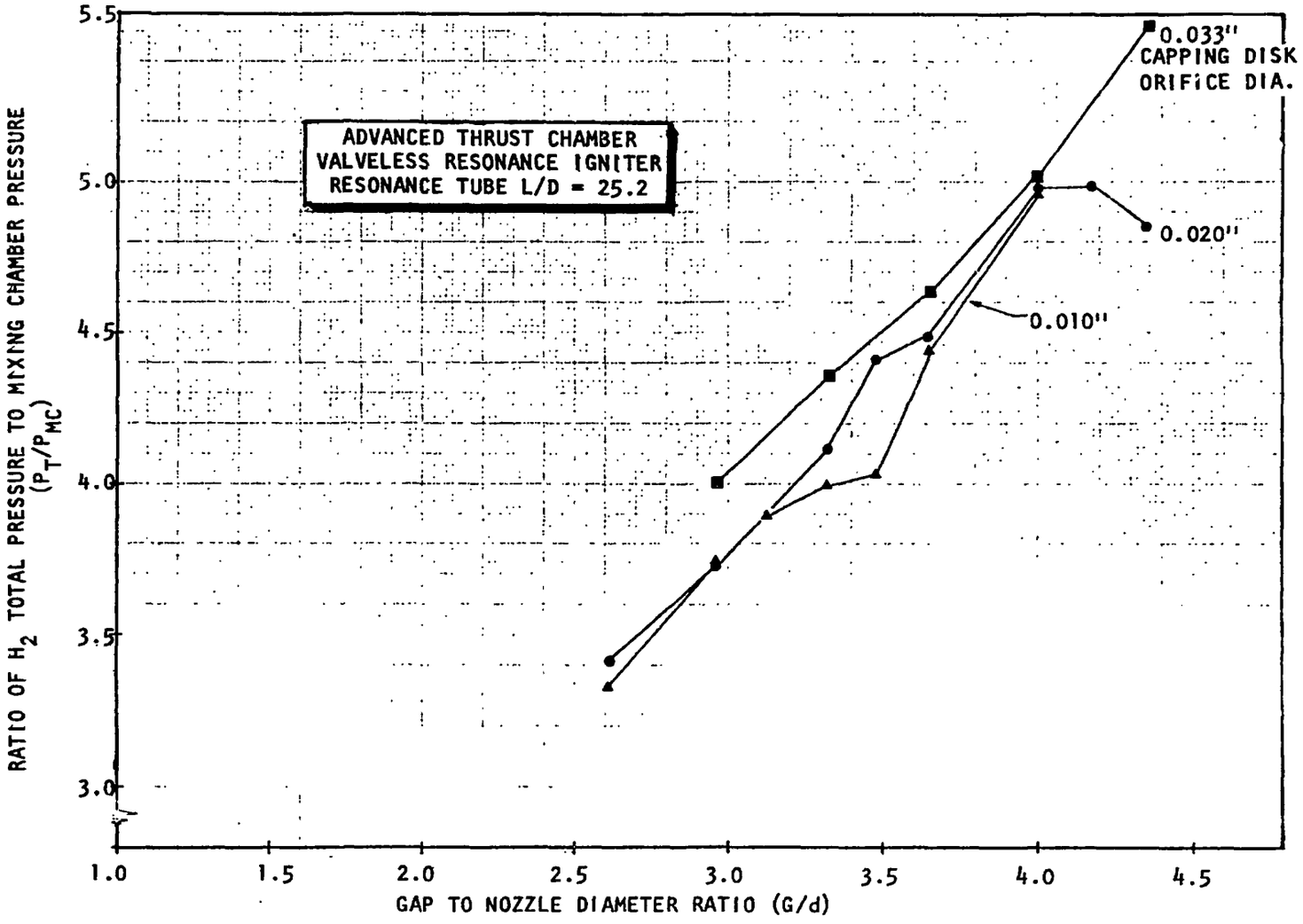

Figure 31. Pressure Ratio vs G/d

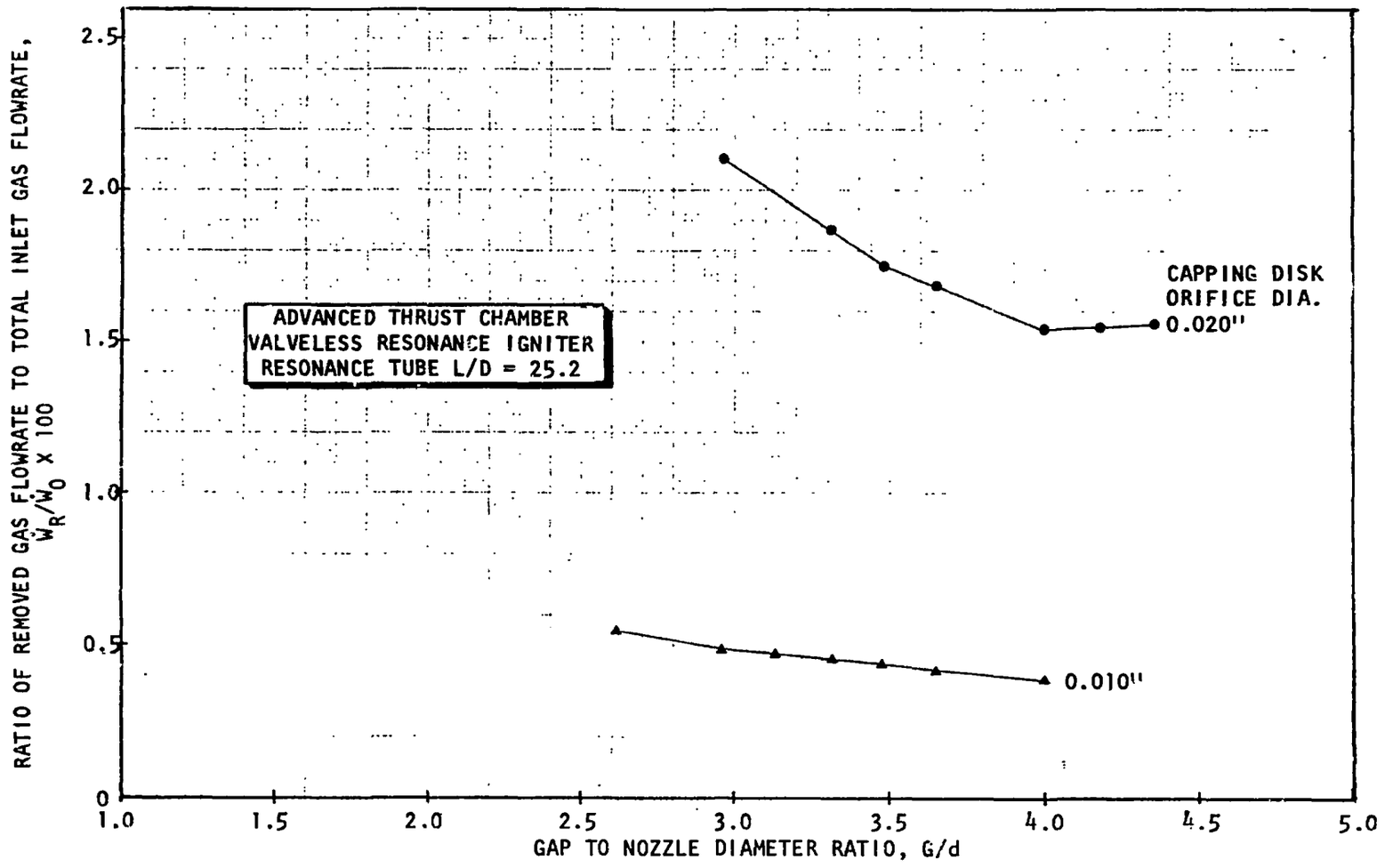

Figure 32. Removed Gas Percent vs G/d

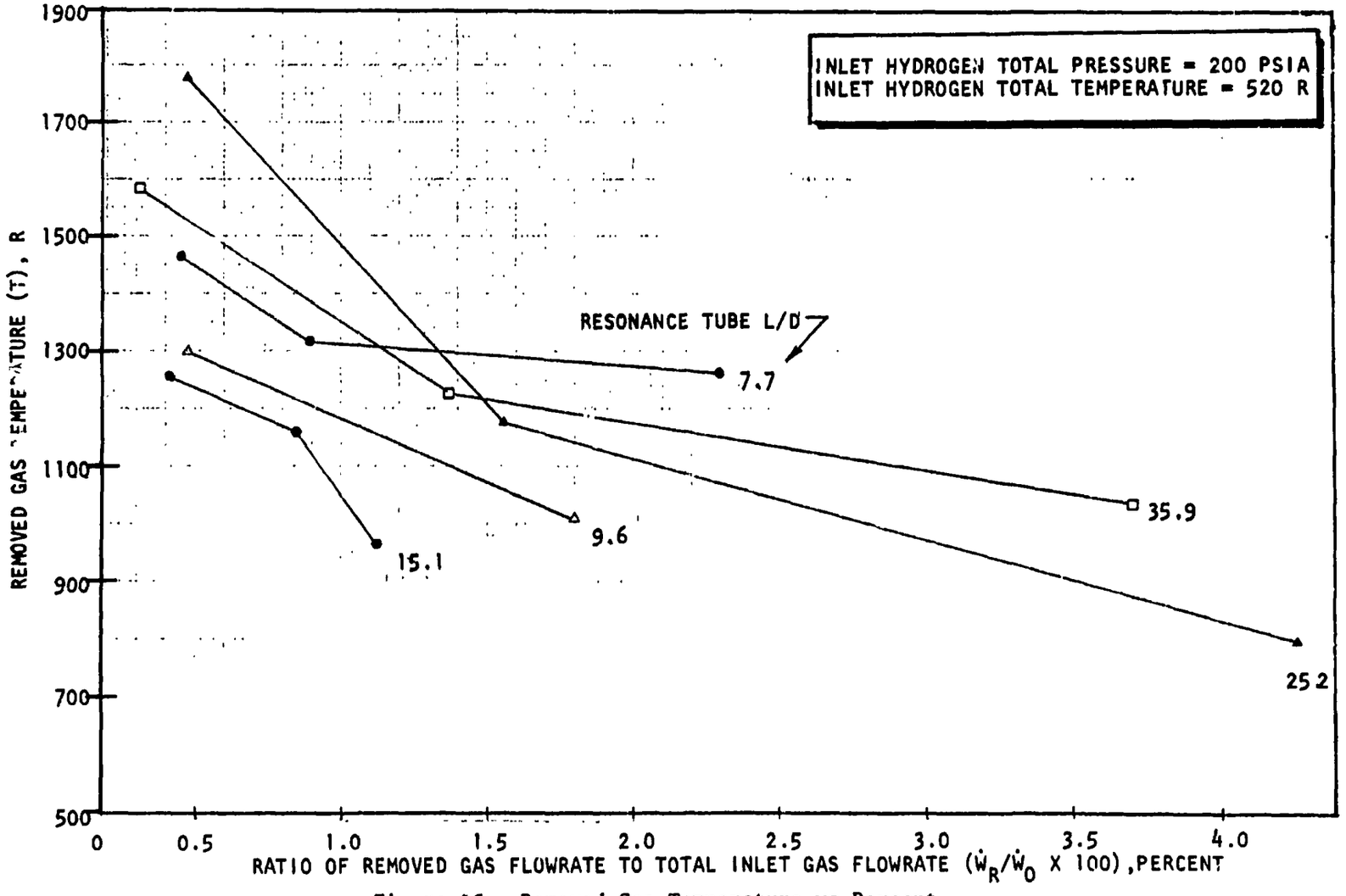

Figure 33. Removed Gas Temperature vs Percent

CONCLUSIONS

The fesibility of the resonance ignition concept as applied to the No. 2 test bed was investigated and demonstrated experimentally. Four phases of the test program provided the following results.

1. Geometry Optimization

   a. The optimum dimensions of a resonance igniter meeting prescribed flowrates were established.

   b. With the optimized configuration, measured hydrogen temperatures of up to 1560 R were achieved in time periods of less than 0.010 second after start of flow.

   c. Dimensional scaling techniques can be successfully applied to provide a basis for resonance configurations having widely different flowrates, i.e., the optimized resonance igniter configuration developed during this program required only small variations from a previously developed resonance igniter having approximately 3 times the flowrate capacity.

2. Combustion Characteristics

   a. Investigations conducted with both hydrogen and oxygen flowing through the igniter resulted in 171 ignitions out of 179 tests. The tests were run over a wide range of mixture ratios ($0.48 < MR < 4.48$) and propellant inlet pressures ($130 < P_T < 310$ psia).

   b. The cause for the eight no-ignition cases was traceable to gas leaks developed in the oxidizer check valve.

   c. Elimination of oxidizer check valve leaks resulted in 100 percent reliable ignitions.

   d. All ignition tests resulted in smooth and stable combustion without pressure overshoots.

e. All ignition tests were achieved with small hydrogen lead times (3 to 5 milliseconds, and 90 percent of steady-state chamber pressure was reached in less than 60 milliseconds from time of electrical signal to first propellant (hydrogen) valve.

3. Oxidizer Augmentation

a. It was demonstrated that increased torch gas temperature can be achieved by means of secondary oxygen injection at the igniter exit plane. Secondary oxygen also provided cooling of the igniter throat tube.

b. Oxidizer augmentation effectively tripled the basic igniter mixture ratio.

c. The limiting igniter mixture ratio necessary to react with the secondary oxidizer was delineated, i.e., the basic igniter mixture ratio must be above 1.3 to complete combustion with the injected secondary oxidizer.

4. Valveless Heating and Resonance Flow

a. The feasibility of generating a continuous high-temperature hydrogen flow (starting with ambient-temperature hydrogen) was demonstrated using a resonance device having no moving parts and requiring no external energy addition.

b. A continuous hydrogen gas stream at 1780 R was obtained by extracting approximately 0.5 percent from one of the resonance cavities tested.

c. Since hydrogen temperatures between 1400 and 1500 R are required to ignite with oxygen, the investigation provided the basis for a flow-through igniter design that eliminates the need for an oxidizer check valve, thus increasing reliability and simplifying system operation.

In summary, a resonance igniter sized specifically for integration with the No. 2 test bed was proved feasible. The experimental program indicated that the igniter will operate reliably with ambient propellants over a wide range of mixture ratios and pressures. To eliminate potential problems with the oxidizer check valve, a new application of the resonance phenomenon was investitated. The results of the latter effort, being very promising, should be pursued in future advanced thrust chamber development programs.

COMBUSTION WAVE IGNITION DEVICE

COMBUSTION WAVE PHENOMENON

If a flowing, explosive gas mixture contained in a tube is ignited with a weak spark, a flame (deflagration wave) will begin to propagate in the direction of flow. The combustion products, having a higher specific volume than the unburned mixture, will compress the mixture and increase the unburned gas velocity. Under suitable conditions, this compression wave will produce a shock wave traveling ahead of the deflagration. If sufficient tube length is available, the combustible mixture is compressed and heated by the shock wave until autoignition occurs behind the shock and a detonation wave develops.

The theory of gaseous detonations has been under continuous development since the turn of the century. Detonations were identified by Mallard and LeChatelier (Ref. 10) and Berthelot and Vielle (Ref. 11) in 1881, and hypotheses leading to mathematical predictions of the speed of propagation of these waves were first given by Chapman (Ref. 12) and Jouguet (Ref. 13). Many experimental investigations have been conducted to determine the effect of mixture ratio and intial conditions on the properties of detonation waves and to further refine the theory; an excellent bibliography is presented in Ref. 14.

A simplified detonation theory can be formulated with the following assumptions: (1) the gases are ideal, (2) the average molecular weight of the gases is not changed across the shock wave, and (3) the specific heat of the gases does not change across the shock wave.

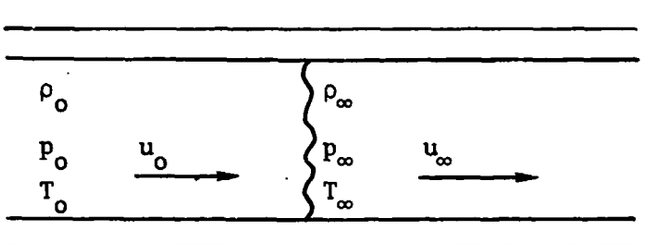

The equations of continuity, momentum, and energy can be written for these assumptions:

$$\rho_o u_o = \rho_\infty u_\infty \qquad \text{Continuity} \qquad (1)$$

$$\rho_o u^2_o + p_o = \rho_\infty u^2_\infty + p_\infty \qquad \text{Momentum} \qquad (2)$$

$$h_\infty - h_o = C_p (T_\infty - T_o) - q \qquad \text{Energy} \qquad (3)$$

where q = the heat of combustion per pound of mixture.

If Eq. 3 is combined with the equation of state:

$$p_\infty/\rho_\infty T_\infty = p_o/\rho_o T_o = R/\overline{M}_o \qquad \text{State} \qquad (4)$$

and it is remembered that $C_p = \frac{\gamma R/\overline{M}_o}{\gamma - 1}$

then:

$$h_\infty - h_o = -q + \frac{\gamma}{\gamma-1}\left(\frac{p_\infty}{\rho_\infty} - \frac{p_o}{\rho_o}\right) \qquad (5)$$

The energy equation for the gas property change across a shock wave with no combustion is the Hugeniot relationship:

$$h_\infty - h_o = \frac{1}{2}\left(\frac{1}{\rho_\infty} + \frac{1}{\rho_o}\right)(p_\infty - p_o) \qquad (6)$$

Since the energy difference between combustion and no combustion across the shock front is the heat of reaction q:

$$q = \left(\frac{\gamma}{\gamma-1}\right)\left(\frac{p_\infty}{\rho_\infty} - \frac{p_o}{\rho_o}\right) - \frac{1}{2}\left(\frac{1}{\rho_\infty} + \frac{1}{\rho_o}\right)(p_\infty - p_o) \qquad (7)$$

Equation 2 may be rewritten as:

$$\frac{p_\infty - p_o}{1/\rho_\infty - 1/\rho_o} = -(\rho_\infty u_\infty)^2 \qquad (8)$$

Equations 7 and 8, therefore, completely define the simplified system. Dimensionless variables are generally introduced to simplify manipulation (Ref. 14):

$$p = p_\infty/p_o$$

$$v = \rho_o/\rho_\infty$$

$$\alpha = q\ \rho_o/p_o$$

$$\mu = \rho_o\ u_o^2/p_o$$

Introducing these variables in Eq. 7 and 8 results in:

$$\left(\frac{\gamma}{\gamma-1}\right)(pv - 1) - \frac{1}{2}\ (p - 1)\ (v + 1) = \alpha \tag{9}$$

$$(p - 1)/(v - 1) = -\mu \tag{10}$$

If the mass flow parameter $-\mu$ is defined as the slope of a straight line tangent to Eq. 9 ($-\mu = dp/dv$), Eq. 9 and 10 may be solved simultaneously to obtain the final Chapman-Jouguent relationships for the properties change across a detonation wave:

$$p = \frac{p_\infty}{p_o} = 1 + \alpha\ (\gamma - 1)\ \left\{1 + \left[1 + \frac{2\ \gamma}{\alpha(\gamma^2-1)}\right]^{1/2}\right\} \tag{11}$$

$$v = \frac{\rho_o}{\rho_\infty} = 1 + \frac{\alpha}{\gamma}\ (\gamma - 1)\ \left\{1 - \left[1 + \frac{2\ \gamma}{\alpha(\gamma^2-1)}\right]^{1/2}\right\} \tag{12}$$

$$\frac{M_o}{M_\infty} = M_o = \left[1 + \frac{\alpha\ (\gamma^2-1)}{2\ \gamma}\right]^{1/2} + \left[\frac{\alpha\ (\gamma^2-1)}{2\ \gamma}\right]^{1/2} \tag{13}$$

$$\frac{T_\infty}{T_o} = pv \tag{14}$$

In Eq. 13, M_o is the starting Mach number of the detonation wave with respect to the unburned gas. The downstream velocity of a Chapman-Jouguet detonation is sonic with respect to the burned gas, i.e., $M_\infty = 1.0$.

These relationships are plotted as a function of the energy release parameter (α) for a specific heat ratio of $\gamma = 1.4$ in Fig. 34.

The energy release parameter for hydrogen/oxygen mixtures may be estimated by realizing that

$$\alpha = q\ \rho_o/p_o = q\ \overline{M}_o/RT_o$$

where $\overline{M}_o$ is the mean molecular weight of the unburned mixture. The mean molecular weight of unburned hydrogen/oxygen mixtures may be calculated from

$$\overline{M}_o = 2\ (1+\overline{R})/(1+\overline{R}/16)$$

where $\overline{R}$ is the oxygen to hydrogen weight mixture ratio. Using a reaction enthalpy of $\Delta H = 104{,}040$ Btu/lb-mole of hydrogen burned, the energy release parameter is calculated as follows:

Fuel-Rich Mixtures

$$\alpha = \frac{\Delta H}{8RT_o} \left\{1 - [1/(1+\overline{R})]\right\} \left\{(1+\overline{R})/(1+\overline{R}/16)\right\} \quad (778)$$

Oxidizer-Rich Mixtures

$$\alpha = \frac{\Delta H}{RT_o} \left\{1/(1+\overline{R})\right\} \left\{(1+\overline{R})/(1+\overline{R}/16)\right\} \quad (778)$$

The energy release parameter for hydrogen/oxygen is plotted as a function of mixture ratio in Fig. 35. For stoichiometric hydrogen/oxygen, the energy-release parameter for ambient gases is seen to be approximately 66. Referring to Fig. 34, a pressure ratio of about 54 and a temperature ratio of 32 can be predicted for a Chapman-Jouguet detonation.

In reality, the high-pressure and temperature ratios predicted by the simplified model are not achieved because of the energy absorbed due to dissociation at high temperature and the molecular weight change across the shock wave. The temperature and pressure ratios of Chapman-Jouguet waves in hydrogen/oxygen have been

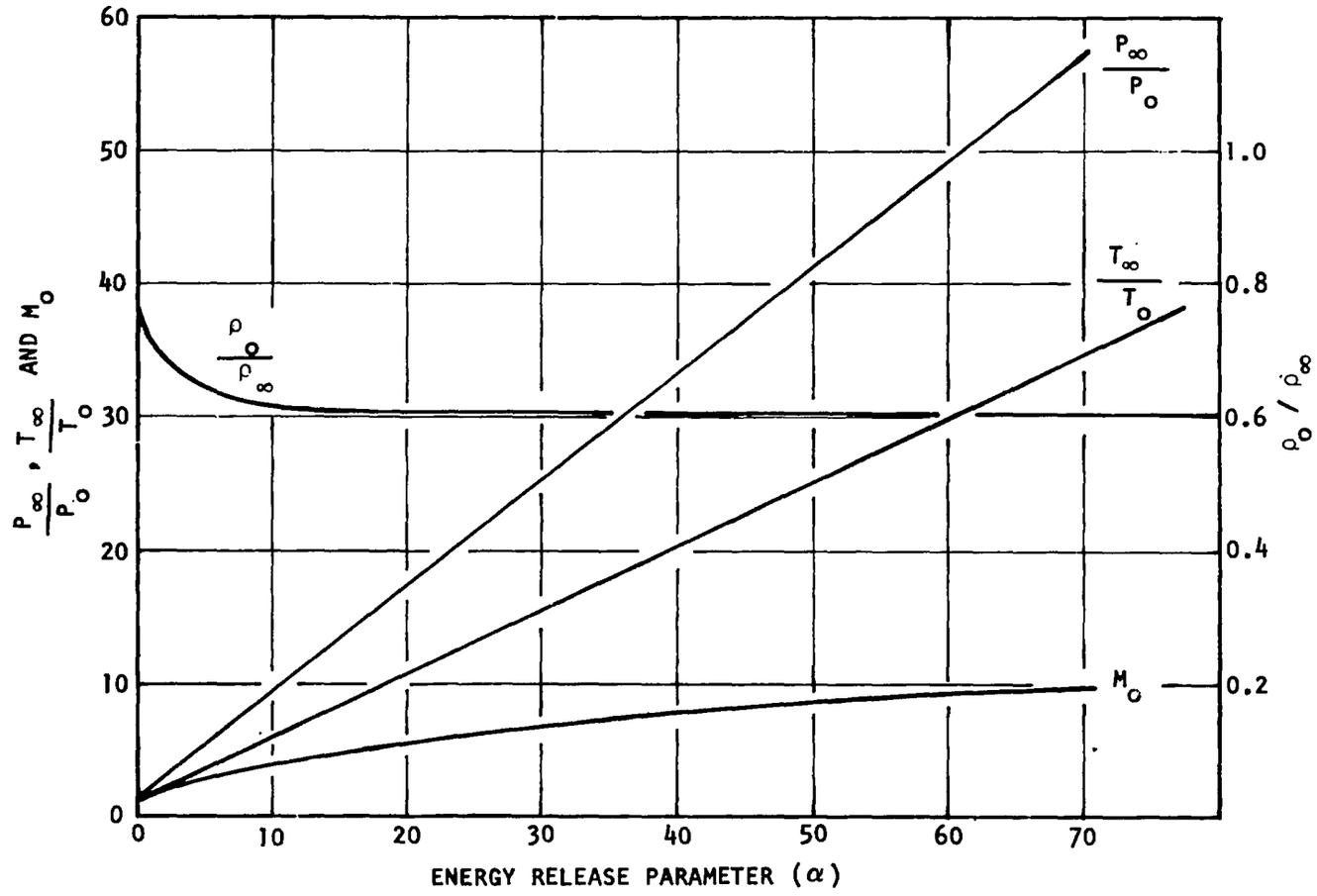

Figure 34. Chapman-Jouguet Ratios vs Energy Release

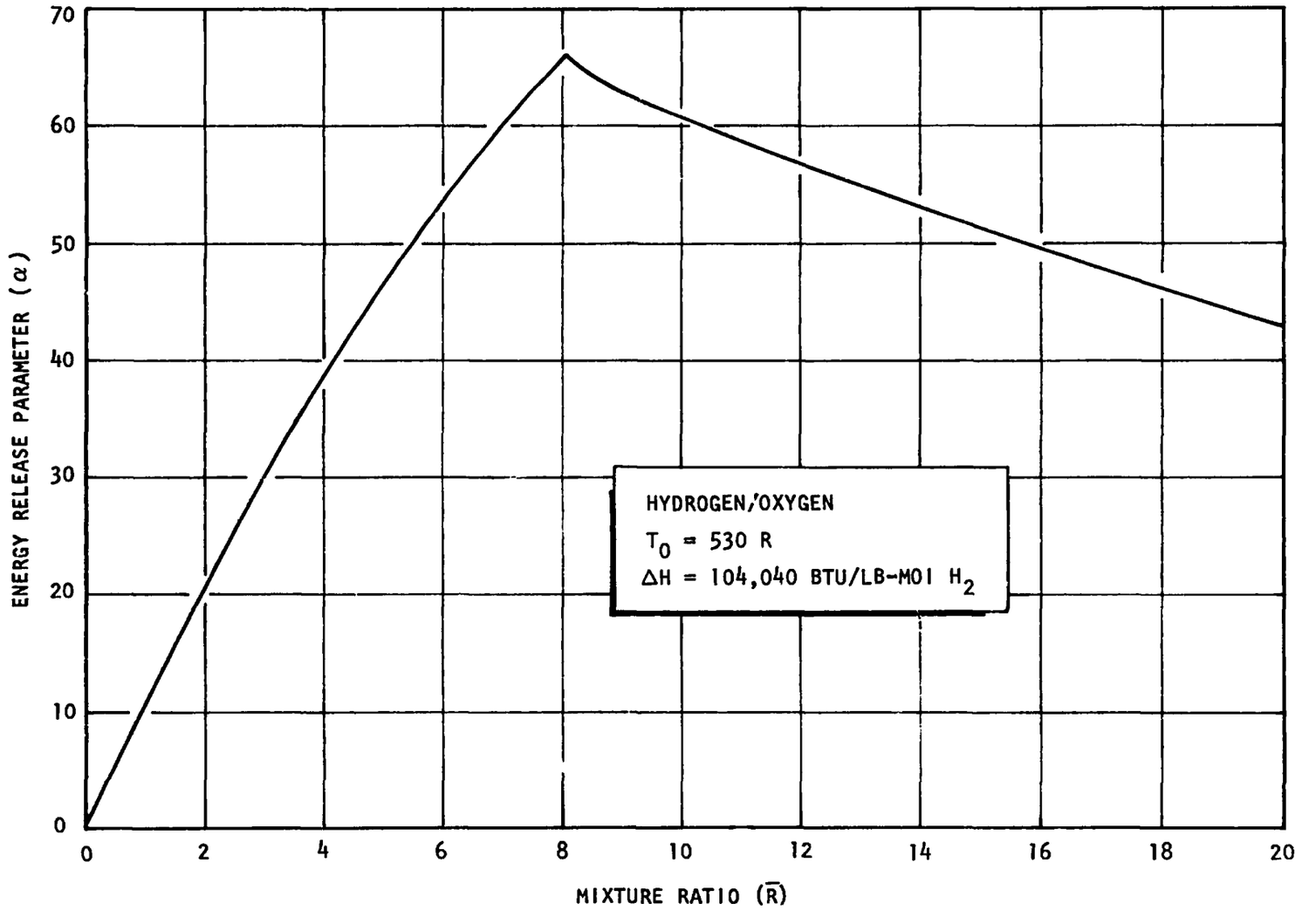

Figure 35. Energy Release vs Mixture Ratio

found to be relatively insensitive to mixture ratio, and are dependent on the initial temperature and pressure of the gas mixture. The effects of initial conditions and mixture ratio on the Chapman-Jouguet temperature and pressure ratios have been determined by Busch and Laderman (Ref. 15) and are presented in Fig. 36 and 37. Ambient temperature temperature stoichiometric mixtures are seen to develop a pressure ratio of 14 to 17, depending on the initial pressure, compared with the value of 54 predicted by the simplified theory. A temperature ratio of 8 to 13 is developed across the wave for ambient propellants, compared to a value of 32 predicted by the simplified theory. A more complex computerized program developed in Ref. 16 successfully predicts values of this order by considering the combustion equilibria of the burnt gas species along with the Hugeniot relationship.

Data from Fig. 36 and 37 are summarized in Table 5. These data imply that:

1. A minimum initial pressure is required to obtain a sufficiently high-temperature ratio for pilot ignition.
2. Higher pressure and temperature ratios will be obtained with low-temperature propellants.
3. At initial pressures of 1 to 2 atmospheres, combustion wave core temperatures in excess of 6000 R can be expected.

Table 5. Effect of Initial Conditions on Chapman-Jouguet Conditions

	Initial Temperature (60 to -180 F), percent	Initial Pressure (1 to 10 atms), percent	Comparison (MR = 8 to MR = 5.3), percent
Wave Velocity	(3)	(4)	(14)
Pressure Ratio	(95)	(4)	(3)
Temperature Ratio	(100)	(6)	(5 to 10)

The minimum length of tubing required to obtain a Chapman-Jouguet detonation wave has been experimentally determined for hydrogen/oxygen mixtures (Ref. 17). Data presented in Fig. 38 were obtained with 0.599-inch-ID tubing and indicate that the induction length increases sharply at low mixture ratios. For typical engine

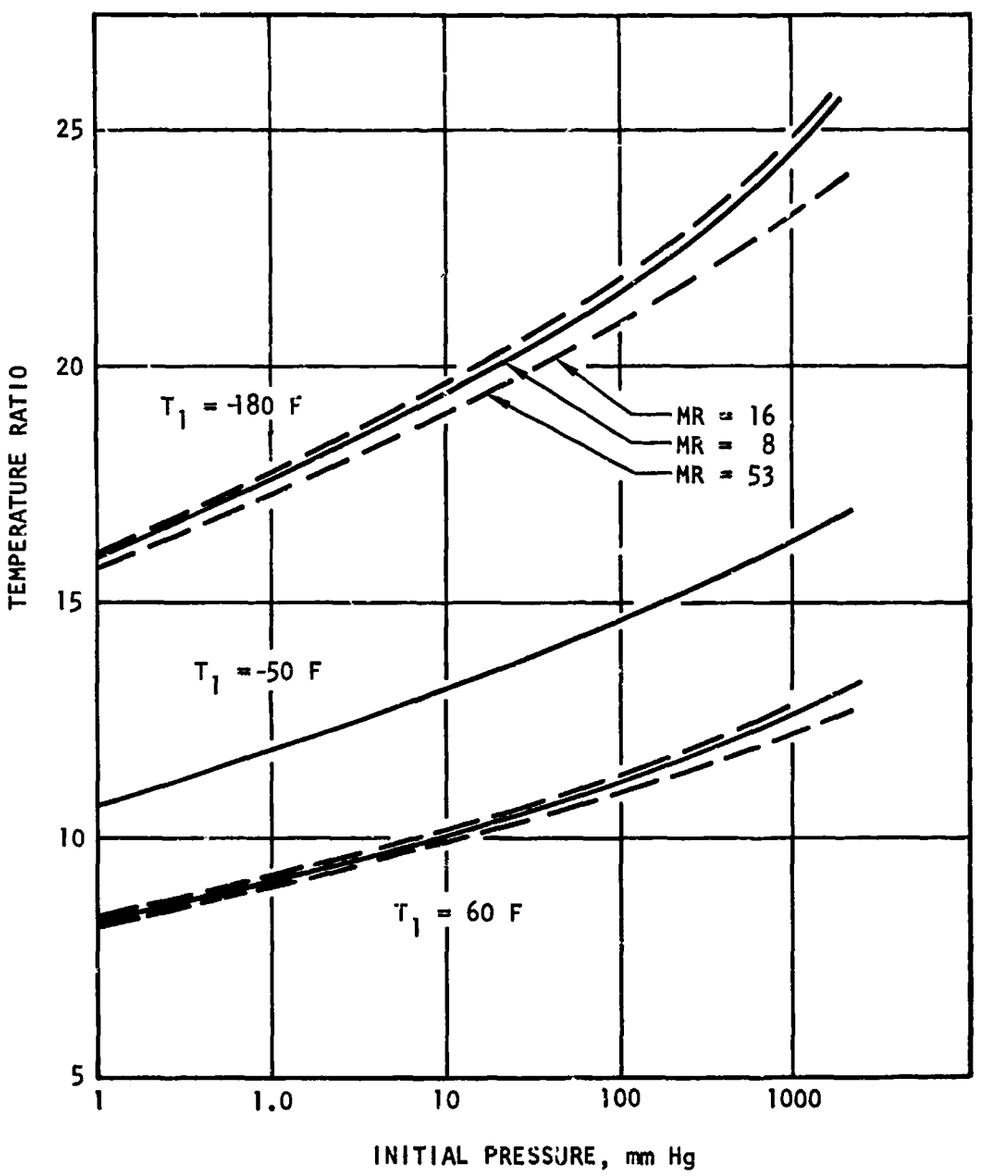

Figure 36. Influence of Initial Conditions on Chapman-Jouguet Temperature Ratio (Ref. 15)

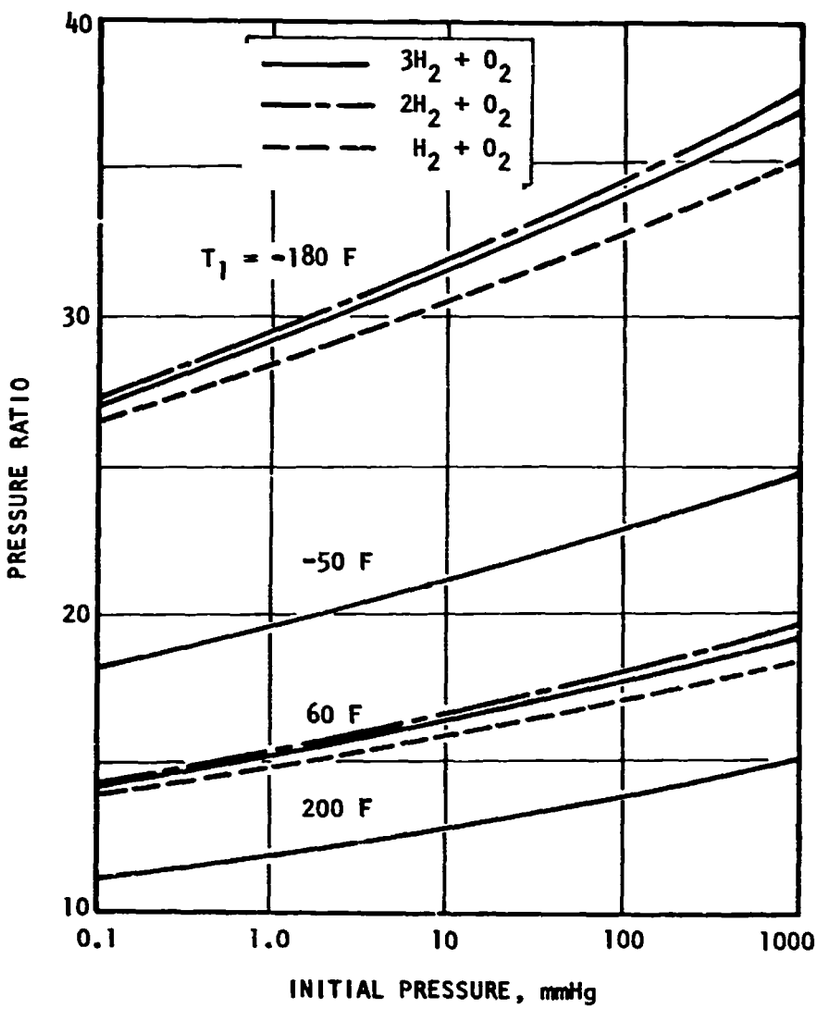

Figure 37. Influence of Initial Conditions on Chapman-Jouguet Pressure Ratio

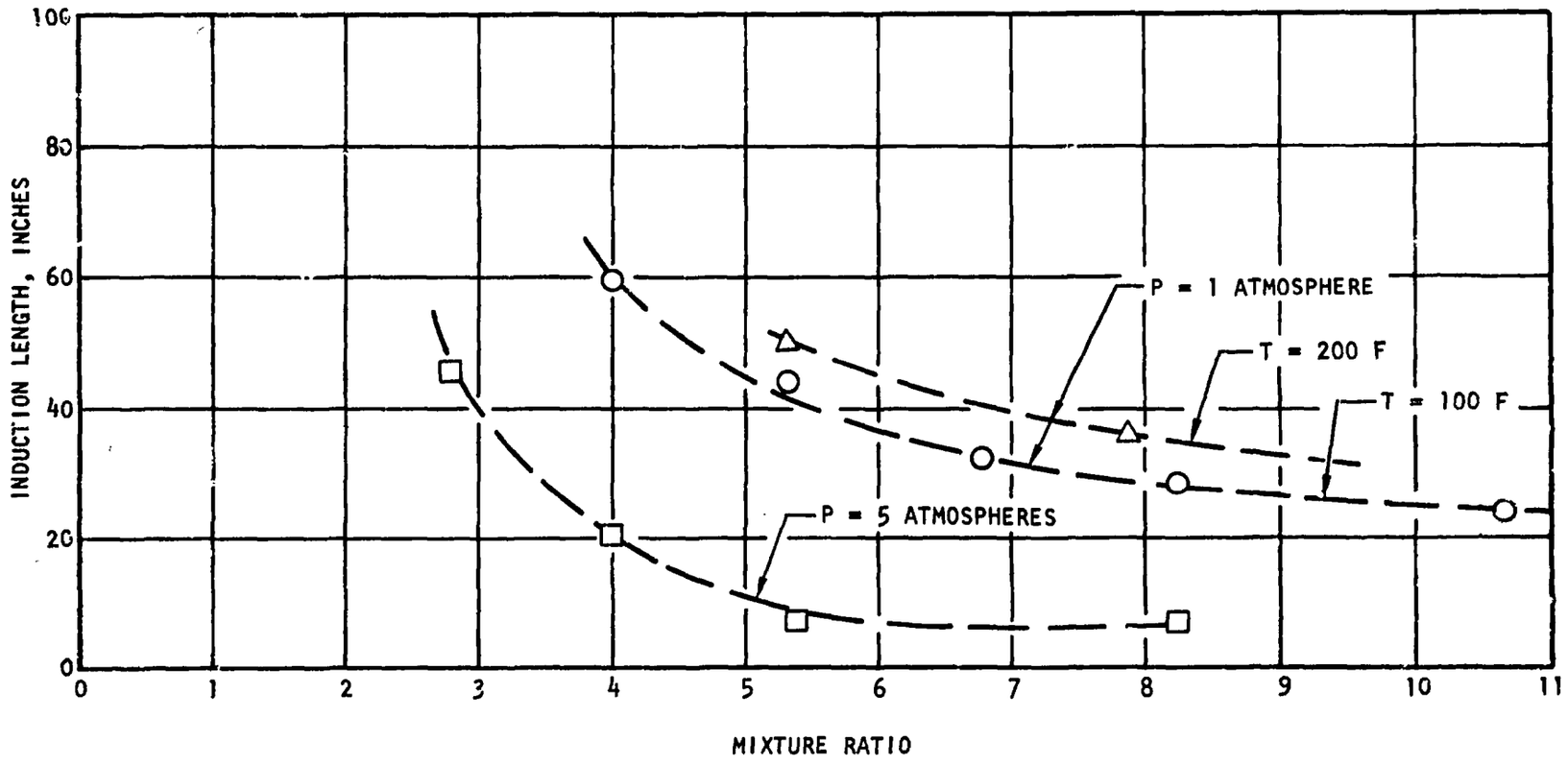

Figure 38. Induction Length vs Mixture Ratio

system tubing lengths of 50 to 60 inches and initial pressures of 1 to 2 atmospheres available from tank head pressures, mixture ratios of less than approximately 2.5 will be marginal for propagating a detonation wave.

TEST PROGRAM OBJECTIVES

Test effort was performed to provide a demonstration of the combustion wave concept and to verify the capability of a combustion wave to ignite a concentric pilot element. The combustion wave demonstration was sized to provide ignition capability for 20 segmented combustors, and at least two pilot elements were to be ignited. The test hardware was sized to meet the dimensional requirements of the No. 2 test bed common igniter port, and to provide the energy requirements discussed in Appendix A.

The test program was conducted in two phases:

1. Detonation wave generation
2. Pilot ignition

Testing was performed in parallel with the resonant igniter test at the Thermodynamics Laboratory of the Los Angeles Division. The facility is described in Appendix C.

COMBUSTION WAVE IGNITER TESTING

Design Description

A triaxial igniter element was designed and fabricated for this program (Fig. 39). The unit comprises a central combustion wave tube (0.180-inch OD x 0.0245-inch wall) chamfered 5 degrees at the exit, a concentric tube (0.291-inch OD x 0.0175-inch wall) chamfered 15 degrees at the exit forming the oxidizer pilot annulus, and an outer tube (0.373-inch OD x 0.027-inch wall) forming the fuel pilot annulus. The inner tubes were chamfered to increase pilot element mixing. The triaxial element is silver soldered to a standard 1/4-inch fitting for attachment to the

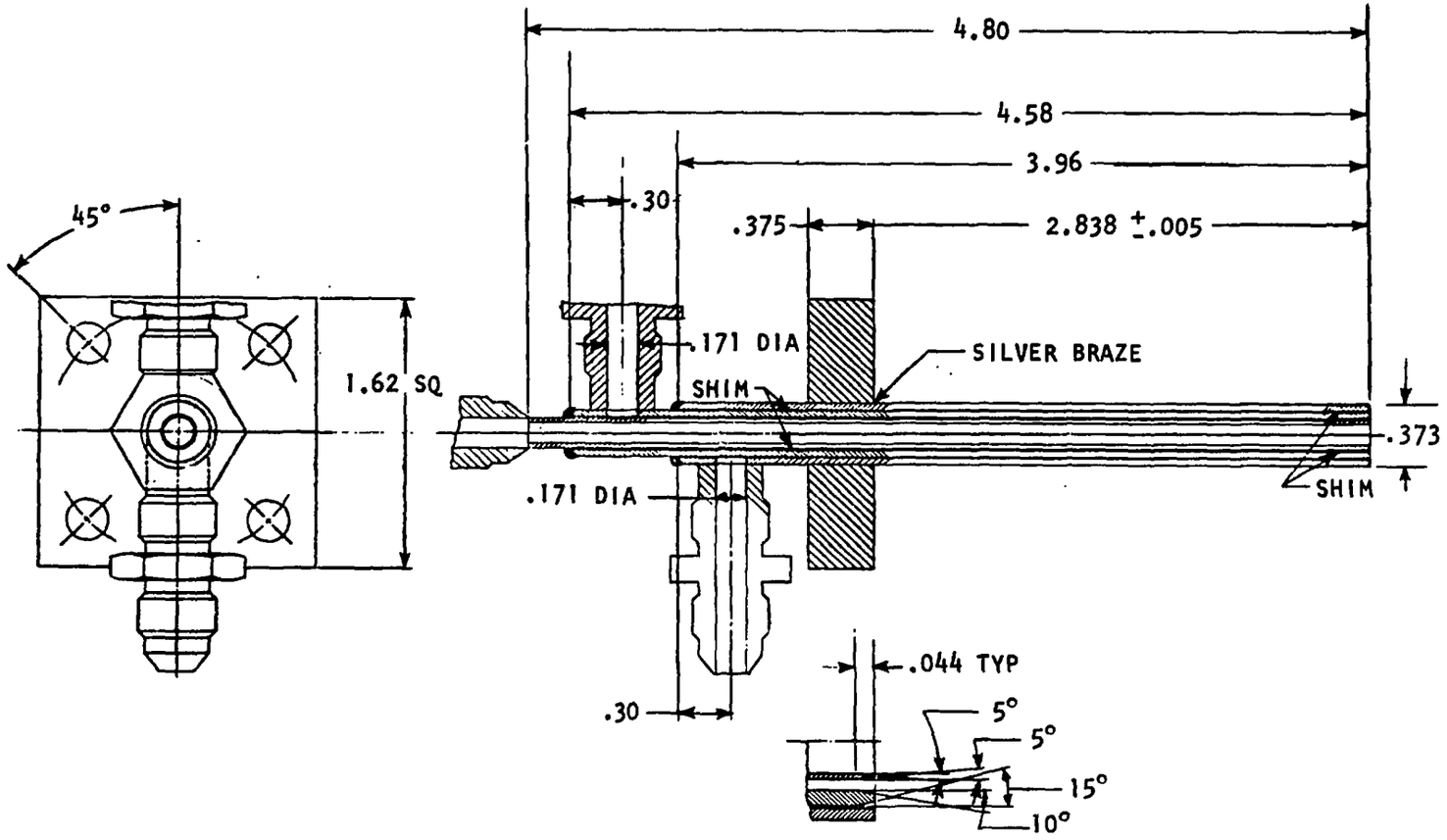

Figure 39. Combustion Wave Element Design

combustion wave supply tube. The completed unit is shown in Fig. 40.

An instrumented premixer chamber (Fig. 41) used on a previous program was obtained to supply premixed gases and generate the combustion wave. This unit has a recessed coaxial injector element to provide sonic hydrogen and oxygen velocities at the nominal operating flowrates. A standard J-2 spark igniter requiring a 4.5-ampere input current at 28 vdc was utilized to provide a 360-millijoule spark. The spark igniter is located approximately 3 inches from the injector element.

A precombustor unit (Fig. 42) was fabricated to provide controlled pressure at the igniter tip during vacuum testing. The unit was drilled and tapped for a chromel-alumel thermocouple installation.

Lengths of standard 1/4-inch tubing were used to connect the triaxial element and the premixer chamber. Tubes 48 to 60 inches long were used as representative of No. 2 test bed manifold lengths.

An assembly of the test hardware is shown in Fig. 43. The premixer flow was directed into a constantly evacuated vacuum tank by two parallel flow paths for single-element ignition.

The flow to the igniter element was 4 to 5 percent of the total premixer flow, which simulated a 20-element flow requirement of 0.035 lb/sec. For two-element operation, a third flow path was provided. Since the No. 2 test bed combustion wave manifold will require bends for adequate packaging, one 90-degree bend was provided in the No. 1 element combustion wave tube, and two 90-degree bends were provided in the No. 2 element tube.

Test Results

An experimental program comprised of 106 tests was conducted to (1) evaluate the feasibility of generating a combustion wave in engine system lengths of standard tubing, (2) map the pressure and mixture ratio limits of combustion wave generation,

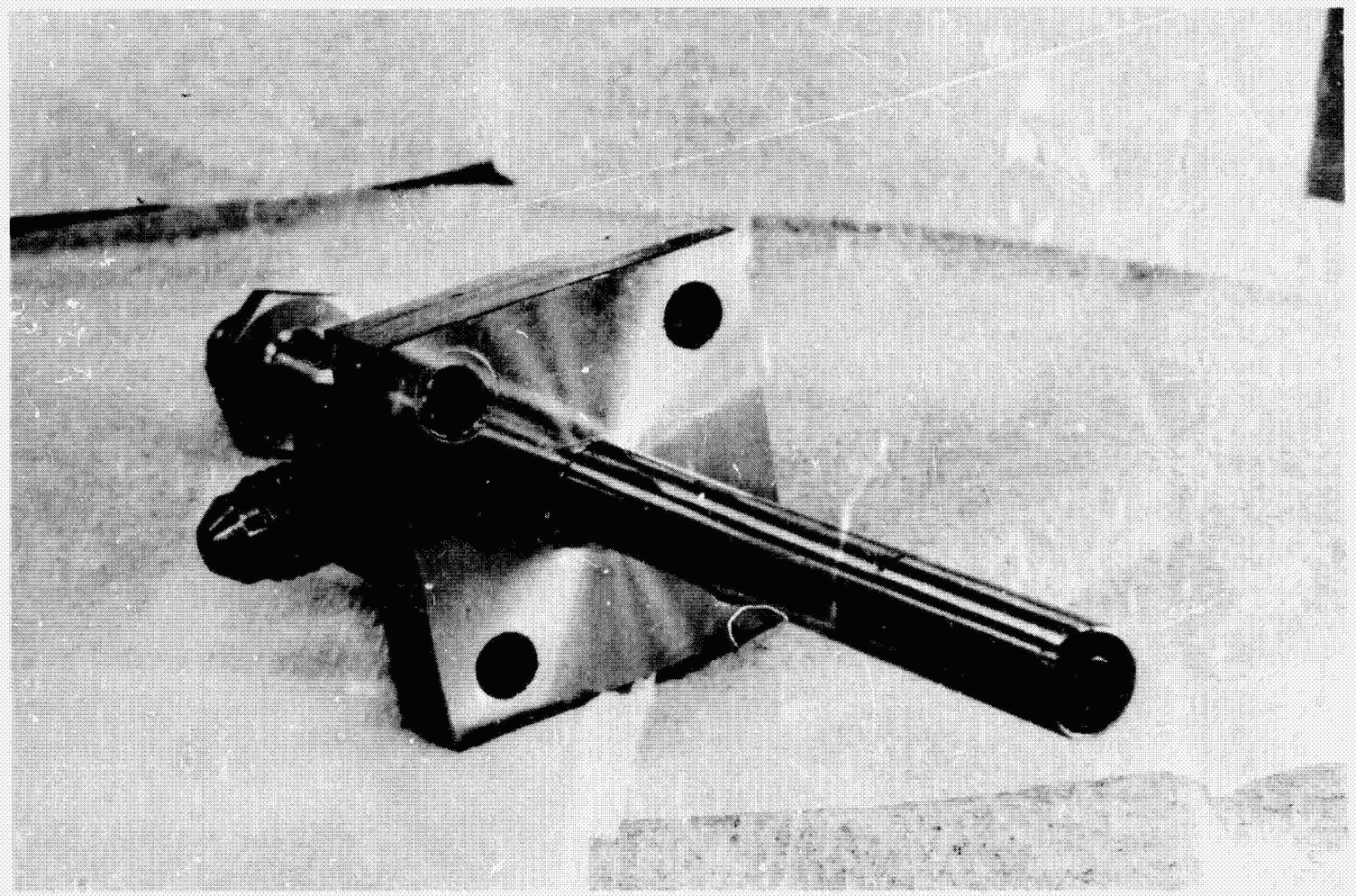

Figure 40. Combustion Wave Igniter Element

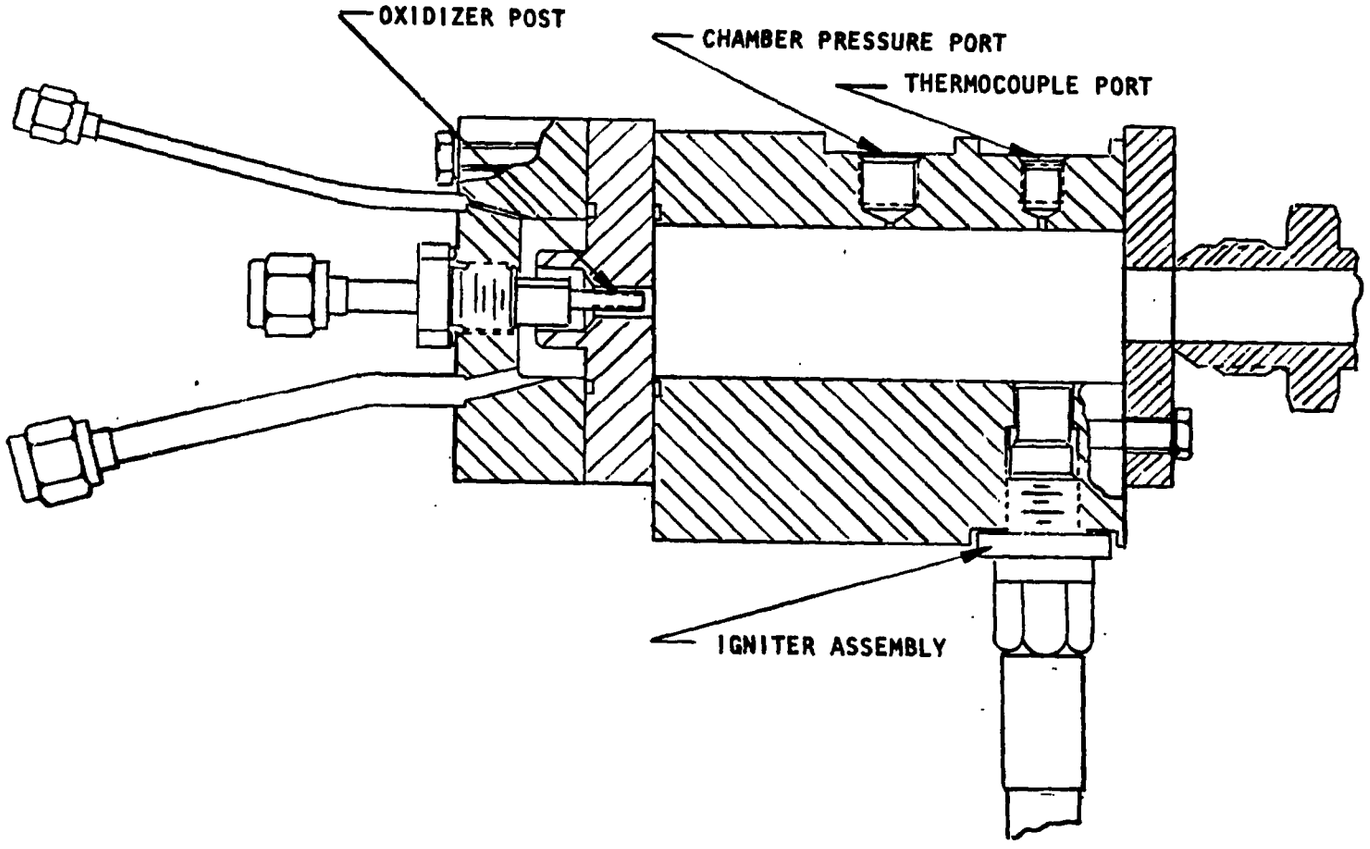

Figure 41. Combustion Wave Igniter Premixer

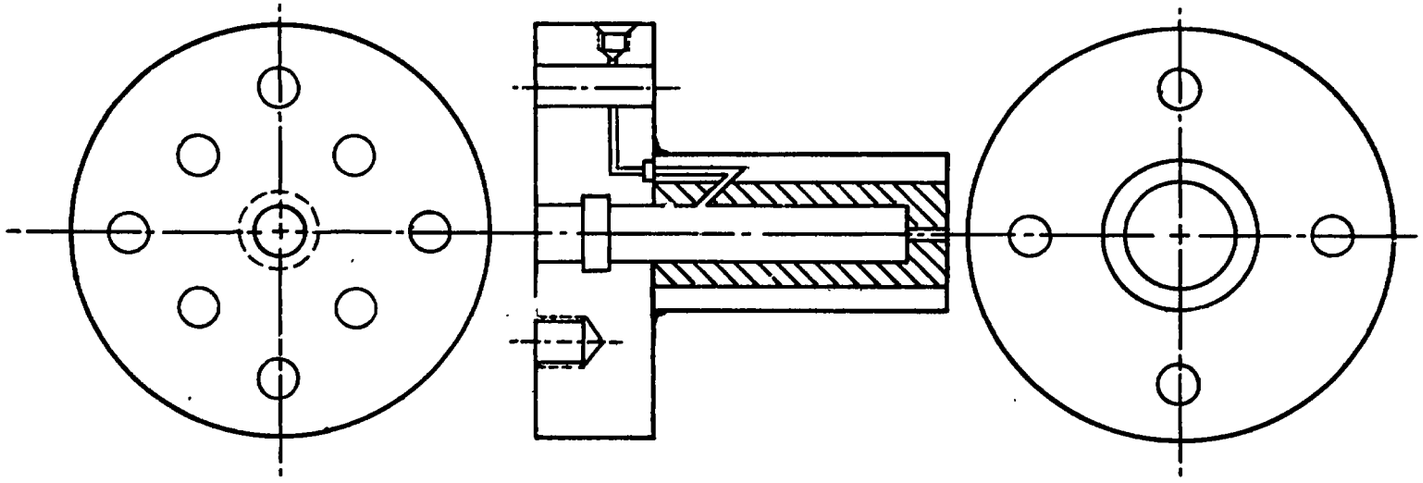

Figure 42. Precombustor

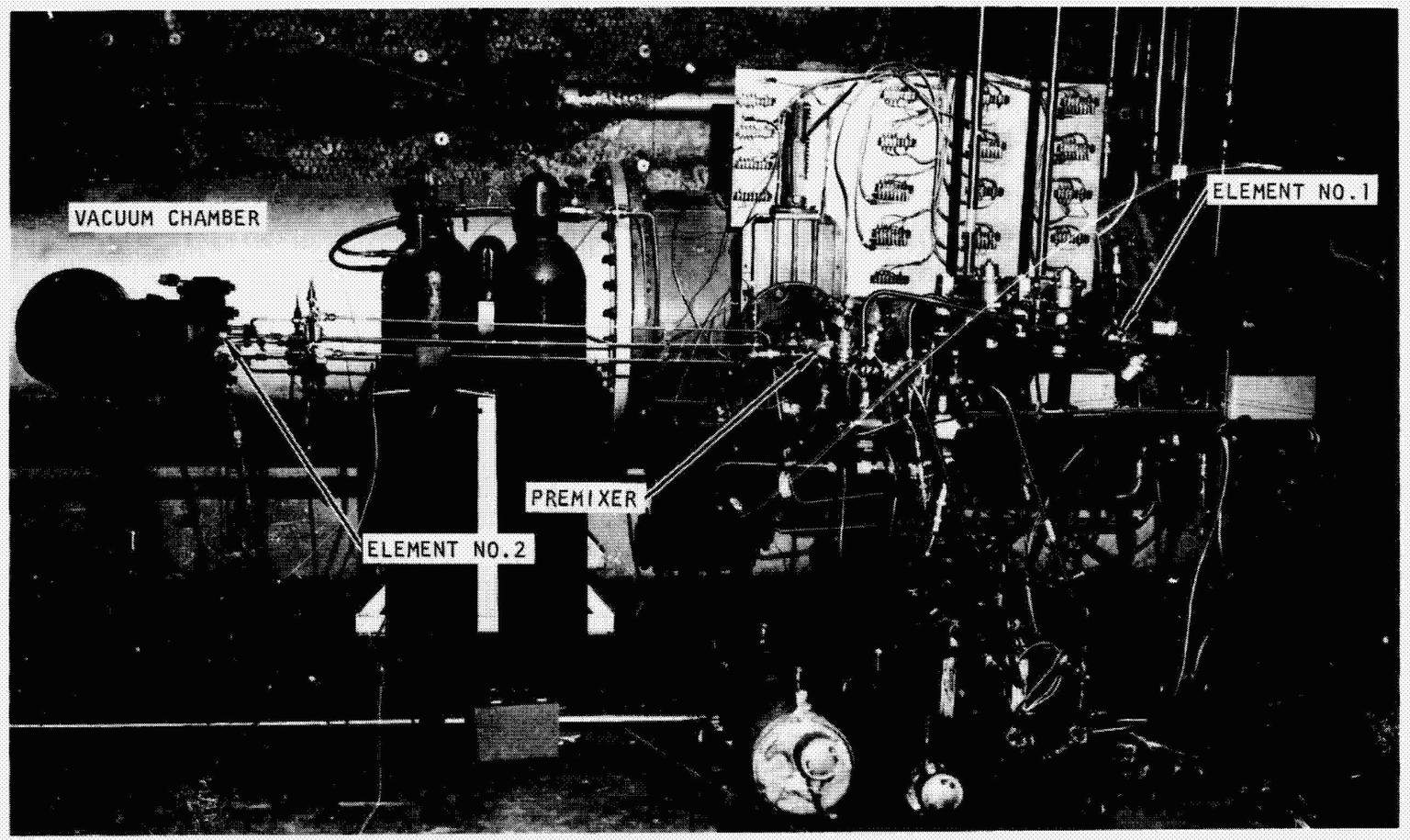

Figure 43. Test Setup

(3) evaluate the feasibility of igniting a pilot element with a combustion wave, (4) simulate proposed engine system valve sequencing, (5) map pilot element ignition limits, and (6) show the feasibility of multiple-element ignition. A test matrix of the experiments is shown in Table 6, and a summary of test results is presented in Table 7. A discussion of the test results is presented in the following paragraphs.

Combustion Wave Limits. Throughout the test program, initial pressure and mixture ratio in the premixer were varied so that the combustion wave propagation limits could be determined. The test results, plotted in Fig. 44, show that the lower limit of initial pressure was about 4.2 psia and the minimum mixture ratio for detonation was 2.3. The lower pressure limit agrees with the results of Ref. 18 in which spark-ignited detonations could not be consistently reproduced in hydrogen/oxygen mixtures at initial pressures below 1/4 atmosphere. The lower mixture ratio limit is in agreement with the induction length results of Ref. 17 presented in Fig. 38, which indicates a lower mixture ratio limit of approximately 2.5 for propagation of a detonation wave.

Pilot Ignition Limits. The investigation of pilot ignition limits was conducted on tests 20 through 106. A typical temperature versus time trace is shown in Fig. 45. The premixer mixture ratio was 4.9 on this test at a pressure of 21.5 psia. At a facility time of 54 seconds, the spark was initiated and a pressure spike was recorded within 5 milliseconds of this event. The temperature in the premixer (TC-3) peaked within 15 milliseconds after the spark and rapidly decayed to ambient temperature within 200 milliseconds. The igniter element indicated ignition approximately 20 milliseconds after the spark, as indicated by the rapid rise of TC-1, a thermocouple located immediately downstream of the element. The oxidizer valve was closed 40 milliseconds after the spark signal, and gaseous fuel was allowed to flow through the combustion wave tube.

The element temperature (TC-1) and a temperature in the vacuum tank 1 inch downstream of the precombustor exit plant (TC-2) showed a continuous temperature rise, indicating sustained pilot ignition until the propellant flows were terminated.

Table 6. Combustion Wave Ignition Test Program

Test Number	Objectives	Results
1 through 19	Obtain combustion wave and map propagation limits	Combustion wave successfully obtained propagation limits determined
20	Obtain pilot ignition	Pilot ignition obtained; igniter element burnout
21 through 27	Calibrate to lower pilot element mixture ratio	Pilot ignition without igniter element damage
28 through 47	Map pilot ignition limits	No igniter damage
48 through 54	Delay spark to simulate proposed engine sequencing	No combustion wave generated with 5-MS spark delay from premixer oxidizer valve closure
55 through 81	Additional mapping tests	No igniter damage
82 through 87	Evaluate ignition in vacuum	Combustion wave generated but no pilot ignition
88 through 93	Alternate testing of two igniter elements	Successful pilot ignition obtained with both elements
94 through 106	Dual igniter tests to evaluate sequencing and ignition limits	No combustion wave with delayed ignition signal.

Table 7. Combustion Wave Igniter Test Results

Test No.	Premixer			Pilot Element				Comments
	Pressure, psia	Mixture Ratio	Combustion Wave Obtained	Precombuster Pressure, psia	Initial Mixture Ratio	Final Mixture Ratio	Pilot Ignition Obtained	
1	N/A	N/A	N/A	N/A	N/A	N/A	N/A	Blowdowns
2	N/A	N/A	N/A	N/A				Blowdowns
3	1.0	3.47	No	2.5				No pilot element flow
4	3.7	17.5	No	2.6				
5	4.2	24.8	No	3.0				
6	4.6	25.5	Yes	3.2				
7	4.8	29.2	Yes	3.5				
8	4.3	28.6	No	3.3				
9	4.3	27.7	No	3.3				
10	4.4	31.6	No	3.5				
11	4.6	32.0	Yes	3.5				
12	9.2	4.5		7.9				
13	9.1	4.45		7.8				
14	10.0	5.31		8.6				
15	10.0	5.35		8.7				
16	10.1	5.43		8.7				
17	11.4	7.41		10.4				
18.	11.8	7.41		10.4				
19	11.9	7.57		13.1				
20	17.2	7.11		25.2	34.3		Yes	Igniter element burnout
21	22.7	8.61		2.1	N/A		N/A	No pilot flow
22	16.7	8.69		1.3	N/A		N/A	No pilot flow

Table 7. (Continued)

Test No.	Premixer			Pilot Element				Comments
	Pressure, psia	Mixture Ratio	Combustion Wave Obtained	Precombuster Pressure, psia	Initial Mixture Ratio	Final Mixture Ratio	Pilot Ignition Obtained	
23	15.1	8.86	Yes	3.6	7.35	7.3	No	No pilot flow
24	20.6	5.14		1.5	N/A	N/A	N/A	
25	27.7	3.00		2.1	N/A	N/A	N/A	
26	27.5	2.99		6.7	2.5	2.45	Yes	
27	27.3	2.89		7.0	2.43	1.15		Pilot ignition limits survey
28	27.5	2.93		7.2	2.45	1.15		
29	27.9	2.93		7.5	2.45	1.15		
30	24.0	1.96	No	N/A	N/A	N/A	N/A	
31	25.4	2.46	Yes	6.8	2.18	1.10	Yes	
32	24.7	2.13	No	N/A	N/A	N/A	N/A	
33	26.6	2.54	Yes	7.2	2.15	1.10	Yes	
34	25.4	2.21	No	N/A	N/A	N/A	N/A	
35	26.0	2.41	Yes	7.1	2.03	1.10	Yes	
36	26.6	2.40		7.0	2.03	1.10		
37	26.1	2.38		7.1	2.03	1.10		
38	23.7	4.08		6.2	3.40	1.55		
39	21.5	4.90		5.7	4.12	1.80		
40	28.0	5.06		7.5	4.23	1.80		
41	18.9	2.30	No	N/A	N/A	N/A	N/A	
42	25.9	2.39	Yes	7.0	2.03	1.05	Yes	
43	24.5	2.45	Yes	6.6	2.06	1.05	Yes	
44	22.0	2.36	No	N/A	N/A	N/A	N/A	

Table 7. (Continued)

Test No.	Premixer			Pilot Element				Comments
	Pressure, psia	Mixture Ratio	Combustion Wave Obtained	Precombuster Pressure, psia	Initial Mixture Ratio	Final Mixture Ratio	Pilot Ignition Obtained	
45	22.7	2.34	Yes	6.2	1.99	1.05	Yes	Pilot ignition limits survey
46	21.9	2.30		6.0	1.95	0.80	No	
47	21.8	2.36		6.0	1.99	0.80	No	
48	27.1	3.01		7.1	2.47	1.40	Yes	
49	23.3	2.00	No	N/A	N/A	N/A	N/A	Spark signal 5 milliseconds after oxidizer valve closed
50	25.5	2.44						
51	26.2	2.69						
52	26.9	2.97						
53	26.9	2.94						
54	27.1	3.01						
55	27.1	3.00	Yes	7.1	2.49	1.14	Yes	Spark signal 40 milliseconds before oxidizer valve closed
56	23.1	2.02	No	6.1	N/A	N/A	N/A	
57	25.4	2.56	Yes	6.6	2.13	1.00	Yes	
58	25.2	2.53	Yes	6.7	2.11	0.98	Yes	
59	24.8	2.45	Yes	6.4	2.06	1.33	Yes	
60	14.2	2.28	No	3.6	N/A	N/A	N/A	
61	14.5	2.69	Yes	3.7	2.08	1.12	No	
62	15.2	3.09	Yes	3.9	2.60	2.13	Yes	
63	--	--	--	--	--	--	--	Test invalid
64	13.1	3.00	Yes	3.5	2.56	1.39	No	
65	13.5	3.27		3.5	2.74	1.49	No	
66	13.9	3.37		3.5	2.87	1.41	No	

Table 7. (Continued)

Test No.	Premixer			Pilot Element				Comments
	Pressure, psia	Mixture Ratio	Combustion Wave Obtained	Precombuster Pressure, psia	Initial Mixture Ratio	Final Mixture Ratio	Pilot Ignition Obtained	
67	14.3	3.65	Yes	3.5	3.06	1.54	No	
68	14.6	3.83		3.6	3.22	2.80	Yes	
69	11.8	3.75		2.8	3.22	1.74	No	
70	12.1	4.05		2.9	3.43	1.87		
71	12.6	4.33		3.0	3.66	1.93		
72	12.8	4.55		3.1	3.85	1.98		
73	13.0	4.70		3.2	3.98	2.06	No	
74	13.0	4.72		3.2	3.98	3.48	Yes	
75	10.3	4.83		2.4	4.06	2.42	No	
76	10.7	5.15		2.5	4.30	2.64		
77	11.0	5.52		2.6	4.65	2.76		
78	11.4	6.12		2.7	5.07	3.15		
79	11.9	6.51		2.9	5.45	3.31		
80	12.0	6.80		3.0	5.71	3.32		
81	13.1	8.18		3.3	6.63	5.86	Yes	
82	25.0	2.39		0.6	2.0	N/A	No	
83	25.7	2.60		0.6	2.2	N/A		
84	26.1	2.68		0.7	2.3			
85	22.3	4.08		0.6	3.50			
86	24.6	2.45		2.0	2.10			
87	22.3	4.15		1.8	3.60			
88	24.7	2.45		7.2	2.09	1.22	Yes	Alternating tests on two elements
89	13.5	3.71		3.7	3.16	1.05	No	

Table 7. (Continued)

Test No.	Premixer			Pilot Element				Comments
	Pressure, psia	Mixture Ratio	Combustion Wave Obtained	Precombuster Pressure, psia	Initial Mixture Ratio	Final Mixture Ratio	Pilot Ignition Obtained	
90	13.3	3.35	Yes	3.6	2.92	0.93	No	Alternating tests on two elements
91	12.6	3.00		3.5	2.58	0.99		
92	12.3	2.75		3.4	2.30	0.85		
93	24.6	2.42		6.7	2.06	1.49	Yes	
94	23.2	2.47		7.1	2.10	1.41		Simultaneous ignition of two elements on tests 94 through 106.
				6.4	2.06	1.53		
95	23.2	2.45		7.2	2.08	1.34		
				6.5	2.04	1.49		
96	23.0	2.44	No	N/A	N/A	N/A	N/A	Delayed spark 15 milliseconds from oxidizer valve close
97	23.2	2.44	Yes	7.2	2.07	1.32	Yes	Advanced spark to 5 milliseconds prior to oxidizer valve closed
				7.6	2.04	1.47		
98	23.3	2.49		7.2	2.09	1.26		Advanced spark to 15 milliseconds
				6.5	2.05	1.39		
99	23.3	2.44		7.3	2.07	1.23		Advanced spark to 35 milliseconds
				6.6	2.04	1.36		
100	23.3	2.44		7.3	2.07	1.15		Advanced spark to 55 milliseconds
				6.5	2.03	1.29		
101	22.6	2.30		7.0	1.94	1.12		
				6.3	1.90	1.23		
102	21.9	2.10	No	N/A	N/A	N/A	N/A	
103	23.2	2.41	Yes	13.0	--	0.37	Yes	
				10.5	0.60	0.39	Yes	

Table 7. (Concluded)

Test No.	Premixer			Pilot Element				Comments
	Pressure, psia	Mixture Ratio	Combustion Wave Obtained	Precombuster Pressure, psia	Initial Mixture Ratio	Final Mixture Ratio	Pilot Ignition Obtained	
104	25.7	3.10	Yes	14.1	--	--	Yes	
				11.6	0.75	0.50		
105	27.8	3.79		15.3	--	--		
				12.6	0.98	0.60		
106	31.3	4.90		16.9	--	--		
				13.8	1.06	0.76		

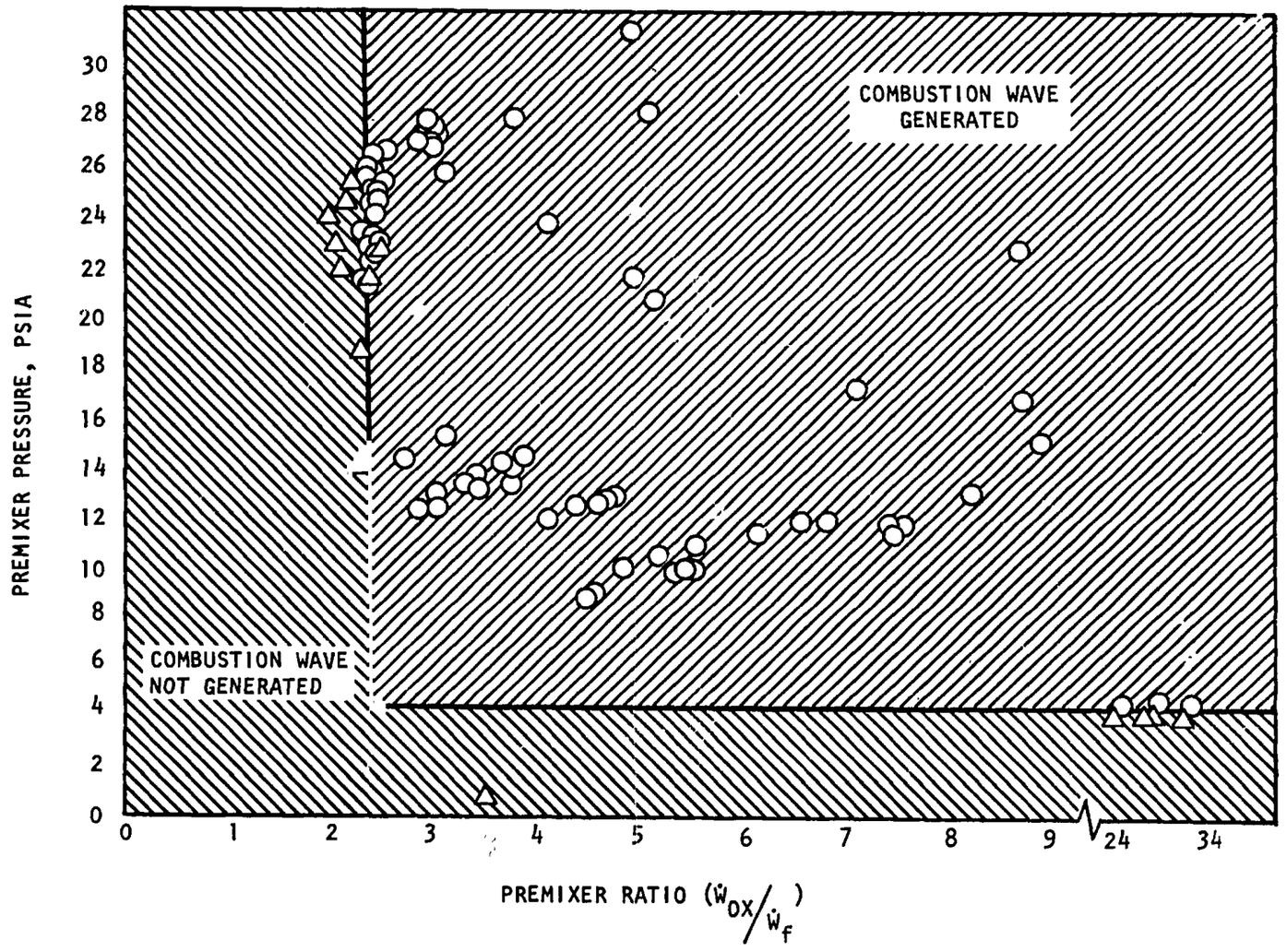

Figure 44. Combustion Wave Map

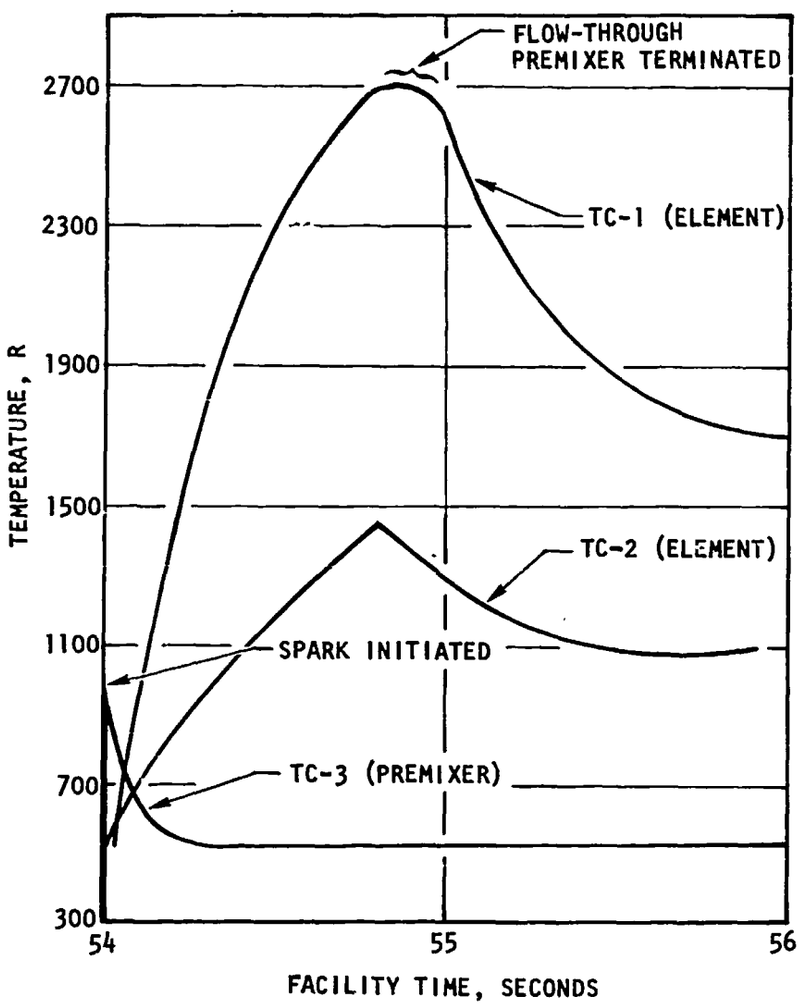

Figure 45. Ignition Temperature vs Time

A pilot ignition map is presented in Fig. 46 where precombustor pressure is plotted against pilot element mixture ratio. If it is assumed that the combustion wave ignites local mixture ratio at the pilot annulus exit plane, the data indicate that pilot ignitions at mixture ratios less than 1.0 can be obtained in a 1-atmosphere environment. No pilot ignitions were obtained below 3 psia precombustor pressure. Since the test setup required a precombustor surrounding the igniter tip to control the environmental pressure, it is possible that the combustion wave ignited the combined mixture ratio of core and pilot annulus flows in the precombustor. A pilot ignition map with precombustor pressure plotted against the combined precombustor mixture ratio is presented in Fig. 47. The connected data points show the precombustor conditions at pilot ignition and at stabilized operation following premixer oxidizer valve closure. If it is assumed that the combustion wave ignited the combined precombustor mixture ratio, a mixture ratio in excess of 2.0 is required for pilot ignition, and a mixture ratio greater than 1.0 is required to sustain pilot ignition. Until testing can be accomplished without a precombustor, the more conservative assumption will be used to design the No. 2 test bed igniter, i.e., a pilot mixture ratio greater than 2.0 will be provided.

Valve Sequencing. The sequencing of the premixer oxidizer valve was investigated on tests 49 through 58 and tests 96 through 102. The test results (Table 7) show that a combustion wave could not be generated if the oxidizer valve was closed prior to the spark signal. Delaying the oxidizer valve between 5 and 55 milliseconds from the spark signal resulted in no hardware damage and consistent combustion wave generation. These results led to the incorporation of a check valve in the premixer oxidizer line on the No. 2 test bed design to prevent hot-gas backflow into the main oxidizer ducting, and eliminated concern about the effect of critical valve timing on hardware integrity.

Dual Element Tests. Tests 94 through 106 were conducted with two igniter elements attached to the premixer. Nine successful pilot ignitions were obtained and ignition was successfully sustained. A typical dual igniter data trace is presented in Fig. 48. On this test (95), the premixer mixture ratio was 2.45 at a pressure of 23.2 psia, and the elements were at a mixture ratio of approximately 2.0 at a pressure of 7 psia. The temperature measurements shown were taken in the

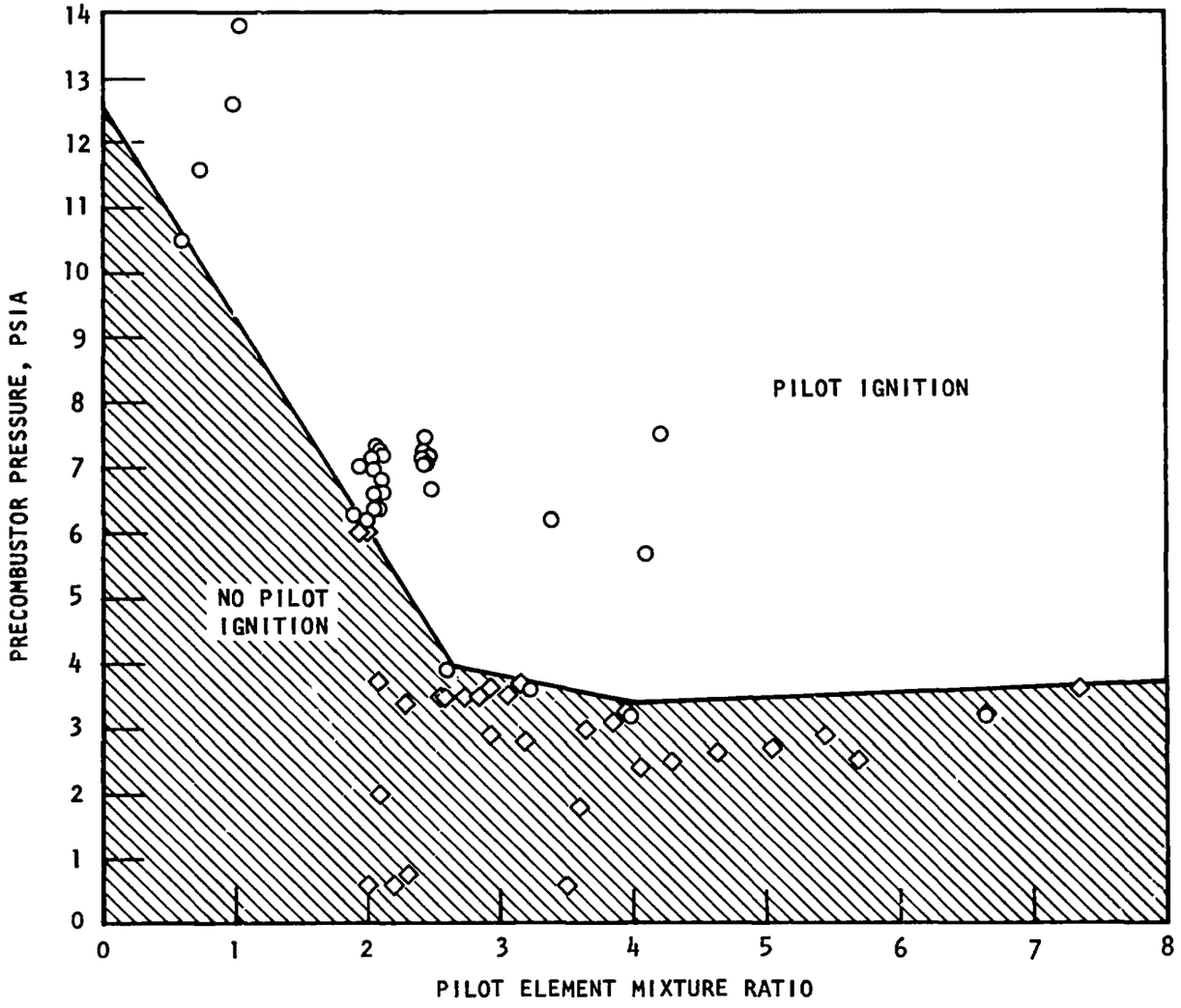

Figure 46. Pilot Ignition Map (Precombustor/Pilot Element)

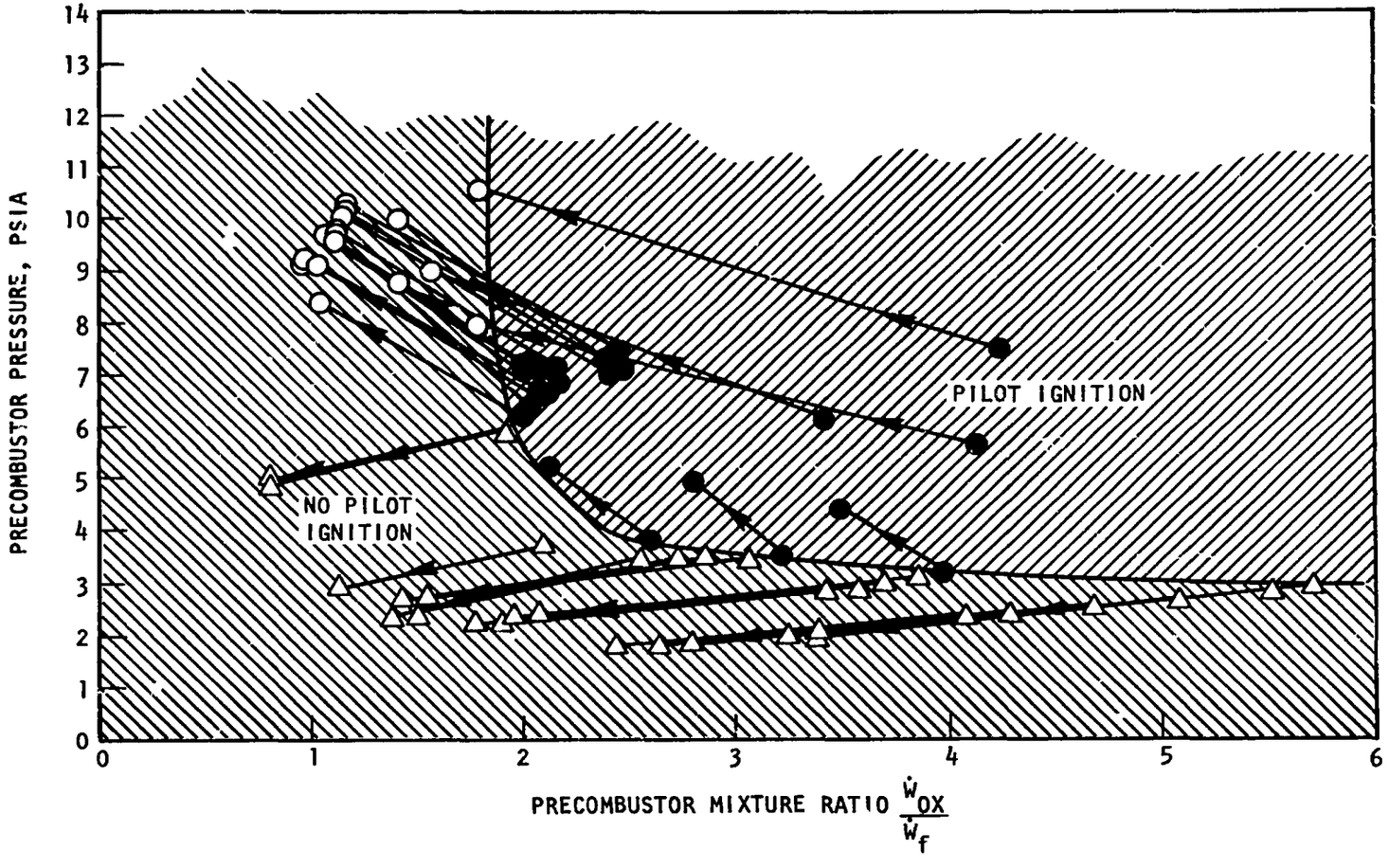

Figure 47. Pilot Ignition Map (Precombustor/Precombustor)

FOLDOUT FRAME 1

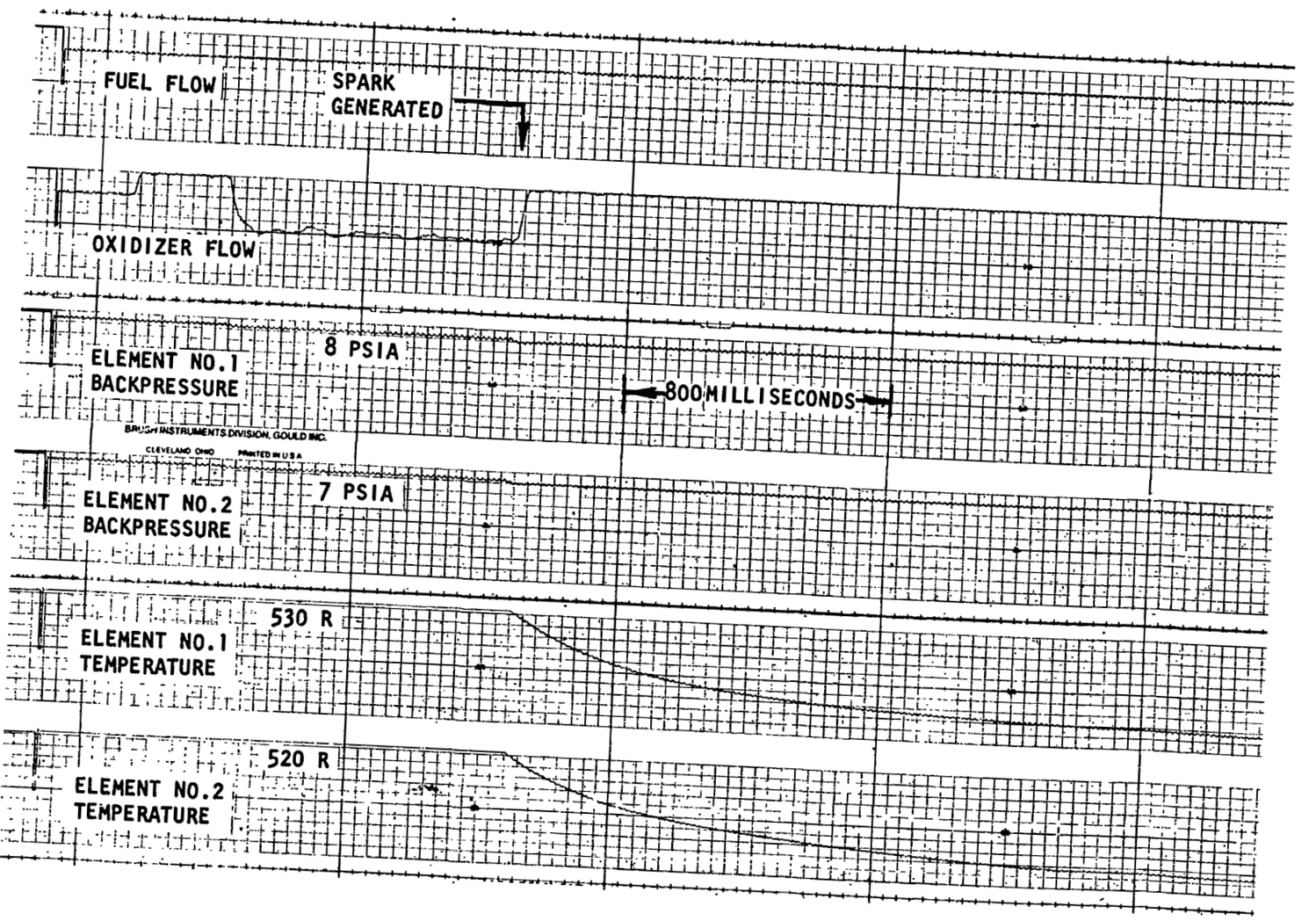

FOLDOUT FRAME 2

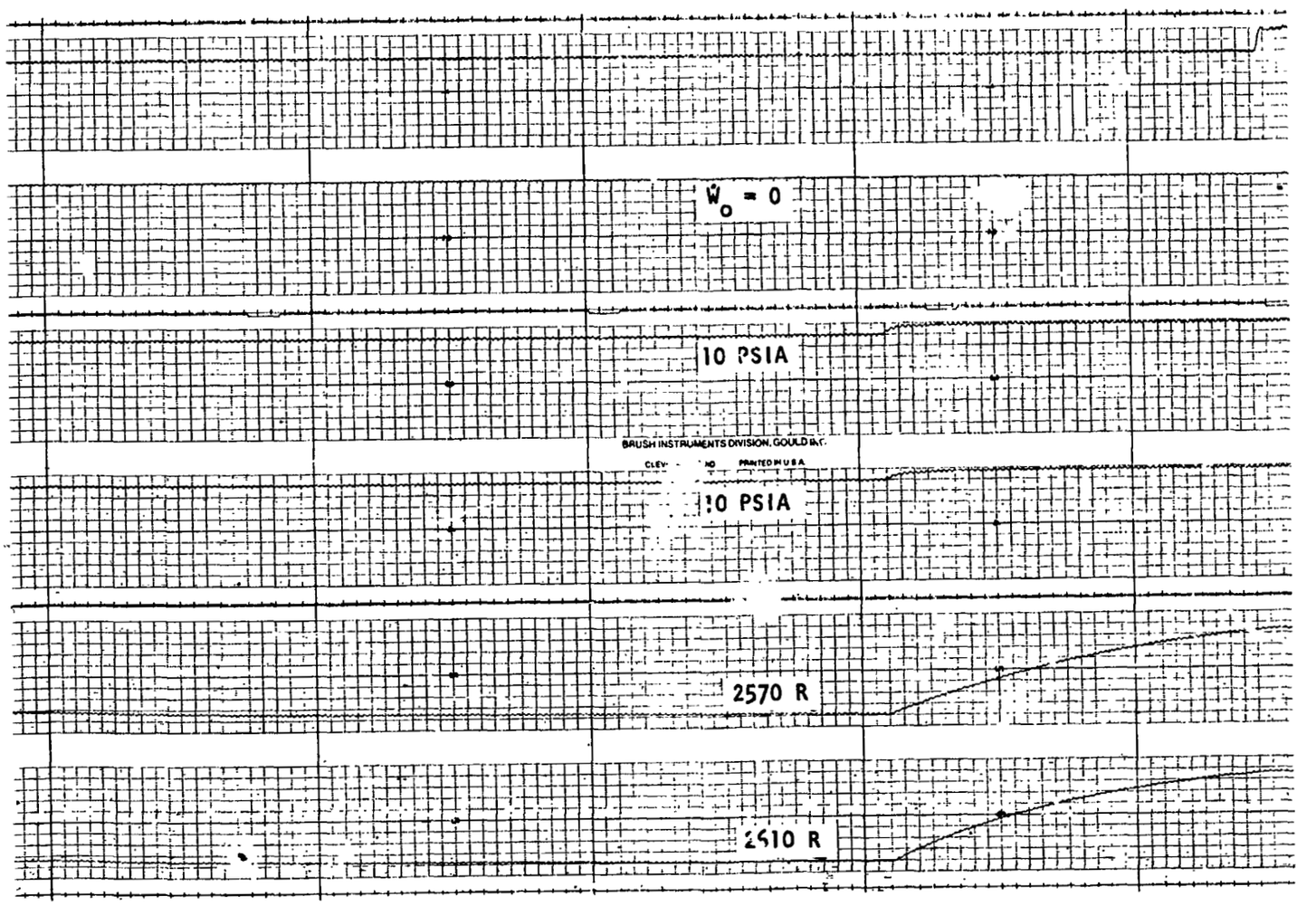

Figure 48. Dual-Element Test Results

precombustor throats and indicate sustained pilot ignitions following premixer oxidizer valve closure. Temperatures of approximately 2600 R were sustained in the elements for 4.3 seconds with no hardware damage. Fuel flow through the element core for approximately 1 second after pilot flow termination provided the necessary purge for element and precombustor cooling.

OPTIMUM COMBUSTION WAVE IGNITION SYSTEM

Because of the common igniter port requirement on the No. 2 test bed, the design of the Combustion Wave igniter was compromised to allow interchangeability with the Resonant Flow igniter. The ignition system and manifolding design was also compromised to allow a common start sequence with the Resonant Flow system. An optimized Combustion Wave ignition system (i.e., an ignition system design and engine start sequence that are mutually dependent) greatly simplifies the combustion wave concept.

The optimized Combustion Wave ignition system, schematically shown in Fig. 49, comprises a spark-detonated premixer unit supplied with propellant from the turbopump discharge ducting. As in the No. 2 test bed design, the propellants are controlled with solenoid valves and the detonation is isolated from the discharge ducting with check valves in the propellant lines. Unlike the No. 2 test bed design, pilot propellant is supplied from the thrust chamber injector manifolds, so that only a single ignition manifold is required on the engine, i.e., the manifold to distribute the combustion wave to the individual thrust chamber combustors. The installation of a combustion wave tube in a thrust chamber combustor is depicted in Fig. 50. The tube is installed coaxially through an existing injector oxidizer post and pilot flows are provided by the standard injector element.

The engine start sequence for this ignition system is presented in Fig. 51. At the engine start signal, the main fuel valve and igniter fuel valve are opened and a 1.0-second fuel lead is provided for hardware chilldown. At the mainstage start signal, the main oxidizer valve is opened to the 15-degree position and the igniter oxidizer valve is opened. Oxidizer is allowed to flow under tank head to

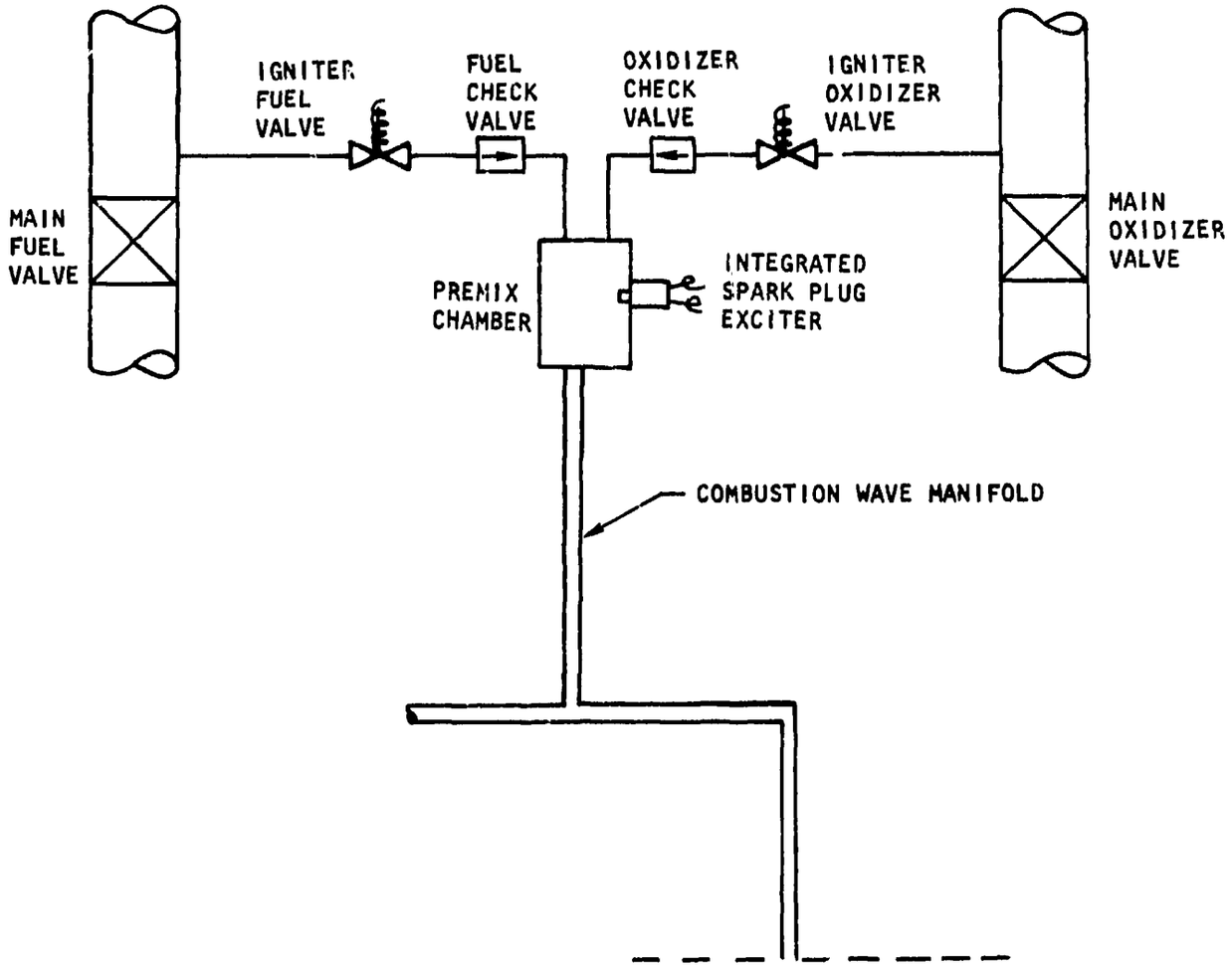

Figure 49. Optimized Combustion Wave Ignition System

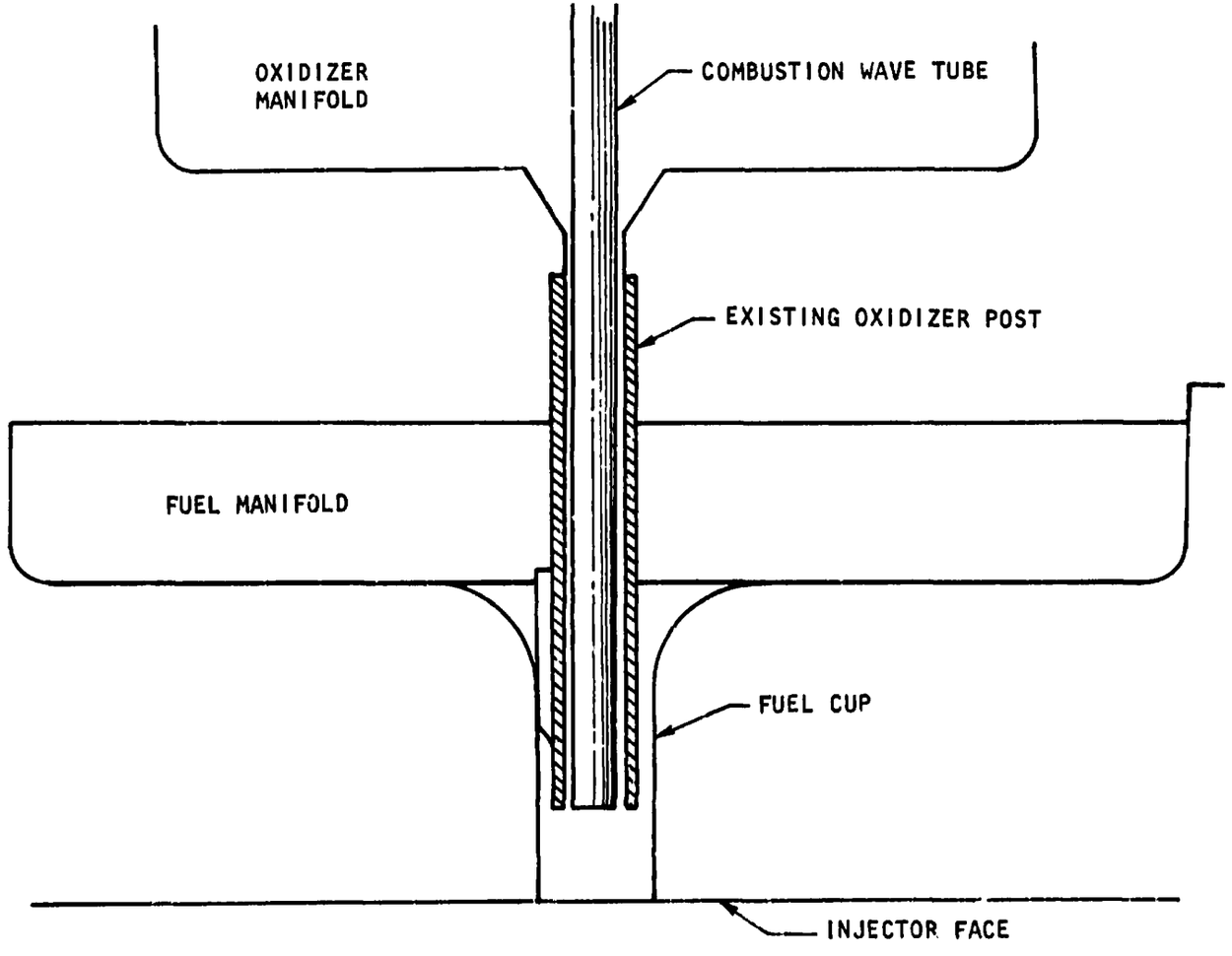

Figure 50. Optimized Combustion Wave Igniter Element

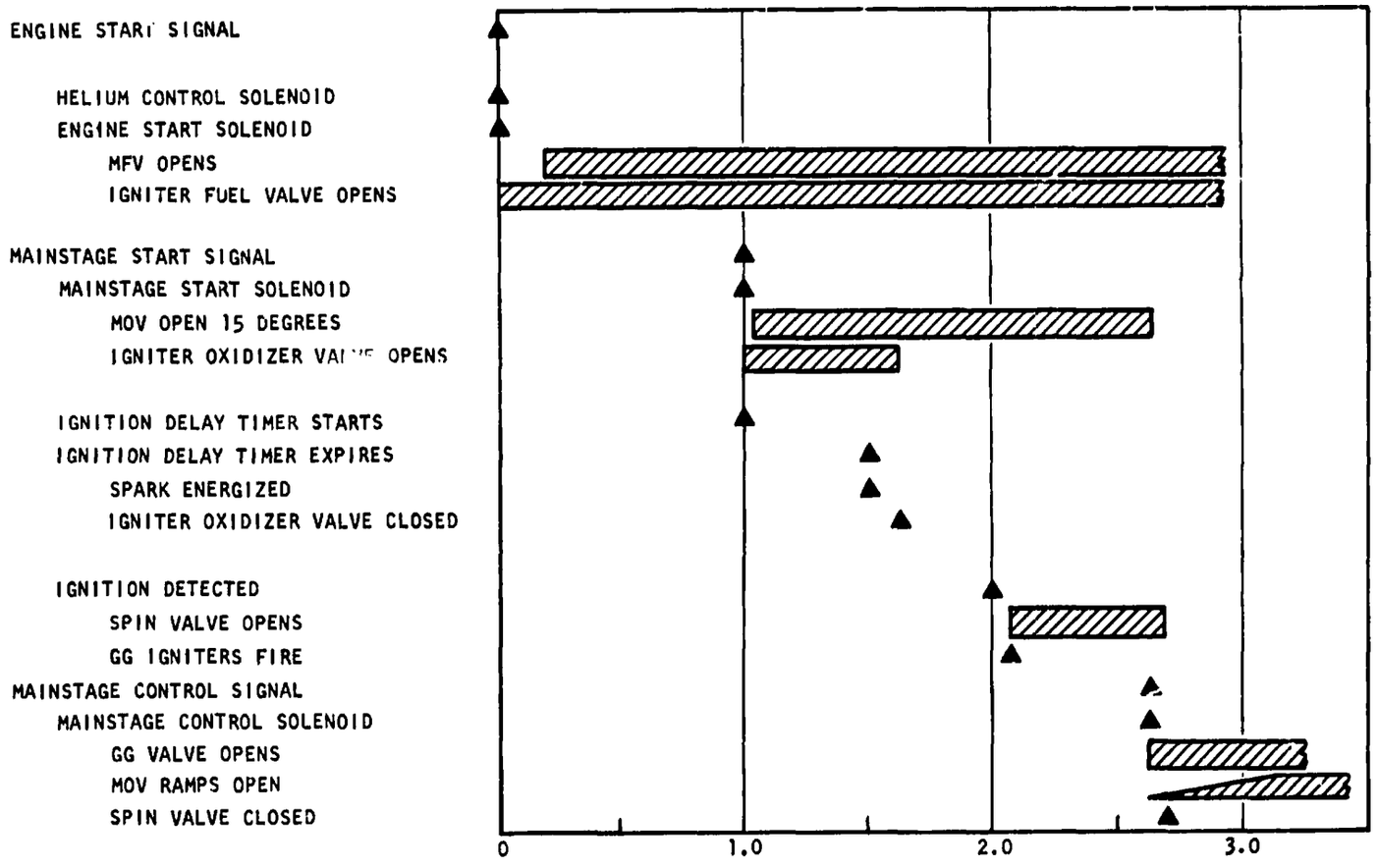

Figure 51. Optimized Combustion Wave Igniter Engine Start Sequence

the thrust chamber manifolds and combustion wave premixer for 500 milliseconds to provide an ignitable injector mixture ratio and to prime the combustion wave manifold. Upon expiration of the 500-millisecond ignition delay timer, the spark is energized and the combustion wave is generated. Upon pilot ignition and ignition detection, the spin valve is opened, the gas generator is fired, and the engine is allowed to bootstrap into mainstage.

CONCLUSIONS

The Combustion Wave Igniter proved feasible for a multiple-combustor ignition system. The following conclusions are drawn from the test effort:

1. The combustion wave process can be utilized to ignite multiple combustors from a single ignition energy source.
2. A low-pressure (30 psia > p > 5 psia) premixed propellant is adequate for establishing a combustion wave when sufficient induction length is available.
3. The combustion wave can ignite pilot elements at varying distances (greater than the induction length) from the ignition energy source.
4. For the igniter element tested (0.131-inch-diameter combustion wave tube, and 48 to 60 inches induction length), a premixed propellant mixture ratio greater than 2.3 is required to initiate a combustion wave.
5. A pilot element mixture ratio greater than 2.0 is required for pilot ignition.
6. The ignition element design demonstrated sustained operation without damage.

REFERENCES

1. Thompson, P. A.: "Jet-Driven Resonance Tube," AIAA Journal V. 2 No. 7, July 1964, p. 1230-1233, See also Thompson P. A.: Resonance Tubes, Sc.D. Dissertation, Massachusetts Institute of Technology, 1961.

2. Shapiro, A. H.: "On the Maximum Attainable Temperature in Resonance Tubes," Readers' Forum, Journal of Aero Space Sciences, V. 27, 1960, p. 66-67.

3. Kang, Sang-Wook: Resonance Tubes, Ph.D. Thesis, Rensselaer Polytechnic Institute, Troy, New York, 1964.

4. McAlevy, R. F., III and A. Pavlak: "Tapered Resorance Tubes: Some Experiments," AIAA Journal, V. 8, No. 3, March 1970, p. 571-572.

5. Walker, D. W., et al.: Investigation of the Ignition Properties of Flowing Combustible Gas Mixtures, Air Force Aero Propulsion Laboratory, Wright-Patterson Air Force Base, AFRPL-TR-69-82, September 1962.

6. Diehl, L. A.: An Experimental Investigation of the Role of Resonance Heating in the Autoignition of Flowing Combustible Gas Mixture, Ph.D. Dissertation, The Ohio State University, Columbus, Ohio, 1970.

7. Falkenstein, G. L. and R. D. Paster: Hydrogen-Oxygen APS Engines Program, Third Quarterly Technical Progress Narrative, NASA Contract NAS3-14352, Rocketdyne Report ASR71-105, April 1971.

8. Lauffer, J. R.: Space Shuttle Auxiliary Propulsion Ignition System, NASA Report CR-R-8724, NASA Contract NAS3-14351, June 1971.

9. Sprenger, H.: "Uber Thermische Effeckte in Resonanzrohren," Mitteilung aums dem Institut für Aerodynamik, Mr. 21, Verlag Leemann, Zurich, 1954, p. 18-35.

10. Mallard, E. and H. LeChatelier: Compt. Rend. Acad. Sci, Paris 93, 145, 1881.

11. Berthelot, M. and P. Vieille: Compt. Rend. Acad. Sci., Paris 93, 18, 1881.

12. Chapman, D.: Philosophy Magazine 47, 90, 1899.

13. Jouguet, E.: Mathamatique, 6, 347, 1905.

14. Williams, F.: Combustion Theory, Addison-Wesely Publishing, Reading, 1965.

15. Busch and Laderman: Computations of Gaseous Detonation Parameters, IER Report No. 64-12.

16. Foreman, K., H. Pevney, and R. MacMillan: "Parametric Studies of Strong Gaseous Detonations," Detonation and Two Phase Flow, Academic Press, New York, 47, 1962.

17. Bollinger, L., M. Fong, and R. Edse: "Experimental Measurements and Theoretical Analysis of Detonation Induction Distances," ARS Journal, May 1961.

18. Richmond, J.: "Spectrographic Analysis of Detonation Wave Structures," Detonation and Two-Phase Flow, Academic Press, New York, 1961.

APPENDIX A

ADVANCED IGNITER ENERGY REQUIREMENTS

The similarity of design parameters on the No. 2 test bed injectors and the J-2S open-compartment injector prompted a study of J-2S engine operating conditions at main propellant ignition. A test series conducted under simulated altitude conditions at AEDC was selected for the ignition study since low-range instrumentation was used in conjunction with low-thrust, idle-mode testing. The test series, J4-1001-6A through J4-1001-15C, was run on J-2S engine J-112 during the months of August through October 1969. The ignition test results are discussed in the following paragraphs.

J-2S IGNITION CONFIGURATION

The J-2S injector incorporates 614 coaxial elements arranged in a concentric circular pattern around a central augmented spark igniter (ASI). The engine is ignited under vehicle tank head pressure, and incorporates a fuel lead followed by the simultaneous introduction of oxidizer to the main injector and the ASI controlled by the idle mode oxidizer valve (IOV). The ASI is spark-ignited with a spark frequency of 50 sparks per second and the sparks are energized at engine start. During the test series studied, low-range pressure transducers were used to measure propellant injection pressures in the ASI and main injector, and injector-end chamber pressure. Propellant temperature measurements were obtained in the main injector fuel and oxidizer manifolds, at the pump discharges, and in the ASI feed lines.

DATA ANALYSIS

Since flowrates were not measured during the test series, a combination ASI and main chamber balance was formulated and programmed on the General Electric computer. A second program, using inputs from the balance program, was formulated to thermochemically determine the heat output of the ASI. Because the instant of

main propellant ignition was of primary interest, the data were sampled in 10-millisecond increments from the engine start signal until main propellant ignition (MPI) was detected by an abrupt increase in the slope of main chamber pressure. A typical data plot is presented in Fig. A-1. Following engine start signal the main fuel valve and IOV are opened and propellants are admitted under tank head pressure to the main injector and the ASI injector. Main chamber pressure increases with fuel flow until MPI occurs and an abrupt chamber pressure increase is noted.

Measured and calculated main chamber and ASI propellant conditions at MPI are presented in Table A-1. All MPI's occurred with gaseous propellants in the main chamber and ASI feed lines. No ignitions occurred at main injector mixture ratios of less than 0.44.

Although many ignition parameter correlations were attempted, only two proved fruitful. The ratio of ASI total propellant flowrate to main injector propellant flowrate proved to be relatively constant at MPI (Fig. A-2) regardless of the injector mixture ratio. The mean value of $\dot{w}_{ASI}/\dot{w}_{INJ}$ for these tests was approximately 0.005. Another correlation was obtained plotting the ASI heat output per pound of injector flow versus injector mixture ratio (Fig. A-3). The data indicate that more heat output is required from the igniter as mixture ratio increases. Since total injector flow is relatively constant, the decrease in flammability with mixture ratio indicates that propellant mixing (mostly a function of fuel momentum) has a profound effect on the required ignition energy.

NO. 2 TEST BED REQUIREMENTS

Because of injector element similarity, the ignition parameters obtained for the J-2S engine will be used for the No. 2 test bed. In the J-2S injector, the igniter is surrounded by 10 of the 614 total elements. If it is assumed that MPI is initiated at the elements surrounding the ignition device, then the ratio of igniter flow to surrounding element flow is:

$$\frac{\dot{w}_{IG}}{\dot{w}_{EL}} = \frac{\dot{w}_{ASI}}{\dot{w}_{INJ}} \frac{\text{(Total Elements)}}{\text{(Surrounding Elements)}} = (0.005)\frac{(614)}{(10)} = 0.3$$

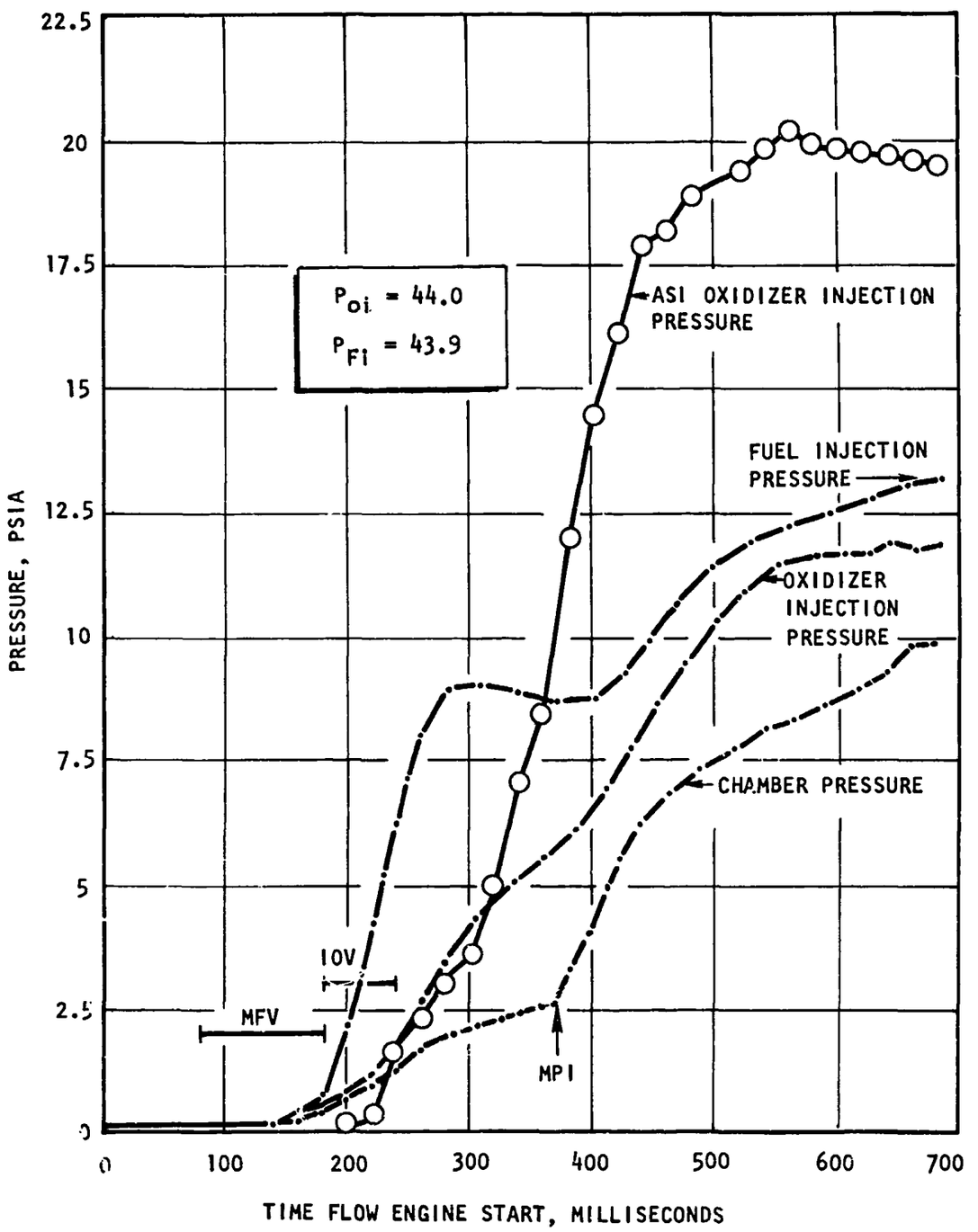

Figure A-1. J-2S Ignition Parameters

Table A-1. J-2S Conditions at Main Propellant Ignition

Test No.	Main Oxidizer Injection Temperature, R	Main Fuel Injection Temperature, R	Main Chamber Pressure, psia	Main Chamber Total Flow,* lb/sec	Main Chamber Mixture Ratio*	ASI Oxidizer Injection Temperature, R	ASI Fuel Injection Temperature, R	ASI Chamber Pressure,* psia	ASI Mixture Ratio*	ASI Flow* / Chamber Flow	Q_{ASI},* Btu/sec	$\frac{Q_{ASI}}{\bar{w}_{INJ}}$
6B	423	524	3.5	2.08	0.93	423	455	5.5	0.94	0.0052	34	16.4
7B	445	552	3.8	2.16	1.18	445	507	5.6	1.27	0.0046	36	16.7
7C	437	498	3.3	3.76	0.44	437	394	7.3	0.47	0.0048	37	10.0
11A	317	555	2.7	2.35	1.31	317	417	6.5	1.55	0.0061	56	23.9
11B	473	512	2.9	2.44	0.69	473	328	5.0	0.54	0.0050	28	11.4
11C	336	529	3.1	2.26	0.88	336	285	6.5	0.86	0.0056	38	16.8
12A	241	543	2.5	2.37	1.14	241	383	7.8	1.74	0.0065	63	26.4
13A	404	519	3.2	2.37	0.67	404	302	5.8	0.42	0.0045	21	8.7
13B	398	486	3.0	2.35	0.65	398	357	5.0	0.60	0.0052	30	12.7
13C	426	506	3.5	1.90	0.61	426	326	4.9	0.44	0.0051	19	10.1
14A	419	531	1.6	1.55	1.41	419	490	3.8	1.33	0.0045	26	16.7
14B	360	200	2.5	2.83	0.64	360	225	4.9	0.47	0.0044	24	8.6
15A	403	510	3.6	2.12	0.72	403	198	5.0	0.54	0.0053	26	12.1
15B	362	192	2.6	2.70	0.58	362	235	5.5	0.63	0.0046	31	11.6
15C	317	428	2.0	1.85	0.85	317	295	6.0	0.60	0.0071	32	17.3

*Calculated Parameters

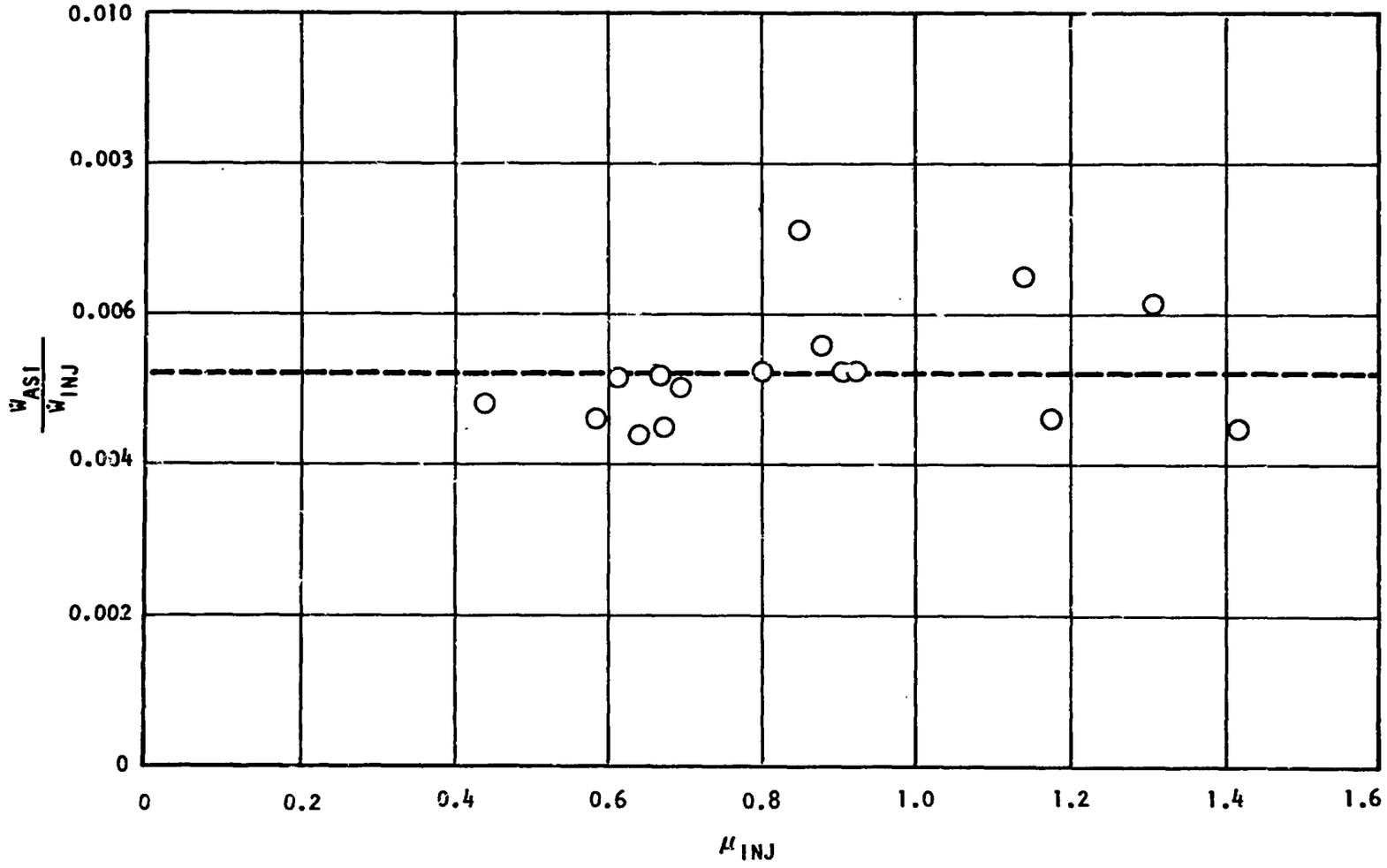

Figure A-2. Flowrate Ratio vs Injector Mixture Ratio at MPI

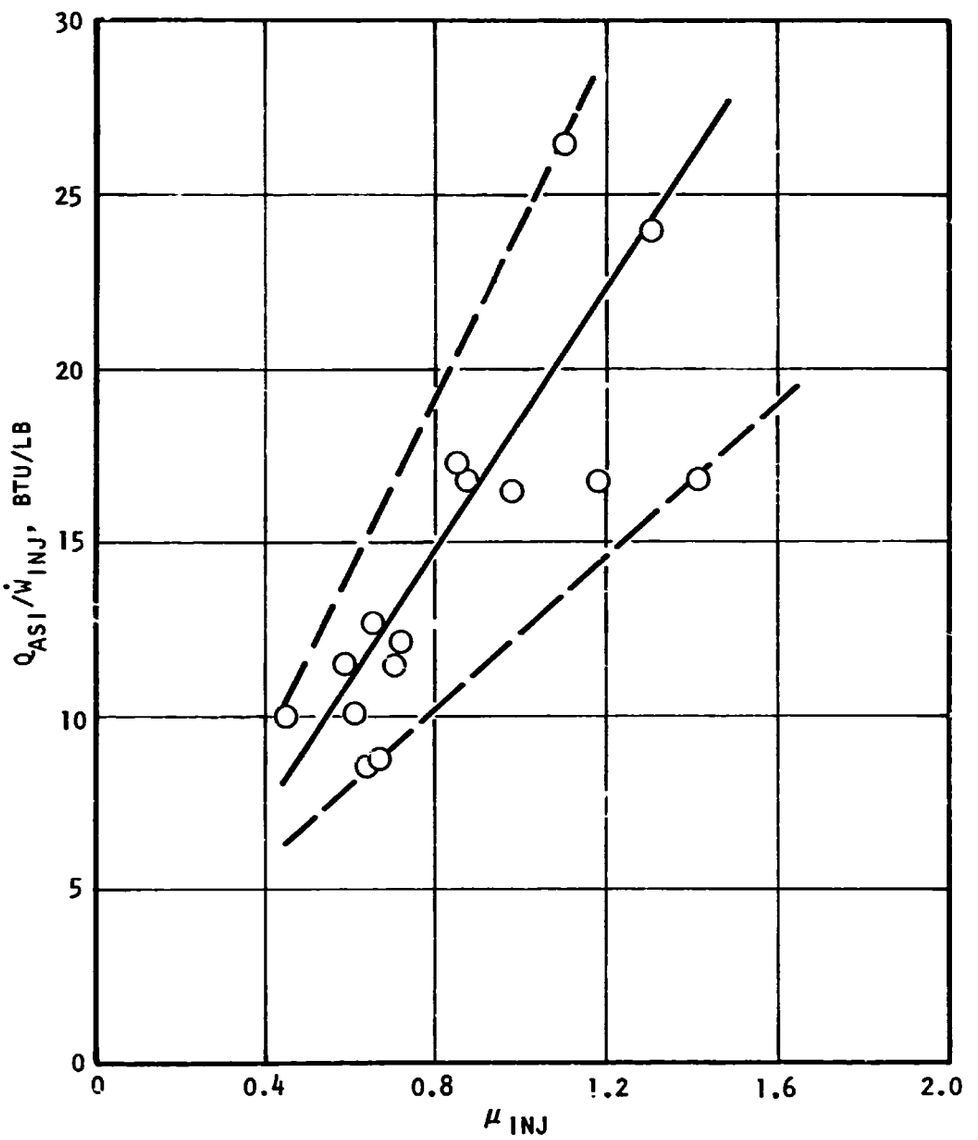
30
25
20
15
10
5
0
0
0.4
0.8
1.2
1.6
2.0
$Q_{ASI}/\dot{W}_{INJ}$, BTU/LB
μ_{INJ}

This ratio should be used for the No. 2 test bed igniter.

Start model studies indicate that the No. 2 test bed will have a maximum injector mixture ratio of 0.8 during the ignition stage. The ignition device should have a heat output per surrounding element of at least (Fig. A-3):

$$\frac{Q_{IG}}{\dot{w}_{EL}} = (15)\left(\frac{614}{10}\right) = 921 \text{ Btu/lb}$$

APPENDIX B

RELATED EXPERIENCE IN RESONANCE IGNITION

Under a NASA contract, Rocketdyne has recently completed an ignition study for the Space Shuttle Auxiliary Propulsion System (SS/APS).* During this contract both the spark and resonance igniters were investigated. The resonance ignition portion of the contractual effort was prompted by the requirement for an ignition system that would (1) have fast response (less than 50 milliseconds from command signal to 90 percent of full SS/APS engine thrust), (2) be simple and reliable (10^6 pulses during its life, and (3) eliminate radio frequency interference. Further impetus to the program was given by the fact that over 200 auxiliary thrustors will be required on the Space Shuttle Vehicle.

The SS/APS resonance igniter investigation was divided into three tasks, each of which was successfully completed. Task I involved preliminary design and analysis, and laboratory-type testing of the basic phenomena. Task II included "igniter only" hot firing and demonstration of igniter/thrustor ignition. Task III was related to ignition system design and analysis. In the following paragraphs, results of the first two tasks will be discussed.

TASK I

Tests were conducted using variable-geometry test hardware (Fig. B-1). During the initial heating evaluation tests, hydrogen was injected into the resonance cavity. A fast-response thermocouple was placed at the end of the resonance cavity to measure temperature response and absolute value of temperature. Resonance cavity configurations and other igniter variables (gap ratio and pressure ratio) were evaluated over a range of inlet pressures and flowrates. The geometry was optimized and temperatures up to 3000 R were recorded. Fast response

*See NASA Report CR-R-8274 (June 1971)

HARDWARE

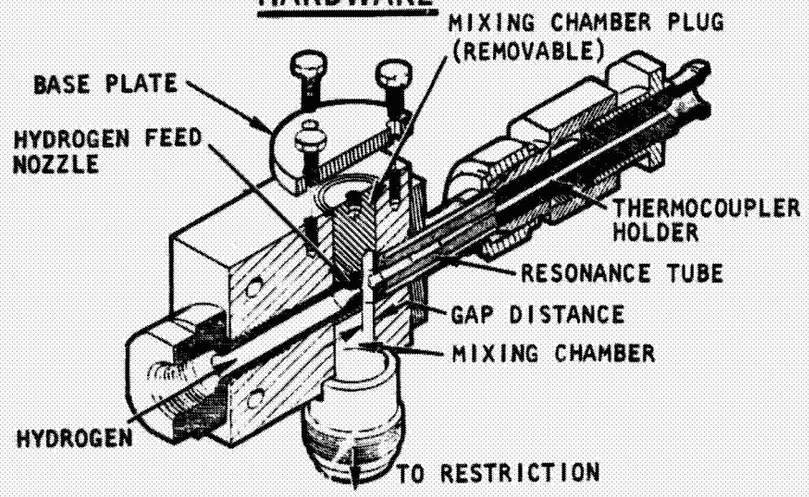

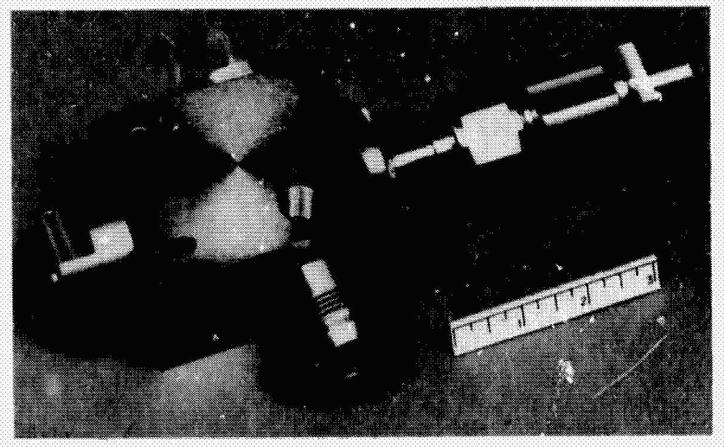

RESULTS

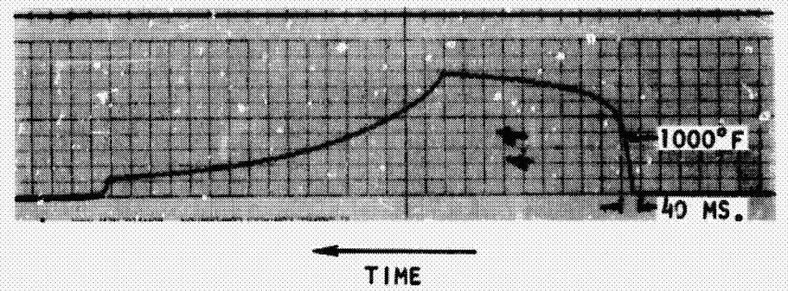

- GEOMETRY OPTIMIZED
- RESONANCE HEATING DEMONSTRATED (~ 3000°R)
- FAST RESPONSE DEMONSTRATED (1000°F IN ~ 20 MSEC.)

Figure B-1. Phenomena Testing (Model 1, Heating)

was indicated by reaching indicated temperatures of 1000 F in approximately 20 milliseconds (gas temperature was higher than that indicated by the thermocouple response).

The variable-geometry test hardware was also used for combustion tests with only minor modifications. An oxidizer valve was installed at the end of the resonance cavity where the thermocouple had been previously (Fig. B-2). One hundred six combustion tests were conducted. Hydrogen leads down to 3 milliseconds resulted in ignitions. Response of 0.020 to 0.030 second was obtained from electrical signal to 90 percent of igniter chamber pressure. A test record of a typical start transient (shown in Fig. B-2) demonstrates the rapid response of the autoigniter. Analysis of the chamber pressure trace indicates no ignition delay or pressure overshoot. The hydrogen lead (heating time) on this test was only 0.008 second. The basic feasibility of the concept was demonstrated with this workhorse-type hardware. These data were then used to design an igniter that would integrate into the SS/APS injector and thrust chamber.

TASK II

Resonance igniter design during this task was similar to the workhorse-type igniter (Fig. B-3); the resonance cavity and other critical dimensions were identical. Oxidizer used to cool the igniter was injected into the igniter exhaust at the thrustor injector face plane. One hundred ninety-four combustion tests were conducted over a range of inlet conditions and flowrates. Tests were conducted successfully with hydrogen propellant temperatures down to 201 R and oxygen propellant temperatures down to 277 R.

Analysis of a typical test record indicates the very rapid response of the autoigniter, which used a 0.004-second hydrogen lead (Fig. B-3). The autoigniter was tested with the high-pressure SS/APS thrustor assembly. Installation with the complete thrustor assembly at the CTL-4 facility is shown in Fig. B-4.

This test program was initiated with eight "igniter-only" tests at sea level to evaluate sequencing (all previous tests were conducted on an "igniter-only"

HARDWARE

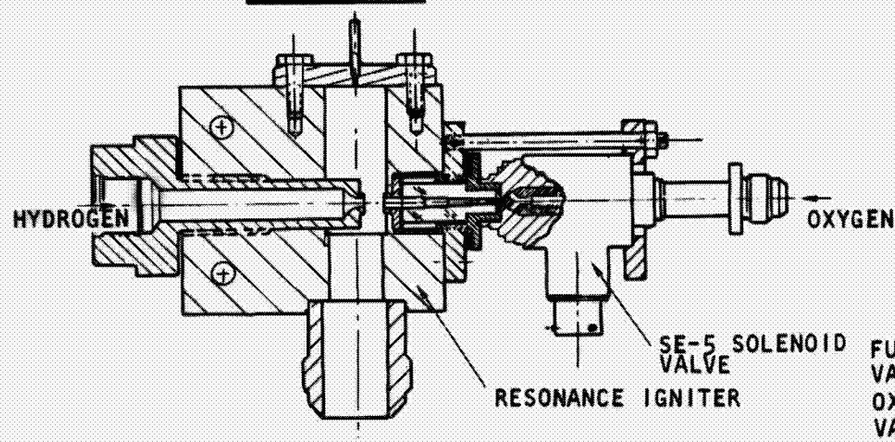

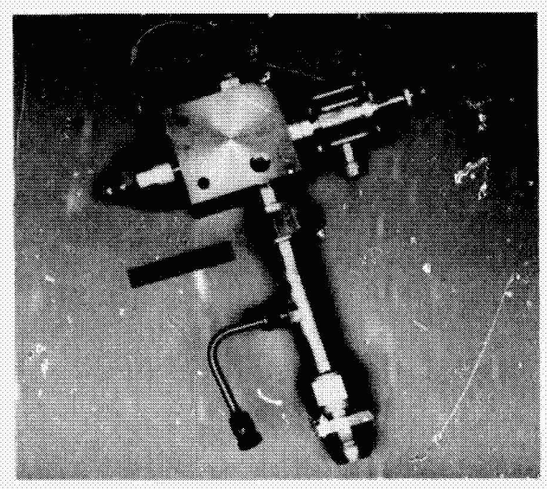

RESULTS

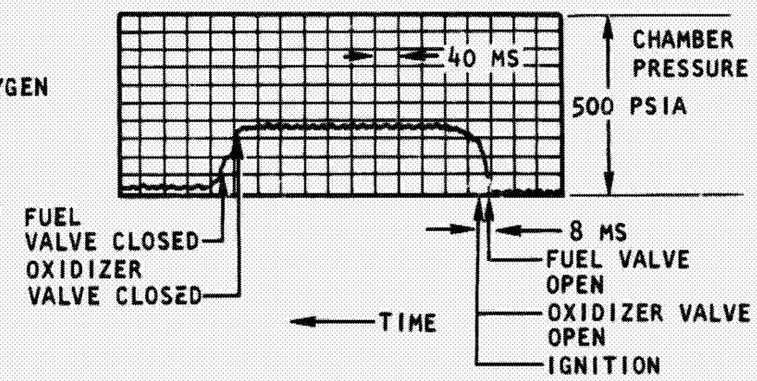

- 106 COMBUSTION TEST CONDUCTED
- RAPID RESPONSE (0.020 - 0.030 SEC)
- BASIC FEASIBILITY DEMONSTRATED
  - $\dot{W}$ = 0.04 LB/SEC
  - MR = 0.4 TO 1.0
  - PROP. TEMP DOWN TO 300°R

Figure B-2. Phenomena Testing (Mode II, Combustion)

HARDWARE

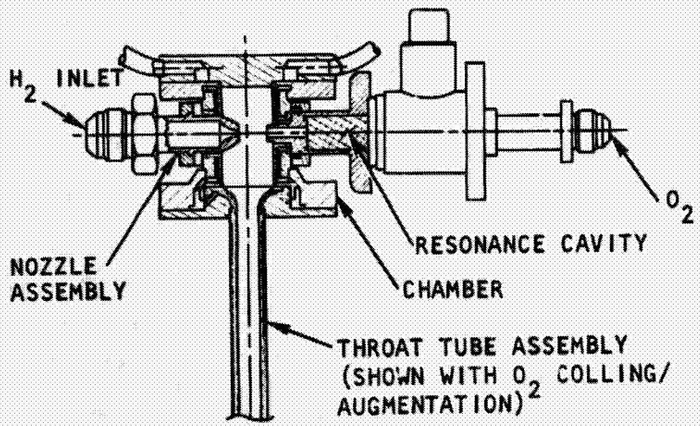

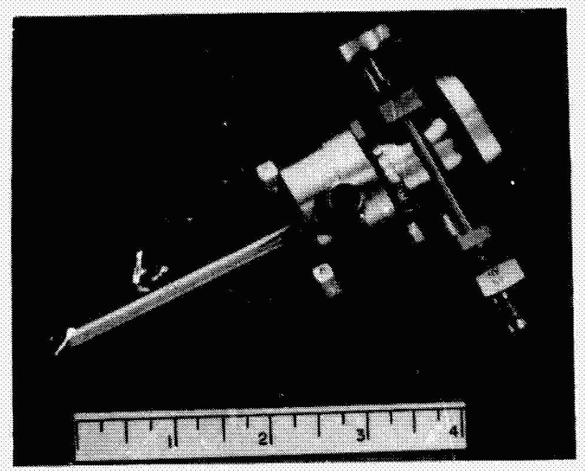

RESULTS

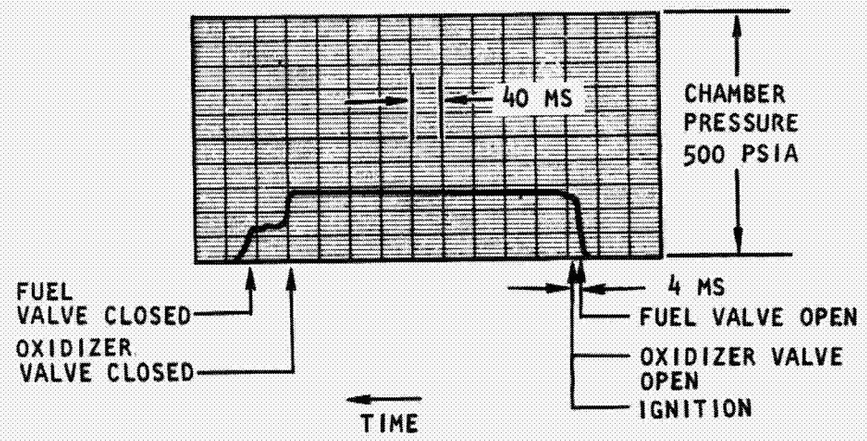

- 190 TESTS CONDUCTED
- RANGE OF PARAMETERS INVESTIGATED
  - MIXTURE RATIOS: 0.45 TO 3.1
  - PROPELLANT TEMPERATURE: 201 TO 540 R
  - PROPELLANT PRESSURES: 160 PSIA TO 335 PSIA

Figure B-3. Autoigniter ("Igniter-Only" Testing)

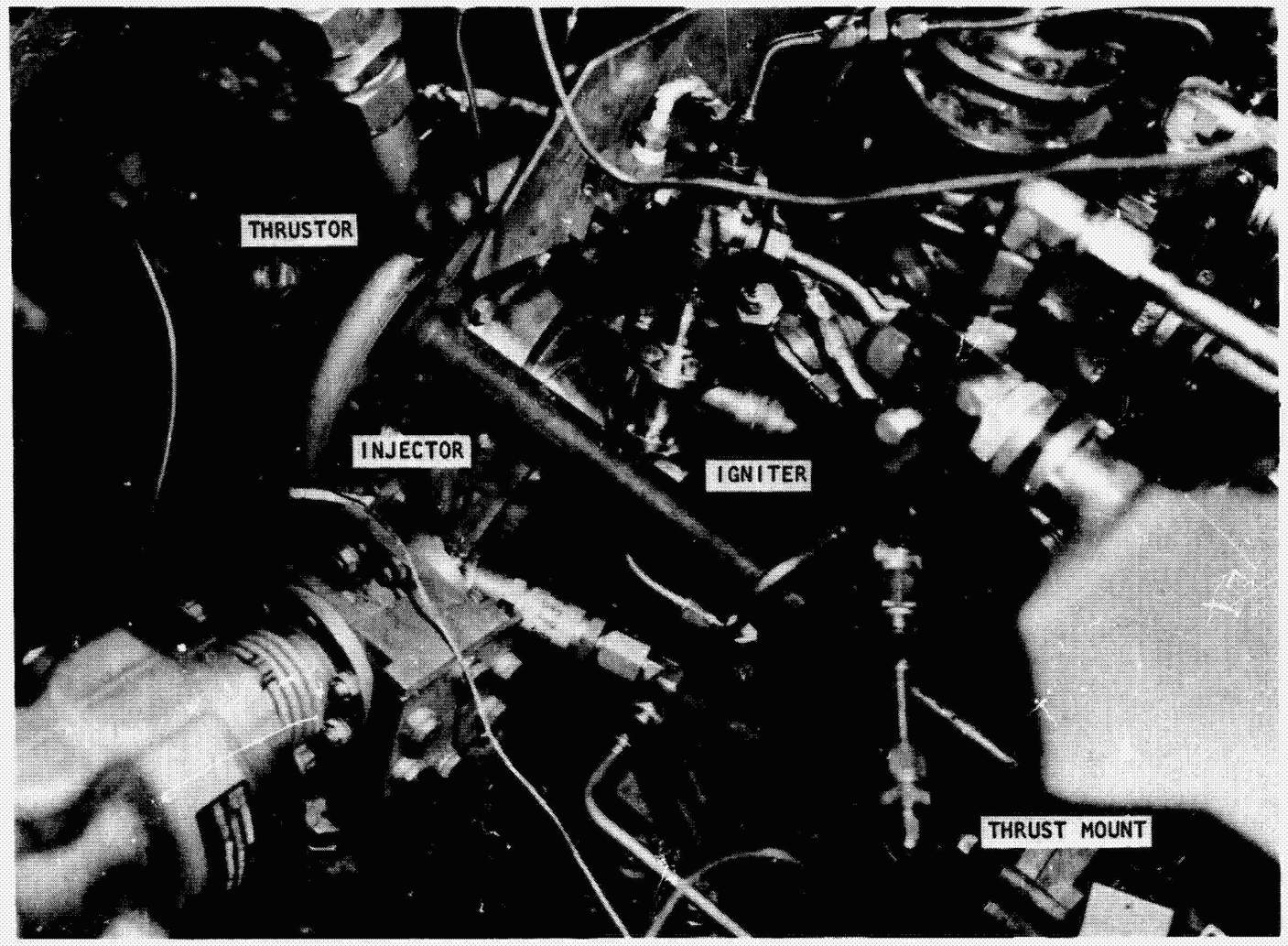

1ST43-3/17/71-S1C

Figure B-4. Thrustor/Igniter Test Setup

facility at altitude conditions). All eight tests resulted in rapid ignitions. A series of six tests was then conducted with ambient propellants, with all tests resulting in successful thrustor ignitions. The final series of tests was successfully conducted with cold propellants (250 R hydrogen and 375 F oxygen). During these 14 tests with conditioned thrustor propellants, igniter mixture ratio and flowrates were varied. The test parameters are listed in Table B-1.

To summarize, the igniter technique employing resonance heating was systematically investigated. Variable-geometry test hardware was used to optimize igniter geometry. A resonance igniter was tested in an "igniter-only" facility to explore operational limits, and complete thrustor assembly tests were conducted at simulated altitude conditions to demonstrate the feasibility of the resonance igniter to ignite the SS/APS thrustor without external power and catalytic agents.

Table B-1. High-Pressure Resonance Igniter/Thrustor Test Matrix

Test No.	Thrustor: Chamber Pressure lb/in.^{2}	Thrustor: Chamber Pressure N/cm^2	Thrustor: Propellant Temperature T_o R	T_o K	T_f R	T_f K	Igniter: $\dot{w}_t$ lbm/sec	$\dot{w}_t$ Kg/sec	$\dot{w}_{ign}$* lbm/sec	$\dot{w}_{ign}$* Kg/sec	Igniter Mixture Ratio (o/f)	Total Mixture Ratio (o/f)	Results
1	290	200	537	298	525	292	0.0798	0.0359	0.0401	0.0180	0.93	2.83	Effect of igniter mixture ratio on thrustor ignition with ambient propellants
2	290	200	536	298	526	292	0.0774	0.0348	0.0369	0.0166	0.61	2.39	
3	290	200	536	298	528	293	0.0777	0.0350	0.0364	0.0164	0.41	2.02	
4	290	200	537	298	526	292	0.0785	0.0353	0.0385	0.0173	0.83	2.72	
5	289	199	537	298	526	292	0.0772	0.0347	0.0366	0.0165	0.62	2.42	
6	289	199	538	299	528	293	0.0769	0.0346	0.0350	0.0158	0.37	2.01	
7	288	199	536	298	526	292	0.0768	0.0346	0.0350	0.0158	0.37	2.01	
8	289	199	537	298	528	293	0.0741	0.0333	0.0330	0.0149	0.57	2.52	
9	280	193	415	231	249	138	0.0819	0.0369	0.0427	0.0192	1.02	2.88	Effect of igniter mixture ratio on thrustor ignition with conditioned propellants
10	281	194	348	193	239	133	0.0792	0.0356	0.0392	0.0176	0.85	2.74	
11	302	208	360	200	221	123	0.0770	0.0347	0.0362	0.0163	0.59	2.37	
12	300	207	365	203	222	123	0.0763	0.0343	0.0346	0.0156	0.33	1.93	
13**	---	---	396	220	239	133	---	---	---	---	--	--	
14	299	206	363	202	217	121	0.0808	0.0364	0.0408	0.0184	0.74	2.46	
15	302	208	357	198	357	198	0.0812	0.0365	0.0408	0.0184	0.59	2.17	
16	301	208	354	197	318	177	0.0766	0.0345	0.0348	0.0157	0.32	1.90	
17	301	208	354	197	219	122	0.0385	0.0173	0.0192	0.00864	0.81	2.63	Effect of igniter mixture ratio on thrustor ignition at reduced igniter flowrate and conditioned propellants
18	304	210	355	197	221	123	0.0371	0.0167	0.0194	0.00873	0.67	2.19	
19	305	210	343	191	213	118	0.0351	0.0158	0.0199	0.00896	0.51	1.65	
20	303	209	344	191	214	119	0.0389	0.0175	0.0193	0.00869	0.82	2.83	
21	303	209	349	194	216	120	0.0371	0.0167	0.0196	0.00882	0.66	2.15	
22	302	208	354	197	204	113	0.0345	0.0155	0.0197	0.00887	0.51	1.64	

*GO_2 coolant flow not included; **No ignition (believed to be the result of valve malfunction)

APPENDIX C

IGNITER TEST FACILITY

The igniter test effort was conducted in Thermodynamics Laboratory located at North American Rockwell Corporation's Los Angeles Division. A schematic of the resonant igniter propellant system is shown in Fig. C-1, and the setup for the combustion wave igniter is shown in Fig. C-2.

PROPELLANT SYSTEMS

Feed systems for both propellants were similar in size and configuration. The propellant was stored in high-pressure bottles and supplied through a 1-1/2-inch (3.8-cm) system and pressure regulator to the test cell. A calibrated sonic venturi was incorporated with a bypass line and valve, which provided a convenient method of calibrating the facility, igniter hardware, and subsonic flowmeters. During blowdowns, the bypass valve was closed and flow was measured and controlled by the sonic venturi while system/hardware parameters were measured. During ignition tests, the bypass valve was opened and the effect of the sonic venturi was negated.

SYSTEM CONTROL

All tests were conducted using an automatic sequencer. The sequence included operation of the fuel, oxidizer, and bleed valves. The sequencer was capable of controlling the valves to any specified relative position in time within 1 millisecond. Prior to each test series, the sequence was verified with the systems pressurized by GN_2.

INSTRUMENTATION

Instrumentation list is presented in Table C-1. Sufficient pressure and temperature sensors were used to establish and monitor the system/hardware conditions.

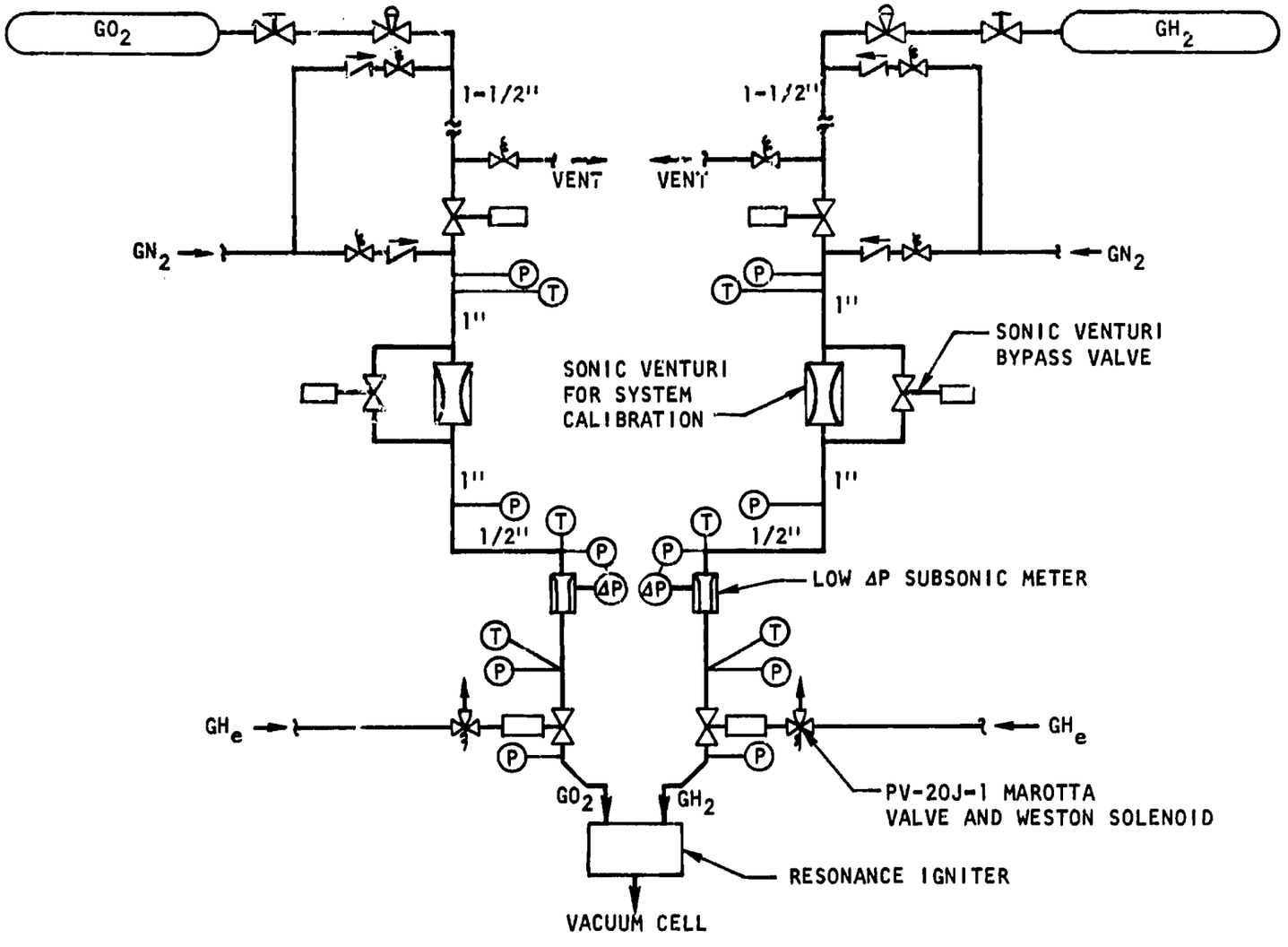

Figure C-1. Resonant Igniter Test Setup

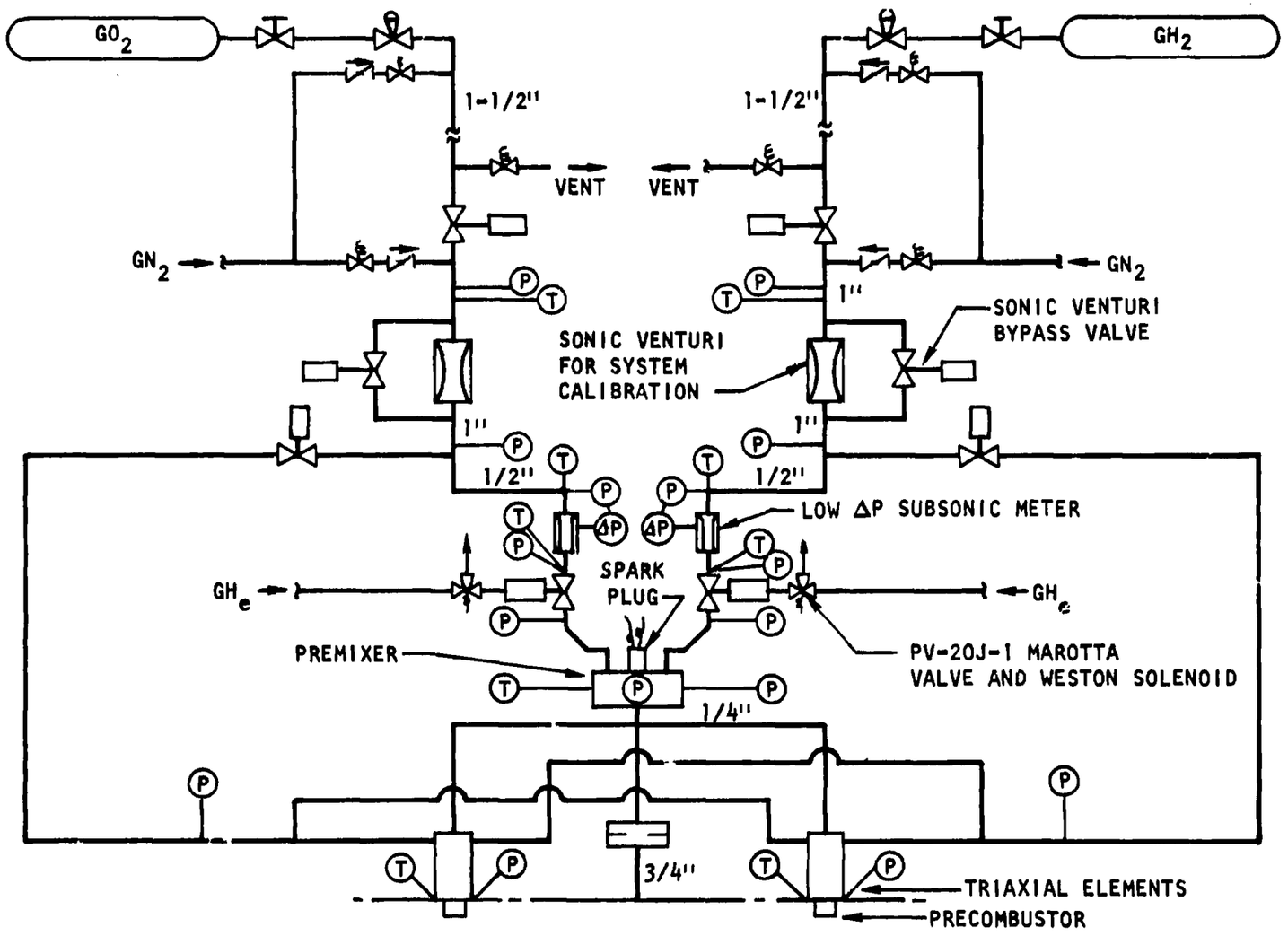

Figure C-2. Combustion Wave Igniter Test Setup

System	Parameter	Range	Recorder Precision, Percent			
			Digital	Oscillograph	Brush	Indication
Fuel	Calibration Venturi Upstream Pressure, psig	0 to 1000	1/2	--	-	2
	Calibration Venturi Upstream Temperature, F	0 to 150	1	--	-	-
	Flowmeter Upstream Pressure, psig	0 to 500	1/2	10	-	-
	Flowmeter Upstream Temperature, F	200 to 800	1	--	-	-
	Flowmeter ΔP,psid	0 to 20	1/2	10		-
	Valve Upstream Pressure, psig	0 to 500	1/2	--	1	2
	Valve Bleed Temperature, R	200 to 800	-	--	-	2
	Injection Pressure, psig	0 to 500	1/2	10	1	-
Oxidizer	Calibration Venturi Upstream Pressure, psig	0 to 1000	1/2	--	-	2
	Calibration Venturi Upstream Temperature, F	0 to 150	1	--	-	-
	Flowmeter Upstream Pressure, psig	0 to 500	1/2	10	-	-
	Flowmeter Upstream Temperature, F	200 to 800	1	--	-	-
	Flowmeter ΔP, psid	0 to 20	1/2	10	1	-
	Valve Upstream Pressure, psig	0 to 500	1/2	--	1	2
	Valve Bleed Temperature, R	200 to 200	-	--	-	2
	Injection Pressure, psia	0 to 500	1/2	10	-	-
	Coolant Flowmeter ΔP, psid	0 to 20	1/2	--	1	-
Igniter	Base Chamber Pressure, psia	0 to 500	1/2	10	1	-
	High-Frequency Chamber Pressure, psig	0 to 1000	-	10	-	-
	Vacuum Pressure, mm Hg	10	-	--	-	2
	Resonance Temperature, R	0 to 3000	1/2	10	1	-
Events	Fuel Valve Signal	--	X	X	X	-
	Oxidizer Valve Signal	--	X	--	X	-
	Fuel Bleed Valve Signal	--	-	--	X	-
	Oxidizer Bleed Valve Signal	--	-	--	X	-
	Time Reference, cps	1	X	X	X	-

Data acquisition included a high-speed digital system, a high-frequency oscillograph recorder, and a 6-channel high-response Brush recorder. Dial indicators were located on the control console for system setup.

The digital system was an Astro Data capable of 6600 samples per second with inputs from up to 100 sensors. Since the instrumentation list has less than 25 inputs, each parameters was multiplexed four times to achieve a sample rate of 264 times per second per parameter. The Astro Data recorded the data on magnetic tape for subsequen computer data reduction on an IBM 360.

The output of a high-frequency Kistler water-cooled transducer was recorded along with other selected system parameters on a high-frequency oscillograph recorder to establish the transient conditions and ignition delays. This recorder output was in the form of permanent strip charts running at speeds of up to 128 inches per second.

A 6-channel Brush recorder was used for on-the-spot monitoring of test results. This recorder was capable of moderately high response and accurate quantitative data. In addition, the recorder contained event channels for recording the electrical valve sequence.

DOCUMENTATION OF RESULTS

A file of test records was maintained, including strip charts and computer data reduction outputs. An informal test book was maintained, which included test setup notes, formal test requests, test data results, and summary of test activities.

DATA REDUCTION

The Astro Data magnetic tape was reduced by a computer data reduction program, which had been written to reduce digital counts to pressures and temperatures in engineering units. The program calculated flowrates and mixture ratio from the subsonic meters, using input tables of real gas properties for each propellant and the in-place calibration factors for each meter as determined by the system calibration blowdowns.

Unclassified

Security Classification

DOCUMENT CONTROL DATA - R & D

(Security classification of title, body of abstract and indexing annotation must be entered when the overall report is classified)

1. ORIGINATING ACTIVITY *(Corporate author)* ROCKETDYNE a division of North American Rockwell Corporation 6633 Canoga Avenue, Canoga Park, California 91304	2a. REPORT SECURITY CLASSIFICATION Unclassified 2b. GROUP

3. REPORT TITLE

Advanced Ignition Systems

4. DESCRIPTIVE NOTES *(Type of report and inclusive dates)*

Final Report, 30 July 1971

5. AUTHOR(S) *(First name, middle initial, last name)*

Rocketdyne Engineering

6. REPORT DATE	7a. TOTAL NO. OF PAGES	7b. NO. OF REFS
30 July 1971	136	18

8a. CONTRACT OR GRANT NO. NAS8-25126 b. PROJECT NO. 09288 c. d.	9a. ORIGINATOR'S REPORT NUMBER(S) R-8756 9b. OTHER REPORT NO(S) *(Any other numbers that may be assigned this report)*

10. DISTRIBUTION STATEMENT

11. SUPPLEMENTARY NOTES	12. SPONSORING MILITARY ACTIVITY

13. ABSTRACT

Two ignition system concepts were experimentally evaluated during laboratory testing for application in hydrogen/oxygen engine system incorporating a multiple-combustor thrust chamber. Both concepts, designated the Resonant Flow Igniter and the Combustion Wave Igniter, proved operationally feasible for the specific engine system application. The ignition concepts are unique and can be used to ignite any hydrogen/oxygen combustion device. The ignition system design requirements are discussed, ignition system configurations for a specific application are described, and the results of feasibility testing with prototype igniter hardware are detailed.

Unclassified

Security Classification

14 KEY WORDS	LINK A ROLE	LINK A WT	LINK B ROLE	LINK B WT	LINK C ROLE	LINK C WT
Resonant Flow Igniter						
Combustion Wave Igniter						
No. 2 Test Bed						
Resonance Heating Phenomenon						
Autoignition						